



With Photo
CD-ROM

2
Edition

MRI

Made Easy[®]

(for Beginners)

JAYPEE

Govind B Chavhan

Copyrighted Material

MRI

Made Easy[®]

(for Beginners)

Second Edition

Govind B Chavhan

MD DNB DABR

Staff Pediatric Radiologist
The Hospital for Sick Children
Toronto, Canada

Assistant Professor
University of Toronto
Ontario, Canada



JAYPEE BROTHERS MEDICAL PUBLISHERS (P) LTD

New Delhi • Panama City • London • Philadelphia (USA)



Jaypee Brothers Medical Publishers (P) Ltd

Headquarters

Jaypee Brothers Medical Publishers (P) Ltd
4838/24, Ansari Road, Daryaganj
New Delhi 110 002, India
Phone: +91-11-43574357
Fax: +91-11-43574314
Email: jaypee@jaypeebrothers.com

Overseas Offices

J.P. Medical Ltd
83 Victoria Street, London
SW1H 0HW (UK)
Phone: +44-2031708910
Fax: +02-03-0086180
Email: info@jpmedpub.com

Jaypee-Highlights Medical Publishers Inc.
City of Knowledge, Bld. 237, Clayton
Panama City, Panama
Phone: +507-301-0496
Fax: +507-301-0499
Email: cservice@jphmedical.com

Jaypee Brothers Medical Publishers (P) Ltd
17/1-B Babar Road, Block-B, Shaymali
Mohammadpur, Dhaka-1207
Bangladesh
Mobile: +08801912003485
Email: jaypeedhaka@gmail.com

Jaypee Brothers Medical Publishers (P) Ltd
Shorakhute, Kathmandu
Nepal
Phone: +00977-9841528578
Email: jaypee.nepal@gmail.com

Website: www.jaypeebrothers.com
Website: www.jaypeedigital.com

© 2013, Jaypee Brothers Medical Publishers

All rights reserved. No part of this book may be reproduced in any form or by any means without the prior permission of the publisher.

Inquiries for bulk sales may be solicited at: jaypee@jaypeebrothers.com

This book has been published in good faith that the contents provided by the author contained herein are original, and is intended for educational purposes only. While every effort is made to ensure accuracy of information, the publisher and the author specifically disclaim any damage, liability, or loss incurred, directly or indirectly, from the use or application of any of the contents of this work. If not specifically stated, all figures and tables are courtesy of the author. Where appropriate, the readers should consult with a specialist or contact the manufacturer of the drug or device.

MRI Made Easy® (for Beginners)

First Edition: 2006

Second Edition: 2013

ISBN 978-93-5090-270-7

Printed at

Dedicated to

*Ravi Sir (Professor Ravi Ramakantan)
the teacher par excellence
unchallengeable Radiologist
'Niswarth Karmayogi' relentlessly working towards
the benefit of thousands of poor patients
the great igniter of minds
this is for you*

Preface to the Second Edition

Between two editions of this book, many new things happened in the field of MRI. 3-Tesla MRI became more widespread in clinical practice. New techniques like SWI, MR Enterography and Urography established their role in the patient management. Nephrogenic systemic fibrosis suddenly surfaced and changed the practice of contrast administration. The second edition of *MRI Made Easy (for Beginners)* remains superficial overview of the subject explaining the basic fundamentals in simple language. This work is done keeping in mind needs of the person beginning to learn MR, especially radiology residents. As before, in attempt to simplify the subject, many complex things have been purposely omitted. This book is by no means complete source of the subject. This should serve as an appetizer for further reading of this interesting subject.

This book is divided into two sections. First section deals with basic principles, instrumentation of MR system, sequences and artifacts. Also discussed are basic principles of MR interpretations. In section 1, there are new chapters on scanning parameters and accessory techniques. The chapter 7 on Clinical Applications of Sequences has been revised to include when and why to use a sequence rather than just listing the applications. Section 2 is on higher applications of MRI. This section has a new chapter on 3-Tesla MRI and discussion of a few new techniques in the chapters on miscellaneous techniques.

Best wishes and happy reading!

Govind B Chavhan

Preface to the First Edition

Radiology is the fastest advancing branch of medical sciences. It is moving from evaluation of anatomy to physiology, structural to functional, morphological to tissue diagnosis and biochemical information. MR takes the lead in this rapid march of advancement of radiology. No other modality has developed so much as MR in the last 20 years. MR has emerged as strong modality, which gives final answer in many conditions in all body systems.

This short introductory book is the superficial overview of the subject explaining the basic fundamentals. This work is done keeping in mind needs of the person beginning to learn MR, especially radiology residents. In attempt to simplify the subject, many complex things have purposely been omitted. This book is by no means complete source of the subject. This should serve as an appetizer for further reading of this interesting subject.

This book is divided into two sections. First section deals with basic principles, instrumentation of MR system, sequences and artifacts. Also discussed are few basic principles of MR interpretations. Section two has some advances and higher applications of MR. Following are few things to remember while reading this book:

- Start reading from the first chapter and go in sequence for better understanding.
- Protons, nuclei and spins are used synonymously; so do not get confused by them. They are one and the same.
- For quick reference to the sequence, list of the common sequences with their long forms is given in the beginning.

Govind B Chavhan

Acknowledgments

The first edition of *MRI Made Easy (for Beginners)* was inspired by high-quality radiology work done by my idols Dr Bhavin Jankharia and Dr Meher Ursekar. The second edition remains reflection of their work and teaching. I am grateful to them for their continued support and love. Most of the images of the first edition are retained in this edition. These images are courtesy of Jankharia Imaging, Mumbai, Maharashtra, India.

I am fortunate enough to have excellent teachers and guides at every step of my career. It started with Ravi Sir in King Edward Memorial (KEM) Hospital, Mumbai, Maharashtra, India, who instilled ability, confidence and values for patient care. This was followed by MRI learning under Dr Jankharia and Dr Ursekar. At my present work place in Toronto, Canada, Dr Manu Shroff and Dr Paul Babyn are my pillars of support and guidance. I am grateful to Dr Babyn for mentoring me in the exciting field of pediatric body MRI.

Thank you to my all colleagues in the department at The Hospital for Sick Children, Toronto, Canada and MRI division under leadership of Albert Aziza for their support. Thank you to Wendy Doda our Research Manager for her help in getting consent for the new images used in this edition.

I take this opportunity to thank all the readers who commented, criticized and made suggestions about the first edition on *Amazon.com*. This has helped to improve the second edition.

My sincere thanks to Shri Jitendar P Vij (Group Chairman), Mr Ankit Vij (Managing Director) and Mr Tarun Duneja (Director-Publishing) of M/s Jaypee Brothers Medical Publishers (P) Ltd, New Delhi, India, for publishing this work.

Last but not least, thanks to my wife, Barakha, and my two sons, Yash and Raj, for their support and time.

Commonly Used Short Forms

ADC	Analog to Digital Converter
CEMRA	Contrast Enhanced MR Angiography
FOV	Field of View
FT	Fourier Transformation
GMR	Gradient Motion Rephasing/Nulling
GRE	Gradient Echo
IR	Inversion Recovery
LM	Longitudinal Magnetization
MTC	Magnetization Transfer Contrast
NEX	Number of Excitation (Averages of Acquisition)
NMV	Net Magnetization Vector
PD	Proton Density
RF	Radiofrequency
SAR	Specific Absorption Rate
SE	Spin Echo
SNR	Signal to Noise Ratio
TE	Time to Echo
TI	Time to Invert (Inversion Time)
TM	Transverse Magnetization
TR	Time to Repeat
VENC	Velocity Encoding

Trade Names of Sequences

SEQUENCES	SIEMENS*	GE *	PHILIPS*
1. Spin Echo Sequences			
Conventional SE (90–180° RF pulses)	SE	SE	SE
Double SE (90° followed by two 180° RF pulses)	PD/T2	PD/T2	PD/T2
Multi-SE (90° followed by multiple 180° RF pulses)	Turbo SE	Fast SE	Turbo SE
Multi-SE with flip-back 90° pulse	RESTORE	FRFSE	DRIVE
Single-shot Multi-SE (Multi-SE with half K-Space filling)	HASTE	Single Shot FSE	Ultrafast SE
Radial K-Space filling	BLADE	PROPELLER	MultiVane
2. Gradient Echo Sequences			
A. Incoherent spoiled TM	FLASH	SPGR	T1-FFE
3D versions	3D FLASH VIBE	LAVA FAME	THRIVE
B. Coherent/Rephased TM			
1. Post-excitation refocused (FID sampled)	FISP	GRASS	FFE
2. Pre-excitation refocused (Spin echo sampled)	PSIF	SSFP	T2-FFE
3. Fully refocused (both FID & spin echo sampled)	True FISP	FIESTA	Balanced FFE
3. Inversion Recovery Sequences Short TI (80–150 ms), e.g. STIR Medium TI (300–1200 ms), e.g. MPRAGE Long TI (1500–2500 ms), e.g. FLAIR			
4. Hybrid			
Combination of SE and GRE	TGSE	GRASE	GRASE
5. EPI Single shot Multishot-segmented			

*Vendor nomenclatures for sequences are taken from References—1. Nitz WR. MR Imaging: Acronyms and clinical applications. Eur Radiol. 1999;9:979-97. and 2. Brown MA, Semelka RC. MR Imaging Abbreviations, Definitions, and Descriptions: A Review. Radiol. 1999; 213:647-62.

Contents

Section 1

Chapter 1. Basic Principles	1
<i>Longitudinal Magnetization</i>	2
<i>Transverse Magnetization</i>	3
<i>MR Signal</i>	4
<i>Localization of the Signal</i>	5
Chapter 2. T1, T2 Relaxations and Image Weighting	8
<i>Longitudinal Relaxation</i>	8
<i>Transverse Relaxation</i>	9
<i>T1</i>	10
<i>T2</i>	11
<i>T2* (T2 star)</i>	11
<i>TR and TE</i>	12
<i>Tl</i>	13
<i>T1 Weighted Image</i>	13
<i>T2 Weighted Image</i>	14
<i>Proton Density (PD) Image</i>	16
Chapter 3. K-Space and Scanning Parameters	17
<i>K-Space</i>	17
<i>Parameters of Scanning</i>	18
<i>Image Quality Determinants</i>	20
Chapter 4. Magnetic Resonance Instrumentation	22
<i>Magnetism</i>	22
<i>Magnetic Field Strength</i>	23
<i>Magnets</i>	24
<i>Gradients</i>	29
<i>Radiofrequency Coils</i>	30
<i>Computers and Accessories</i>	32
Chapter 5. Sequences I: Basic Principles and Classification	33
<i>Classification</i>	34
<i>Spin Echo (SE) Pulse Sequence</i>	34
<i>Gradient Echo (GRE) Sequence</i>	37

<i>Inversion Recovery (IR) Sequence</i>	40
<i>Echo Planar Imaging (EPI)</i>	44
Chapter 6. Sequences II: Accessory Techniques	47
<i>Fat Suppression</i>	47
<i>Parallel Imaging</i>	52
<i>Respiratory Compensation Techniques</i>	53
<i>Gradient Moment Rephasing (GMR)</i>	53
<i>Magnetization Transfer</i>	55
<i>Keyhole Imaging</i>	56
<i>Saturation Band</i>	56
Chapter 7. Sequences III: When to Use What Sequences	58
<i>T1-Weighted Sequences</i>	58
<i>T2-Weighted Sequences</i>	61
<i>T2* Weighted Sequences</i>	70
<i>Cartilage Sensitive Sequences</i>	70
Chapter 8. Magnetic Resonance Imaging Artifacts	73
<i>Ghosts/Motion Artifacts</i>	73
<i>Aliasing/ Wraparound</i>	75
<i>Chemical Shift Related Artifacts</i>	76
<i>Truncation Artifact</i>	78
<i>Magnetic Susceptibility Artifact</i>	78
<i>Straight Lines and Zipper Artifacts</i>	80
<i>Shading Artifacts</i>	81
<i>Cross Excitation and Cross Talk</i>	82
<i>Parallel Imaging Artifact</i>	84
Chapter 9. Magnetic Resonance Safety	85
<i>MR Bioeffects</i>	85
<i>Safety Related Issues</i>	86
Chapter 10. Magnetic Resonance Contrast Media	91
<i>Classification of MR Contrast Media</i>	91
<i>Mechanism of MR Contrast Enhancement</i>	92
<i>Gadolinium</i>	93
<i>Nephrogenic Systemic Fibrosis (NSF)</i>	96
<i>Other MR Contrast Agents</i>	97
<i>Oral Contrast Agents</i>	98
<i>Role of Contrast in MRI</i>	98

Chapter 11. Principles of Interpretation: Neuroimaging	102
Normal signal intensity	102
Sequence Selection	103
Chapter 12. Principles of Interpretation: Body Imaging	115
Sequences	115
Section 2	
Chapter 13. 3-Tesla MRI	125
Physics Differences	125
Artifacts	126
Safety Issues	126
Clinical Applications	128
Chapter 14. Magnetic Resonance Angiography	129
Types of MRA	129
Noncontrast MRA Techniques	131
Contrast Enhanced MRA (CEMRA)	136
Chapter 15. Magnetic Resonance Diffusion	137
What is Diffusion?	137
How do we Acquire Diffusion Weighted Images?	138
Clinical Applications of DWI	140
Diffusion Tensor Imaging	146
Chapter 16. Magnetic Resonance Perfusion	148
Principles	148
Technique of MR Perfusion with Exogenous Contrast Agent	149
Clinical Applications	150
Arterial Spin Labeling (ASL)	155
Chapter 17. Magnetic Resonance Spectroscopy	158
Basic Principles	158
Localization Techniques in MRS	160
Steps in MRS Acquisition	161
Metabolites of ¹ H MRS	164
Clinical Uses of MRS	167
Chapter 18. Cardiac Magnetic Resonance Imaging	172
ECG Gating	172
Imaging Sequences	172

xx MRI Made Easy (for Beginners)

<i>Imaging Planes</i>	173
<i>Clinical Applications of CMRI</i>	176

Chapter 19. Magnetic Resonance

Cholangiopancreatography 183

<i>Principles</i>	183
<i>Sequences used in MRCP</i>	183
<i>MRCP Protocol and Technique</i>	185
<i>Clinical Applications of MRCP</i>	186

Chapter 20. Miscellaneous Neuroimaging

MR Techniques 190

<i>fMRI : Functional MRI</i>	190
<i>Susceptibility Weighted Imaging</i>	192
<i>Cerebrospinal Fluid Flow Study</i>	192

Chapter 21. Miscellaneous Body Imaging

MR Techniques 196

<i>Magnetic Resonance Enterography</i>	196
<i>MR Urography</i>	198
<i>Iron Overload Imaging</i>	199
<i>Magnetic Resonance Elastography</i>	201
<i>Magnetic Resonance Arthrography</i>	201

<i>Index</i>	203–208
--------------	---------

Section 1

CHAPTER

1

Basic Principles

Four basic steps are involved in getting an MR image—

1. Placing the patient in the magnet
2. Sending Radiofrequency (RF) pulse by coil
3. Receiving signals from the patient by coil
4. Transformation of signals into image by complex processing in the computers.

Now let us understand these steps at molecular level. Present MR imaging is based on proton imaging. Proton is a positively charged particle in the nucleus of every atom. Since hydrogen ion (H^+) has only one particle, i.e. proton, it is equivalent to a proton. Most of the signal on clinical MR images comes from water molecules that are mostly composed of hydrogen.

How do protons help in MR imaging?

Protons are positively charged and have rotatory movement called spin. Any moving charge generates current. Every current has a small magnetic field around it. So every spinning proton has a small magnetic field around it, also called magnetic dipole moment.

Normally the protons in human body (outside the magnetic field) move randomly in any direction. When external magnetic field is applied, i.e. patient is placed in the magnet, these randomly moving protons align (i.e. their magnetic moment align) and spin in the direction of external magnetic field. Some of them align parallel and others anti-parallel to the external magnetic field. When a proton aligns along external magnetic field, not only it rotates around itself (called

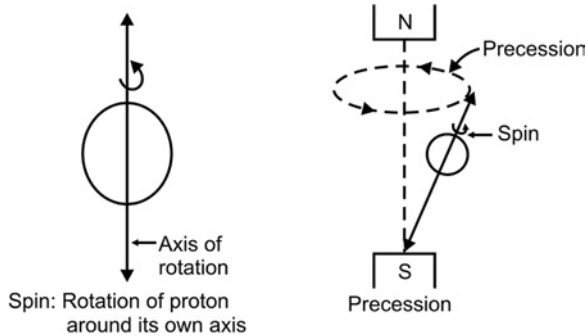


Fig. 1.1: Spin versus precession. Spin is rotation of a proton around its own axis while precession is rotation of the axis itself under the influence of external magnetic field such that it forms a 'cone'

spin) but also its axis of rotation moves forming a 'cone'. This movement of the axis of rotation of a proton is called as *precession* (Fig. 1.1).

The number of precessions of a proton per second is called precession frequency. It is measured in Hertz. Precession frequency is directly proportional to strength of external magnetic field. Stronger the external magnetic field, higher is the precession frequency. This relationship is expressed by Larmors equation—

$$\omega_0 = \gamma B_0$$

Where ω_0 = Precession frequency in Hz

B_0 = Strength of external magnetic field in Tesla

γ = Gyromagnetic ratio, which is specific to particular nucleus

Precession frequency of the hydrogen proton at 1, 1.5 and 3 Tesla is roughly 42, 64 and 128 MHz respectively.

Longitudinal Magnetization

Let us go one step further and understand what happens when protons align under the influence of external magnetic field. For the orientation in space consider X, Y, and Z axes system. External magnetic field is directed along the Z-axis. Conventionally, the Z-axis is the long axis of the patient as well as bore of the magnet. Protons align parallel and

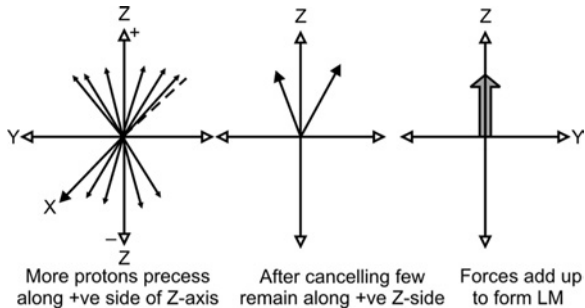


Fig. 1.2: Longitudinal magnetization

antiparallel to external magnetic field, i.e. along positive and negative sides of the Z-axis. Forces of protons on negative and positive sides cancel each other. However, there are always more protons spinning on the positive side or parallel to Z-axis than negative side. So after canceling each others forces there are a few protons on positive side that retain their forces. Forces of these protons add up together to form a magnetic vector along the Z-axis. This is called as **longitudinal magnetization** (Fig. 1.2).

Longitudinal magnetization thus formed along the external magnetic field can not be measured directly. For the measurement it has to be transverse.

Transverse Magnetization

As discussed in the previous paragraph when patient is placed in the magnet, longitudinal magnetization is formed along the Z-axis. The next step is to send radiofrequency (RF) pulse. The precessing protons pick up some energy from the radiofrequency pulse. Some of these protons go to higher energy level and start precessing antiparallel (along negative side of the Z-axis). The imbalance results in tilting of the magnetization into the transverse (X-Y) plane. This is called as transverse magnetization (Fig. 1.3). In short, RF pulse causes titling of the magnetization into transverse plane.

The precession frequency of protons should be same as RF pulse frequency for the exchange of energy to occur between protons and RF pulse. When RF pulse and protons have the same frequency protons

4 MRI Made Easy (For Beginners)

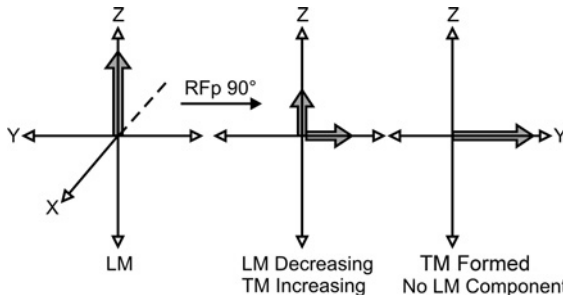


Fig. 1.3: Transverse magnetization. Magnetization vector is flipped in transverse plane by the 90 degree RF pulse

can pick up some energy from the RF pulse. This phenomenon is called as “resonance”- the R of MRI.

RF pulse not only causes protons to go to higher energy level but also makes them precess in step, in phase or synchronously.

MR Signal

Transverse magnetization vector has a precession frequency. It constantly rotates at Larmor frequency in the transverse plane and induces electric current while doing so. The receiver RF coil receives this current as MR signal (Fig. 1.4). The strength of the signal is proportional to the magnitude of the transverse magnetization. MR signals are transformed into MR image by computers using mathematical methods such as Fourier Transformation.

Revision:

Basic four steps of MR imaging include:

1. Patient is placed in the magnet—
All randomly moving protons in patient’s body align and precess along the external magnetic field. Longitudinal magnetization is formed long the Z-axis.
2. RF pulse is sent—
Precessing protons pick up energy from RF pulse to go to higher energy level and precess in phase with each other. This results in reduction in longitudinal magnetization and formation of transverse magnetization in X-Y plane.

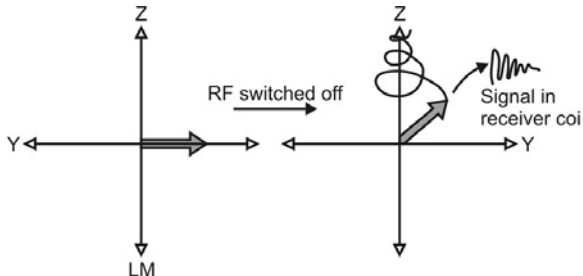


Fig. 1.4: MR signal. The TM vector starts reducing in its magnitude immediately after its formation because of dephasing of protons. The LM starts gradually increasing in its magnitude. The resultant net magnetization vector (NMV) formed by addition of these two (LM and TM vectors) gradually moves from transverse X-Y plane into vertical Z-axis. As long as the NMV is in the transverse plane it produces current in the receiver coil. This current is received by the coil as MR signal

3. MR signal is received—

The transverse magnetization vector precesses in transverse plane and generates current. This current is received as signal by the RF coil.

4. Image formation—

MR signal received by the coil is transformed into image by complex mathematical process such as Fourier Transformation by computers.

Localization of the Signal

Three more magnetic fields are superimposed on the main magnetic field along X, Y, and Z axes to localize from where in the body signals are coming. These magnetic fields have different strength in varying location hence these fields are called “gradient fields” or simply “gradients”. The gradient fields are produced by coils called as gradient coils.

The three gradients are—

1. Slice selection gradient
2. Phase encoding gradient
3. Frequency encoding (read out) gradient.

6 MRI Made Easy (For Beginners)

Slice Selection Gradient

Slice selection gradient has gradually increasing magnetic field strength from one end to another (Fig. 1.5). It determines the slice position. Slice thickness is determined by the bandwidth of RF pulse. Bandwidth is the range of frequencies. Wider the bandwidth thicker is the slice.

Phase Encoding and Frequency Encoding Gradients

These gradients are used to localize the point in a slice from where signal is coming. They are applied perpendicular to each other and perpendicular to the slice selection gradient (Fig. 1.6).

Typically, for transverse or axial sections following are axes and gradients applied even though X and Y axes can be varied.

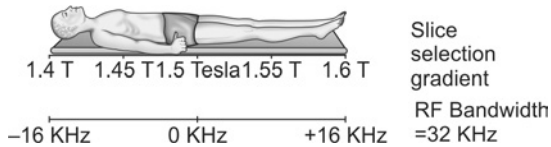


Fig. 1.5: Slice selection gradient

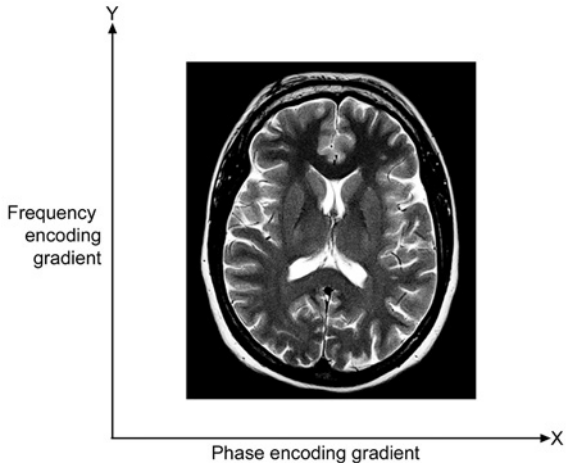


Fig. 1.6: Frequency and phase encoding gradients

1. Z-axis—Slice selection gradient
2. Y-axis—Frequency encoding gradient
3. X-axis—Phase encoding gradient.

In a usual sequence, slice selection gradient is turned on at the time of RF pulse. Phase encoding gradient is turned on for a short time after slice selection gradient. Frequency encoding or readout gradient is on in the end at the time of signal reception.

Information from all three axes is sent to computers to get the particular point in that slice from which the signal is coming.

Why Proton only?

Other substances can also be utilized for MR imaging. The requirements are that their nuclei should have spin and should have odd number of protons within them. Hence theoretically ^{13}C , ^{19}F , ^{23}Na , ^{31}P can be used for MR imaging.

Hydrogen atom has only one proton. Hence H^+ ion is equivalent to a proton. Hydrogen ions are present in abundance in body water. H^+ gives best and most intense signal among all nuclei.

T1, T2 Relaxations and Image Weighting

CHAPTER 2

Relaxation means recovery of protons back towards equilibrium after been disturbed by RF excitation. Relaxation times of protons such as T1 and T2, and number of protons in tissues (proton density) are the main determinant of the contrast in an MR image.

As discussed in chapter 1, RF pulse causes tilting of magnetization in the transverse plane, where it rotates at Larmor frequency. This chapter discusses processes happening after this and their implications on the image contrast.

What happens when RF pulse is switched off?

When RF pulse is switched off, LM starts increasing along Z-axis and TM starts reducing in the transverse plane. The process of recovery of LM is called *Longitudinal Relaxation* while reduction in the magnitude of TM is called as *Transverse Relaxation*.

The components of magnetization in longitudinal and transverse planes (i.e. LM and TM) can be represented by a single vector. This vector represents sum of these components and is called as *net magnetization vector* (NMV). NMV lies some where between LM and TM. If there is no magnetization in transverse plane LM will be same as NMV. Similarly if there is no LM, TM will be equal to NMV.

Longitudinal Relaxation

When RF pulse is switched off, spinning protons start losing their energy. The low energy protons tend to align along the Z-axis. As more

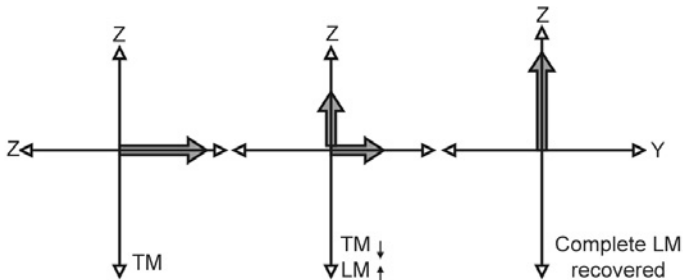


Fig. 2.1: Longitudinal relaxation

and more protons align along the positive side of the Z-axis there is gradual increase in the magnitude (recovery) of the LM (Fig. 2.1). The energy released by the protons is transferred to the surrounding (the crystalline lattice of molecules) hence the longitudinal relaxation is also called as 'spin-lattice' relaxation. The transfer of energy involves dipole-dipole interaction of fluctuating small magnetic fields that originate in adjacent protons and electrons in the surrounding. For the transfer of energy to occur, it is necessary that these fluctuations occur at the Larmor frequency.

The time taken by LM to recover to its original value after RF pulse is switched off is called longitudinal relaxation time or **T1**.

Transverse Relaxation

The transverse magnetization represents composition of magnetic forces of protons precessing at similar frequency. More the number of protons precessing at the same frequency (in-phase) stronger will be the TM. These protons are constantly exposed to static or slowly fluctuating local magnetic fields. Hence they start losing phase after RF pulse is switched off. This, going out of phase of protons (dephasing) results into gradual decrease in the magnitude of TM and is termed as transverse relaxation (Fig. 2.2). Since the dephasing is related to the static or slowly fluctuating intrinsic fields caused by adjacent spins (protons), transverse relaxation is also called 'spin-spin relaxation'.

The time taken by TM to reduce to its original value is transverse relaxation time or **T2**.

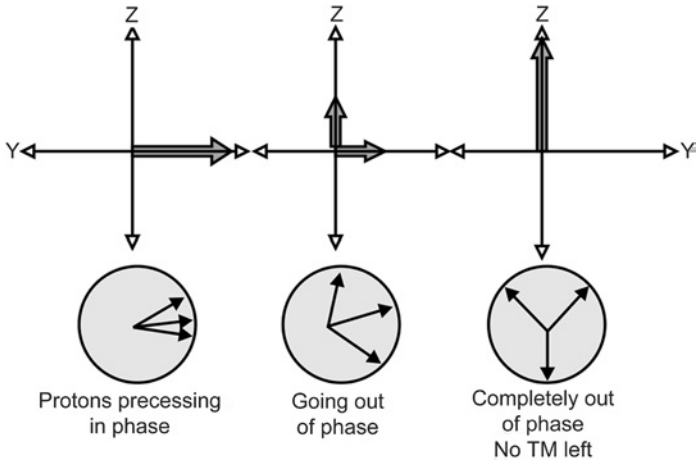


Fig. 2.2: Transverse relaxation

Even though they appear as the parts of same process the longitudinal and transverse relaxations are different processes because underlying mechanisms are different.

T1

T1 is the time taken by LM to recover after RF pulse is switched off. This is not an exact time, but it is a 'constant'. T1 is the time when LM reaches back to 63% of its original value. The curve showing gradual recovery of LM against time is called T1 curve (Fig. 2.3). $1/T1$ is the longitudinal relaxation rate.

T1 depends upon tissue composition, structure and surroundings. If the surrounding matter has magnetic fields, which fluctuate at Larmor frequency, transfer of energy from protons to the surrounding is easy and fast. Protons in such surrounding or chemical environment have shorter T1. Since water molecules move too rapidly the protons in water take long time to transfer their energy. Hence water has long T1. On the other hand, the fluctuating magnetic fields in the fatty acids have frequency near the Larmor frequency. There is fast energy transfer from fat protons to the surrounding. Hence fatty tissues have short T1.

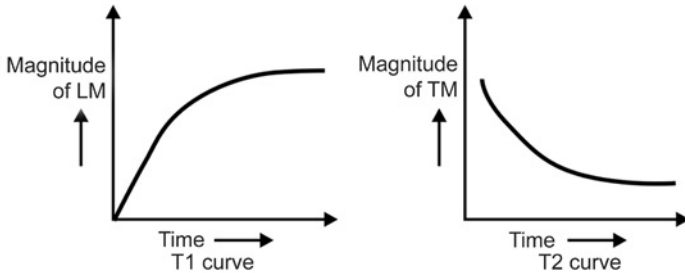


Fig. 2.3: T1 and T2 curves

T1 increases with the strength of the external magnetic field. T1 at 3T is longer than T1 of the same tissue at 1.5T.

T2

T2 is the time taken by TM to disappear. Similar to T1, it is a 'constant' and not an exact time. It is the time taken by the TM to reduce to 37% of its maximum value. The curve showing decrease in magnitude (decay) of the TM plotted against time is called T2 curve (Fig. 2.3). $1/T2$ is transverse relaxation rate.

T2 depends on inhomogeneity of local magnetic fields within the tissues. As water molecules move very fast, their magnetic fields fluctuate fast. These fluctuating magnetic fields cancel each other. So there are no big differences in magnetic field strength inside such a tissue. Because of lack of much inhomogeneity protons stay in phase for a long-time resulting into long T2 for water.

If liquid is impure or the tissue has larger molecules, the molecules move at slower rate. This maintains inhomogeneity of the intrinsic magnetic field within the tissue. As a result protons go out of phase very fast. Hence impure liquids or tissues with larger molecules have short T2. Fat has shorter T2.

T2* (T2 star)

In addition to the magnetic field inhomogeneity intrinsic to the tissues causing spin-spin relaxation, inhomogeneity of the external magnetic field (B_0) also causes decay of the TM. Decay of the TM caused by

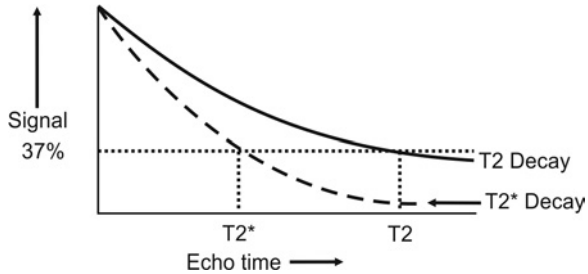


Fig. 2.4: T2* curve

combination of spin-spin relaxation and inhomogeneity of external magnetic field is called $T2^*$ relaxation. Dephasing effects of external magnetic field inhomogeneity are eliminated by 180° RF pulses used in spin-echo sequence. Hence there is 'true' T2 relaxation in a spin-echo sequence. The T2* relaxation is seen in gradient-echo sequence as there is no 180° RF pulse in gradient-echo sequence. T2* is shorter than T2 (Fig. 2.4) and their relationship can be expressed as follows:

$$1/T2^* = 1/T2 + \gamma\Delta B_{\text{in hom}}$$

Where, γ = gyromagnetic ratio

$\Delta B_{\text{in hom}}$ = magnetic field inhomogeneity.

TR and TE

A typical spin-echo sequence consists of 90 degree pulse followed by 180 degree pulse. After 180 degree pulse the signal (echo) is received (Fig. 2.5).

TR (Time to Repeat) is the time interval between start of one RF pulse and start of the next RF pulse. For a spin-echo sequence time interval between beginnings of 90 degree pulses is the TR.

TE (Time to Echo) is the time interval between start of RF pulse and reception of the signal (echo).

Short TR and short TE gives T1 weighted images.

Long TR and long TE gives T2 weighted images.

Long TR and short TE gives Proton density images.

TR is always higher than TE. Typical long and short TR/TE values are shown in Table 2.1.

Table 2.1: Typical TR and TE values in milliseconds

	Spin-echo sequence	Gradient-echo sequence
Short TR	300-800	<50
Long TR	>2000	>100
Short TE	10-25	1-5
Long TE	>60	>10

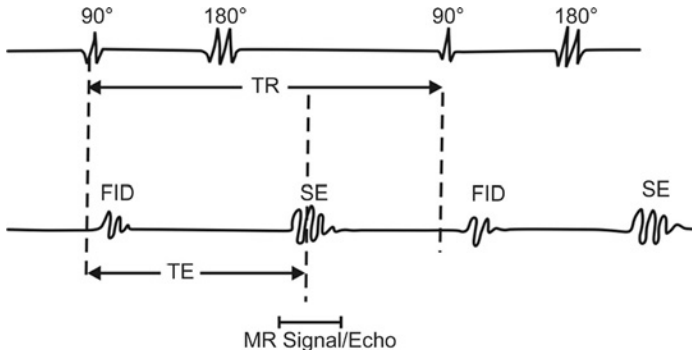


Fig. 2.5: Spin Echo (SE) sequence. (90° = 90 degree RF pulse; 180° = 180 degree RF pulse; FID = free induction decay; SE = spin-echo; TE = time to echo and TR = time to repeat)

T1

T1 is Time of Inversion. It is the time between inverting 180 degree pulse and 90 degree pulse in Inversion Recovery (IR) sequence. T1 determines the image contrast in IR sequences.

T1 Weighted Image

The magnitude of LM indirectly determines the strength of MR signal. Tilting of stronger LM by 90 degree RF pulse will result into greater magnitude of TM and stronger MR signal. The tissues with short T1 regain their maximum LM in short-time after RF pulse is switched off. When the next RF pulse is sent, TM will be stronger and resultant signal will also be stronger. Therefore, material with short T1 have bright signal on T1 weighted images.

How does one make images T1 weighted?

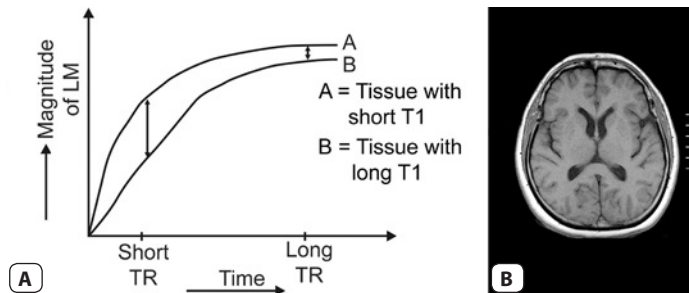
This is done by keeping the TR short (Fig. 2.6). If TR is long the tissues with long T1 will also regain maximum LM giving stronger signal with next RF pulse. This will result in no significant difference between signal intensity of tissues with different T1. With short TR only the tissues with short T1 will show high signal intensity. On T1-W images, differences in signal intensity of tissues are due to their different T1.

T2 Weighted Image

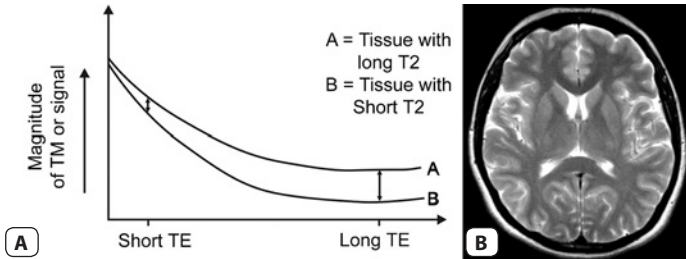
Immediately after its formation TM has greatest magnitude and produces strongest signal. Thereafter it starts decreasing in magnitude because of dephasing, gradually reducing the intensity of received signal. Different tissues, depending on their T2, have variable time for which TM will remain strong enough to induce useful signal in the receiver coil. Tissues or material with longer T2, such as water, will retain their signal for longer time. Tissues with short T2 will lose their signal earlier after RF pulse is turned off.

How does one make images T2 weighted?

The images are made T2-wighted by keeping the TE longer. At short TE, tissues with long as well as short T2 have strong signal. Therefore,



Figs 2.6A and B: T1-weighted image. (A) At short TR the difference between LM of tissue A (with short T1) and of tissue B (long T1) is more as compared to long TR. This results in more difference in signal intensity (contrast) between A and B at short TR. The contrast on the short TR image is because of T1 differences of tissues. Hence it is T1-weighted image. (B) T1-weighted axial image of brain: CSF is dark, white matter is brighter than gray matter and scalp fat is bright because of short T1



Figs 2.7A and B: T2-weighted image. (A) Tissue B has short T2 that results into early loss of magnitude of TM and reduction in signal. At short TE, there is no significant difference between magnitude of TM of A and B. At long TE, signal difference between A and B is more because tissue B will lose most of its signal while tissue A will still have good signal. Since the image contrast is because of differences in T2 of tissues, it is T2-weighted image. (B) T2-weighted axial image of brain: CSF is bright; white matter is darker than gray matter

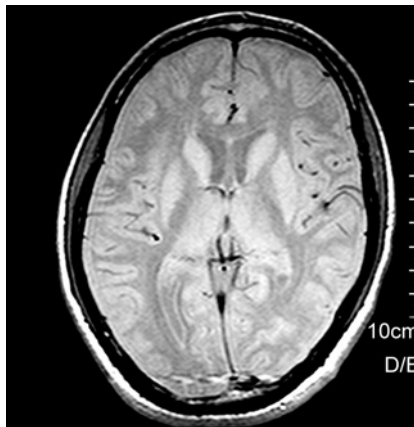


Fig. 2.8: Proton-density image. Long TR used for PD image eliminates T1 effects and short TE eliminates T2 effects

on the images acquired at short echo time, there will not be significant signal intensity difference between tissues with short and long T2. At longer TE, only those tissues with long T2 will have sufficiently strong signal and the signal difference between tissues with short and long T2 will be pronounced (Fig. 2.7). So the image with long TE is T2-weighted since the signal difference amongst tissues (contrast) is determined by T2 of tissues. Tissues with long T2 are bright on T2-weighted images. TR is kept long for T2-weighted images to eliminate T1 effects.

Proton Density (PD) Image

Contrast in the PD image is determined by the density of protons in the tissue. T1 effect is reduced by keeping long TR and T2 effect is reduced by keeping TE short. Hence long TR and short TE give PD-weighted image (Fig. 2.8). The signal intensity difference amongst tissues is function of the number of protons they have.

K-Space and Scanning Parameters

CHAPTER 3

This chapter discusses K-Space, image characteristics and various imaging parameters that can be altered by the scanning person in order to get desired images.

K-Space

K-Space is an imaginary space which represents a raw data matrix. It represents stage between reception of signals and image formation. After acquisition all signals are stored in K-Space in a particular fashion. This raw data from K-Space is used to reconstruct image by Fourier Transformation.

K-Space has two axes. Horizontal axis represents the phase axis and is centered in the middle of several horizontal lines. The frequency axis of K-Space is vertical and is perpendicular to the phase axis (Fig. 3.1).

Signals are filled in K-Space as horizontal lines. The number of lines of K-Space that are filled is determined by the number of different phase encoding steps. If 128 different phase encoding steps are selected then 128 lines of K-Space are filled to form an image. In conventional spin-echo imaging one line of K-Space is filled every TR. If matrix size is 128×128 then 128 TRs will be required to form an image.

Array of signals as lines in the K-Space does not correspond with rows or columns of pixel in the image. It is a complex transformation of this data into an image where center part of K-Space represents contrast of the image and the periphery corresponds with resolution and fine details.

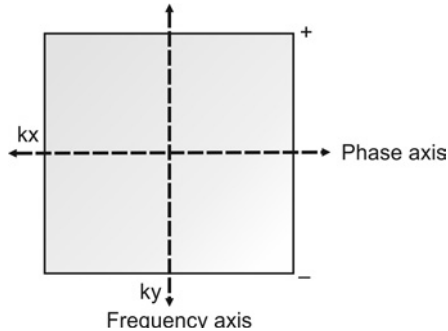


Fig. 3.1: K-Space

Two halves of K-Space—right and left or upper and lower—are exact symmetric conjugate and represent same information. This fact is used to manipulate K-Space sampling (partial sampling) to get same image in less time. In fast imaging like single-shot fast spin-echo sequence such as HASTE, just more than half of K-Space is filled. In ultrafast Echo Planar Imaging (EPI) all the K-Space lines required to form an image are filled within a single TR, thus reducing the scanning time in seconds.

Parameters of Scanning

- 1. Matrix:** A pixel (picture element) is the smallest unit of a digital image. Matrix consists of rows and columns of pixels (Fig. 3.2). Matrix of 256×256 means the image has 256 rows and 256 columns of pixels. Greater the size of the matrix better is the resolution. If the matrix is increased keeping the FOV same, pixel size will reduce. So smaller the pixel better is the resolution. An image acquired with matrix of 512×512 will have better resolution than the image acquired with matrix of 256×256 . However, increasing the matrix size increases the scanning time and reduces SNR. A pixel has two dimensions. If third dimension is added the smallest unit of the imaging data is called voxel (volume element). Voxel volume is determined by matrix size, FOV and slice thickness.
- 2. FOV (field of view):** It is the area from which information is obtained and represented on the image. It is selected as per requirement

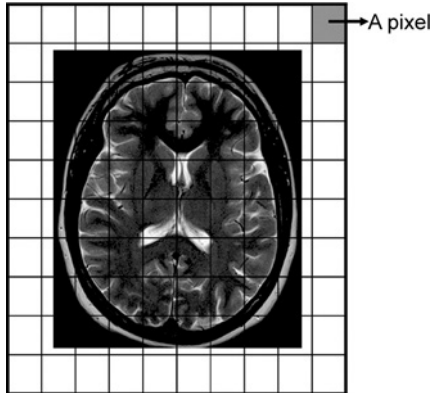


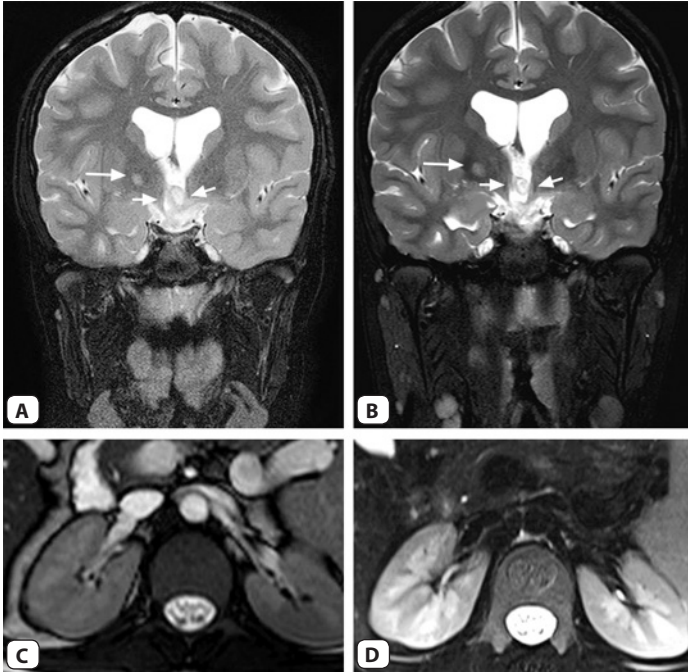
Fig. 3.2: Matrix and FOV schematic. The grid box outlined by thick line represents field of view (FOV). It is divided into multiple rows and columns of small squares (each representing a pixel). The whole grid represents matrix

of the part under examination by the technologist. It should be sufficient enough to cover the area of interest. Increasing FOV improves SNR but reduces resolution.

3. **Number of excitations (NEX)/ Number of signal averages (NSA):** It represents number of time the data is acquired to form the same image. More the number of averages better will be SNR but it increases the scan time.
4. **Flip angle:** It is the angle by which longitudinal magnetization vector is rotated away from Z-axis by a RF pulse. Shorter the flip angle less will be scanning time. Shorter flip angles are used in Gradient-Echo (GRE) sequences. Flip angle also determine the contrast in GRE sequences. T1-weighting of a GRE sequence increases with increasing flip angle. Flip angles are specific to the sequence and are not usually changed at the time of scanning.
5. **Bandwidth:** Bandwidth is the range of frequencies. Reducing receiver bandwidth of the receiver RF coil increases SNR. However, it also increases chemical shift and minimum TE that can be used.

Image Quality Determinants

Signal-to-noise ratio (SNR): It is the ratio of useful signal to unwanted signal (noise) in the image. It is one of the most important image quality determinants. An image with high SNR is less grainy and has more details (Fig. 3.3). Factors affecting SNR could be fixed or changeable.



Figs 3.3A to D: SNR and resolution. Coronal T2-w images acquired at 1.5T (A) and at 3T (B) in a patient with neurofibromatosis type 1 show a focus of abnormal signal intensity in right basal ganglion (large arrow) and optic glioma (small arrows). The image at 1.5T is grainier and has less detail suggestive of lower SNR as compared to image at 3T. Axial TruFISP (C) and Axial T2-w fat sat (D) images of the kidneys are shown. TruFISP image is crisp and less grainy as compared to T2-w image suggesting better SNR. Even though TruFISP has very good SNR it has less resolution than T2-w image as corticomedullary differentiation is better seen on the T2-w image

Fixed factors include magnetic field strength, pulse sequence design and tissue characteristic. Factors that can be changed include RF coil, voxel size, NSA, receiver bandwidth and slice cross talk. SNR improves with number of averages, FOV, surface and phased array coils.

Spatial resolution: Spatial resolution is the ability to discern two points as distinct and separate. Smaller the points that are seen separately better is the resolution. It improves with matrix size.

Contrast: Contrast in an image is the signal intensity difference between adjacent structures. More the contrast easier will be differentiation of the adjacent structures. Contrast in an image is determined by tissue-specific parameters, such as T1, T2, proton density, chemical environment, and macromolecules and hydration layers. Contrast-to-noise ratio (CNR) is the difference in SNR between adjacent structures.

Imaging time:

$$aT = TR \times N^* \times NEX$$

where aT = acquisition time

TR = Time to repeat

N^* = Number of pixels (matrix)

NEX = Number of excitations.

WHEN YOU SCAN.....

While scanning, the aim should be to get good quality images with reasonable SNR and spatial resolution in shorter time. Therefore three important determinants of image quality, which are balanced in the interplay of parameters, are SNR, spatial resolution and scanning time. Effect of various scanning parameters on these three determinants is shown in Table 3.1.

Table 3.1: Effect of imaging parameters on image quality determinants

Increasing parameters	Spatial resolution	SNR	Scanning time
FOV	↓	↑	↔
Slice thickness	↓	↑	↔
Matrix	↑	↓	↑
NSA (signal averages)	↔	↑	↑
Receiver bandwidth	↔	↓	↓
Keys: ↑ = increases; ↓ = decreases; ↔ = no change			

Magnetic Resonance Instrumentation

CHAPTER 4

In this chapter equipments required to acquire MR images are discussed. Basic four components make MR system.

1. The magnet to produce external magnetic field
2. Gradients to localize the signal
3. Transmitter and receiver coils for RF pulses
4. Computer system.

Magnetism

Magnetism is fundamental property of matter. All substances possess some form of magnetism. Degree of magnetism depends upon the magnetic susceptibility of the atoms that make the substance.

Magnetic susceptibility is the ability of the substance to get affected by external magnetic field and is related to electron configuration of the atom. Depending on the magnetic susceptibility, i.e. substance's response to magnetic field, substances can be paramagnetic, diamagnetic or ferromagnetic.

Paramagnetism

Paramagnetic substances have unpaired electrons within the atom. This result into a small magnetic field around them called magnetic moment. When external magnetic field is applied, these moments add together and align in the direction of external magnetic field. Thus paramagnetic substances affect external magnetic field in a positive

way by attraction towards the field resulting in a local increase in magnetic field. Examples of paramagnetic substances are gadolinium, oxygen, and melanin.

Diamagnetism

Diamagnetic substances react in an opposite way when external magnetic field is applied. They are repelled by the magnetic field. Thus diamagnetic substances have negative magnetic susceptibility and show slight decrease in magnetic field strength within the sample. Examples of diamagnetic substances include bismuth, mercury, copper, and carbon.

Ferromagnetism

Ferromagnetic substances get strongly attracted towards the externally applied magnetic field. Moreover, they retain their magnetism even when external magnetic field is removed. Such substances are used to make permanent magnet. The magnetic field in permanent magnet can be hundred or even thousands of times greater than applied external magnetic field. Examples of ferromagnetic substances are Iron, Cobalt and Nickel.

Magnetic Field Strength

Magnetic field is expressed by notation 'B', the primary field as B₀ and the secondary field as B₁. The units of magnetic field strength are Gauss and Tesla. Tesla was the father of alternating current and Gauss was German mathematician.

$$1 \text{ Tesla} = 10 \text{ k G} = 10,000 \text{ Gauss}$$

Gauss is a measure of low magnetic field strength. Earth's magnetic field strength is approximately 0.6 G.

MR systems used for clinical purpose have strength ranging from 0.2 to 3 Tesla. Field strengths higher than 3T are used for research purposes. SNR and resolution increase with the field strength. Advanced MR applications like Spectroscopy, functional MRI, cardiac MR are possible only on higher field strengths like 1.5 T and above.

Magnets

Three types of magnets are in use for clinical MRI machines.

1. Permanent magnet
2. Electromagnet
3. Superconducting magnet.

Permanent Magnet

Permanent magnet is made up of ferromagnetic substances. Usually MR magnets are made up of *alnico*, which is alloy of aluminium, nickel and cobalt.

Permanent magnets do not require power supply and are of low cost. The magnetic field of permanent magnet is directed vertically (Fig. 4.1). Open MRI is possible with permanent magnet, which are useful in claustrophobic patients. Magnetic field strength achievable with permanent magnet is low in the range, typically 0.2 to 0.5 Tesla. Hence they have low SNR and low resolution. Higher applications like spectroscopy cannot be performed on them.

Electromagnets

These are based on principle of electromagnetism. The law of electromagnetism states that moving electric charge induces

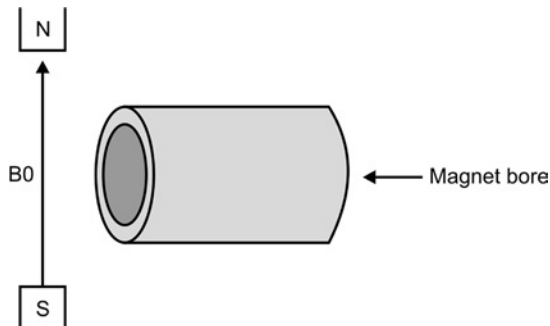


Fig. 4.1: Magnetic field: The magnetic field (B_0) of the permanent magnet is vertically directed perpendicular to the long axis of the bore

magnetic field around it. If a current is passed through a wire, a magnetic field is created around that wire. The strength of the resultant magnetic field is proportional to the amount of current moving through the wire.

When a wire is looped like a coil and current is passed through it, the magnetic field generated is directed along the long axis of the coil. Magnets made of such coils are called solenoid or resistive electromagnets.

All wires at normal temperature tend to resist the passage of current. As the resistance increases, current decreases with resultant reduction in field strength. To get a homogeneous field current must be steady and stable. The heat generated during this process is removed by running cooled water through tubes passing over the ends of the coil. The field strength obtained with electromagnets is limited to 0.2 to 0.3 Tesla because of continuous power and cooling requirements. Even though capital cost is low operational cost is high for electromagnets because enormous power requirement. However, electromagnets are easy to install and can readily be turned on and off inexpensively.

Superconducting Magnets

Some metals like mercury or Niobium-Titanium alloy lose their electric resistance at very low temperature and become superconductors. As discussed in the section on electromagnets, as resistance decreases current increases and as current increases magnetic field strength increases. Therefore in superconducting magnet higher field strength is achieved by completely eliminating the resistance to the flow of current. Moreover, once superconductor wires or coils are energized the current continues in the loop as long as the superconducting wire is maintained below the critical temperature. There is no power loss and continuous power supply is not required to maintain magnetic field. The structure of the superconducting magnet is shown in Fig. 4.2. Important components are as follows.

1. *Superconducting Wires:* Magnetic field is produced when current is passed through the superconducting wires. These wires are made up of Nb/Ti alloy. This alloy becomes superconducting at

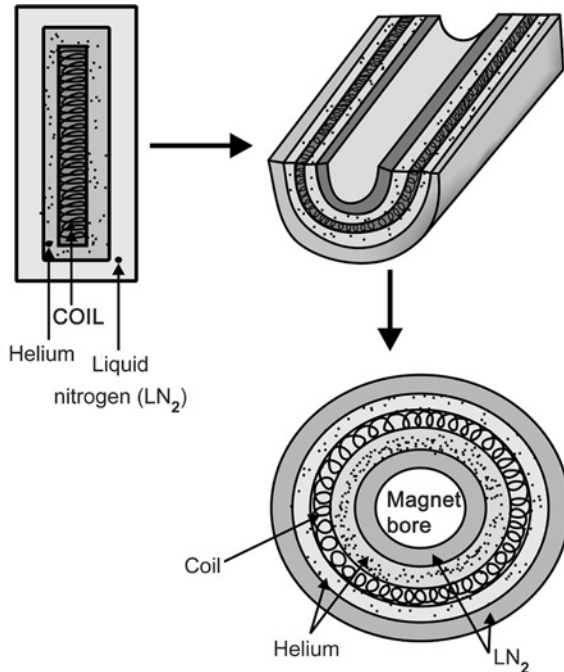


Fig. 4.2: The structure of the superconducting magnet

10K (kelvin). A wire containing filaments of Nb/Ti alloy embedded in a copper matrix, is wound tightly and precisely on insulated aluminium bore tube. It is fixed in place with a viscous, high thermal conductivity epoxy binder. The superconducting wire could be as long as 30 Kilometers. Hence there are thousands of turns of the wire. Since it is not possible to wound the coil with a single continuous strand, coil has several interconnecting joints.

2. *Helium*: The coil made of superconducting material is cooled to 4K (-269 degree Celsius) by *cryogen*s like liquid helium, which surrounds the coil all around. Because of smaller heat leaks into the system, helium steadily boils off. This boil off is reduced by much

cheaper liquid nitrogen. However, helium needs to be replenished on regular basis, usually every six months.

3. *Liquid Nitrogen and Radiation Shield*: The can of liquid helium is surrounded by cooled liquid nitrogen and radiation shields. This prevents any heat exchange between helium and the surrounding. Nitrogen boils at 80 degree K and is much cheaper than the helium. The liquid nitrogen and radiation shields reduce evaporation of liquid helium to approximately 0.3 liter per hour.

Starting the Magnet

When magnet is started first time, it is done in a particular way or sequence. First, superconducting coil is cooled to -269 degree Celsius by helium and liquid nitrogen. Then the magnet is energized by delivering current from external power source to the superconducting coil. This process is called *ramping*. Once desirable level of current is achieved, power supply is cut off. The current continues to circulate through the coil as long as the temperature is maintained below -269 degrees Celsius. The current and the magnetic field produced remain constant and subjected only to minor changes.

Quench

Quench is discharge or loss of magnetic field of the superconducting magnet. This occurs because of increased resistance in the superconducting coil, which results in heat formation. This heat in turn causes cryogenes to evaporate. This sets in a vicious cycle, which ultimately results in increased temperature, increased resistance, evaporation of all cryogenes and complete loss of magnetic field. Triggering factor for the increase in resistance could be minor motion of wire in the coil or flux jumping, which results in heat production.

Rarely quench can be deliberately performed to save patient's life. This is done in situations where patient accidentally gets trapped in the magnet by objects such as oxygen cylinder or wheel chair.

All MR systems should have a vent to allow the helium to escape outside in case quench occurs. Helium released inside the scan room can replace the oxygen completely and can cause asphyxia. It also produces

increased pressure in the scan room, which may prevent opening of the door. Every scan room should have oxygen monitor that will alarm if oxygen level falls below critical level.

To restart the magnet after quench, cryogenes are filled and wires are cooled to -269 degree Celsius. Then the ramping is done till desirable level of magnetic field is achieved.

Magnetic Field Homogeneity

Magnetic field should be uniform all over its extent to get correct information (signal) from the patient. Even though magnetic field is more or less uniform there might be minor inhomogeneity. The process of making the magnetic field homogeneous is called as "*shimming*". This process is necessary as the magnetic field is prone to become inhomogeneous because of the difficulty of winding a perfect coil and presence of metal within the environment.

Shimming can be active or passive. Passive shimming is done by keeping metal pieces, called shim plates, in the field to oppose the inhomogeneity.

Active shimming is done by passing current through the gradient coils, which generate small magnetic field gradients superimposed on main magnetic field (B_0). These coils are called shim coils. Shim coils make field homogeneous by adding or subtracting from the field at desired points. Shim coils can be resistive windings located within the room temperature compartment of the magnet bore or superconducting windings located within the helium vessel.

Homogeneity is expressed as parts per million (ppm). Homogeneity of 10 ppm may be sufficient for routine spin echo imaging. However, for proton spectroscopy a highly homogeneous field of 0.1 ppm is required to be able to detect metabolites with smaller chemical shift differences.

Shielding

The stray magnetic field outside the bore of the magnet is known as *fringe field*. This stray field can cross conventional walls, floors or ceilings and can potentially harmful to patients with pacemakers, for monitoring devices, and other magnetically activated devices

present nearby. Fringe field and its effects can be prevented by either passive shielding or active shielding.

Passive shielding is done by lining the wall of MR room by steel or copper. This shielded chamber is called as '*Faraday cage*'.

Active shielding uses additional solenoid magnet outside the cryogen bath that restricts the B_0 lines to an acceptable location. However, active shielding is an expensive alternative.

Gradients

Gradients or gradient coils are used to vary magnetic field strength over the extent of magnetic field. Gradient system consists of three sets of coils that produce field with changing strength in X, Y, Z directions. The three gradients applied along X, Y and Z axes are perpendicular to each other and are used for slice selection, phase encoding and frequency encoding. In a typical spin-echo imaging slice selection gradient is on for 3 ms, the phase encoding gradient for 4 ms and frequency encoding (readout) gradient for 8 ms.

How gradient coils are produced?

Magnetic field strength is proportional to the amount of current passed through the loop of wire, number of loops in wire, the size of the loop and how closely the loops are spaced. By changing these factors a coil can be produced, which increases or decreases magnetic field strength in particular direction.

Gradient strength (stiffness) is measured in units of G/cm or mT/m. This means that the magnetic field strength changes by one Gauss over each centimeter or 10 milliTesla over each meter. Stronger gradients (15 or 20 mT/m) allow high speed and high resolution imaging. Gradient strength has effect on slice thickness and FOV that can be used. For the same bandwidth, weaker gradient will produce thicker slice and stronger gradient will produce thinner slice and smaller FOV. The time taken by gradient to reach its maximum amplitude is called as *rise time*. The *slew rate* is the rate of rise obtained by dividing gradient amplitude by rise time and is measured in T/m/sec. *Duty cycle* is the time during which the gradient system can be run at maximum power.

Gradient coils are located coaxially in the room temperature compartment of the magnet bore. A problem associated with gradient system is generation of eddy current. Eddy current degrades the homogeneity of the magnetic field. It also causes heat production, which results in evaporation of cryogenes. Various methods are used to minimize the eddy current.

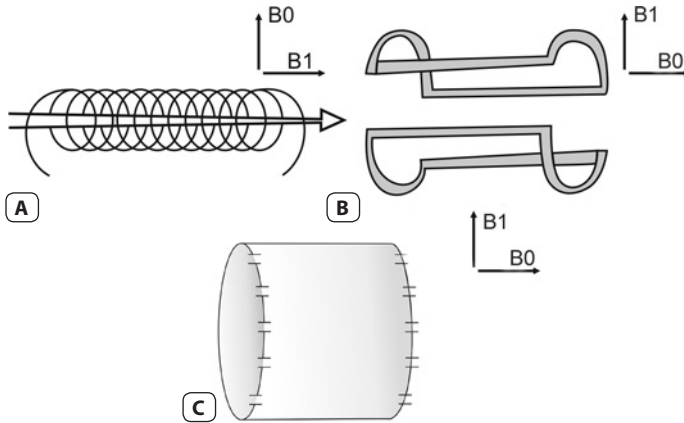
Apart from localization, gradients are also useful in the gradient echo sequences. Gradients are used for spoiling or rewinding transverse magnetization. Gradients are used to rephase the protons when they are going out of phase after RF pulse is switched off. Thus they eliminate 180 degree pulse and make the gradient echo sequences much faster.

Radiofrequency Coils

A loop of wire is a coil. Radiofrequency (RF) coils are used to transmit RF pulses into the patient and to receive the signals from the patient. RF coils can be transmitters, receivers or both (*transceivers*). Energy is transmitted in the form of short intense bursts of radiofrequencies known as radiofrequency pulses. These RF pulses cause phase coherence and flip some of the protons from a low energy states to high energy states. A RF pulse that causes net magnetization vector to flip away from longitudinal axis by 90 degree is called as 90 degree RF pulse. Rotating transverse magnetization (TM) induces current in the receiver coil, which forms the MR *signal*. Based on design RF coils can be divided as volume coil, surface coil and phased-array coil.

Volume coil

A volume coil typically surrounds either the whole body or a specific region. It provides a homogeneous B1 field (RF field perpendicular to main field B0) in the imaging volume circumscribed by the coil. However, the SNR of the images obtained with volume coil is usually less than that obtained with surface or phased-array coil. Body and Head coils are example of volume coils. The main coil of the magnet, also called the *body coil*, is a volume coil. It is located in the magnet bore as the inner most ring. Some configurations of the volume coil include solenoid, saddle and bird cage coils (Fig. 4.3).



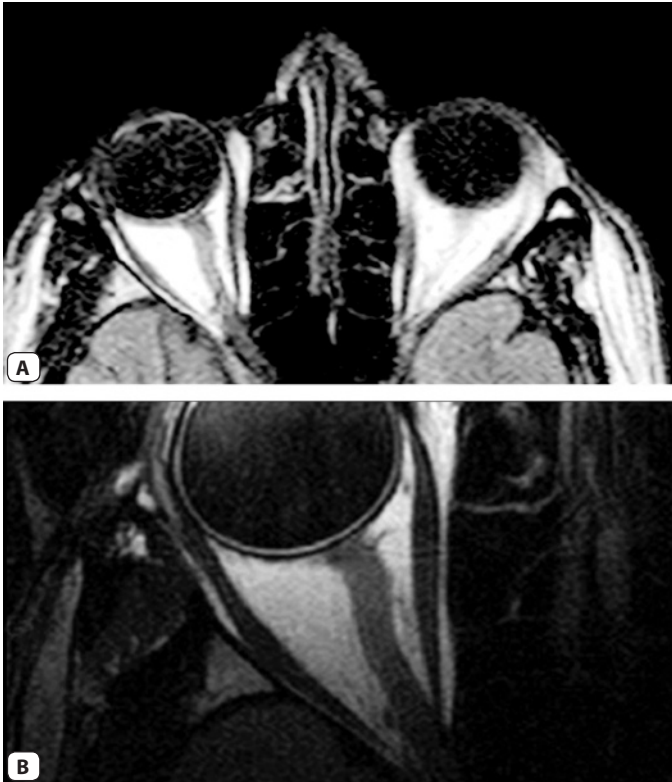
Figs 4.3A to C: (A) Solenoid coil, (B) Saddle coil and (C) Bird cage coil

Surface coil

A surface coil is placed on the surface of a region of interest to acquire images with very high SNR. High SNR is obtained at the cost of limited volume coverage and decreasing B_1 homogeneity with distance from the coil (Fig. 4.4). Surface coils are operated in receive-only mode, and RF transmission is performed separately, typically by a volume coil. Surface coils can be either flexible (can be wrapped around the region of interest) or rigid in design.

Phased-array (PA) coil

A phased-array coil consists of two or more geometrically aligned surface coils used in conjunction. This coil combines advantages of surface coil (high SNR) and volume coil (large FOV). The advantages of high SNR and resolution obtained from a PA coil may be traded off for reduced scan time by decreasing the number of signal averages. Depending on the number of surface coil elements PA coils are called 4, 6, 8 or 32 channel PA coils. The increasing number of elements allows faster dynamic scans with the consequent reduction of motion artifacts. The parallel imaging capability is another distinct advantage of PA coils.



Figs 4.4A and B: Surface versus volume coil. Note the increased resolution and detail in the image with orbit coil (B) as compared to the image with head coil (A) Also note decreased signal beyond the orbital apex in image B

Computers and Accessories

Computer system controls every application. They perform functions of data collection and manipulation, image viewing, storage, retrieval and documentation.

Sequences I: Basic Principles and Classification

CHAPTER 5

A pulse sequence is interplay of various parameters leading to a complex cascade of events with RF pulses and gradients to form a MR image (Fig. 5.1).

So pulse sequence is a time chart of interplay of—

1. Patient's net longitudinal magnetization
2. Transmission of RF pulses (90, 180 degree or any degree)
3. X, Y and Z gradient activation for localization and acquisition of signal (echo)
4. K-Space filling with acquired signals or echoes.

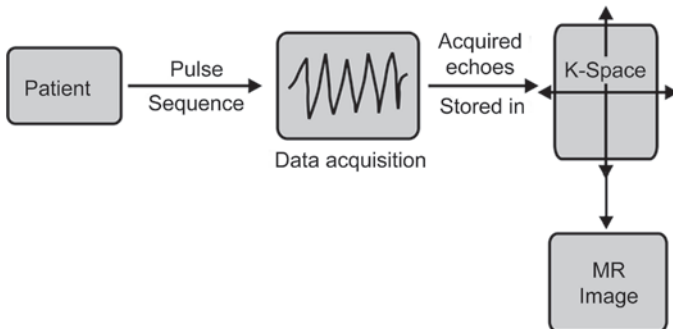


Fig. 5.1: Steps in image acquisition

In this chapter, basic designs and types of sequences will be discussed. Differences in contrast provided by sequences reflecting their clinical applications will be discussed in the chapter 7 on clinical applications of sequences.

Classification

Pulse sequences can be broadly divided into two categories- spin-echo and gradient echo sequences. Inversion recovery and echo planar imaging (EPI) can be applied theoretically to both spin-echo and gradient echo sequences. However, in practice inversion recovery is applied to spin-echo sequences and EPI is used with gradient echo sequences. For practical purposes, let's consider following four types of sequences:

1. Spin-echo sequence (SE)
2. Gradient Echo sequence (GRE)
3. Inversion Recovery sequences (IR)
4. Echo Planar Imaging (EPI).

Spin Echo (SE) Pulse Sequence

It consists of 90 and 180 degree RF pulses. The excitatory 90 degree pulse flips net magnetization vector along Z-axis into the transverse (X-Y) plane. The transverse magnetization (TM) precessing at Larmor frequency induces a small signal called free induction decay (FID) in the receiver coil. FID is weak and insufficient for image formation. Also, the amount of TM magnetization reduces as protons start dephasing. Hence a rephasing 180 degree pulse is sent to bring protons back into the phase. This rephasing increases magnitude of TM and a stronger signal (spin echo) is induced in the receiver coil. This gives the sequence its name. The time between two 90 degree pulses is called as TR (Time to Repeat). The time between 90 degree pulse and reception of echo (signal) is TE (Time to Echo) (Fig. 5.2).

For the localization of the signal, slice selection gradient is turned on when RF is sent. Phase encoding gradient is turned on between excitation (90 degree) pulse and signal measurement. Phase encoding gradient has different strength for each TR. Frequency encoding (read out gradient) is turned on during signal measurement.

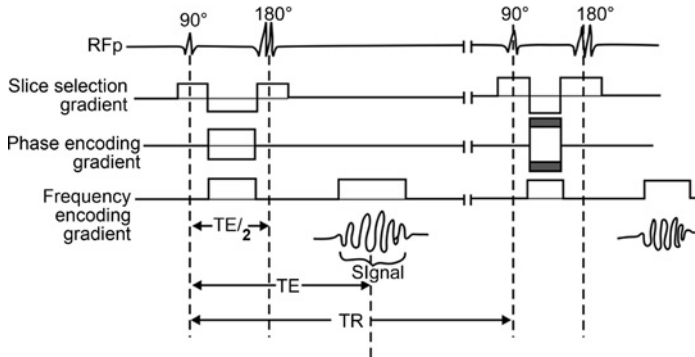


Fig. 5.2: Spin-echo (SE) sequence

SE sequence forms the basis for understanding all other sequences. It is used in almost all examinations. T1-weighted images are useful for demonstrating anatomy. Since the diseased tissues are generally more edematous and/or vascular, they appear bright on T2-weighted images. Therefore, T2-weighted images demonstrate pathology well.

Modifications of SE Sequences

In conventional SE sequence, one line of K-Space is filled per TR. SE sequence can be modified to have more than one echo (line of K-Space) per TR. This is done by sending more than one 180 pulses after the excitatory 90 degree pulse. Each 180 degree pulse obtains one echo. Three routinely used modifications in the SE sequence include dual SE (two 180 degree pulses per TR), fast SE (multiple 180 degree pulses per TR) and single-shot fast SE (fast SE with only half of the K-Space filled).

1. DUAL SPIN-ECHO Sequence

Two 180 degree pulses are sent after each 90 degree pulse to obtain two echoes per TR. The PD + T2 double echo sequence (Fig. 5.3) is an example of this modified SE sequence. This sequence is run with long TR. After the first 180 degree pulse, since TE is short, image will be proton density weighted (long TR, short TE). After second 180 degree pulse, TE will be long giving a T2-W image (long TR, long TE). Both these echoes contribute separate K-Space lines in two different K-Spaces.

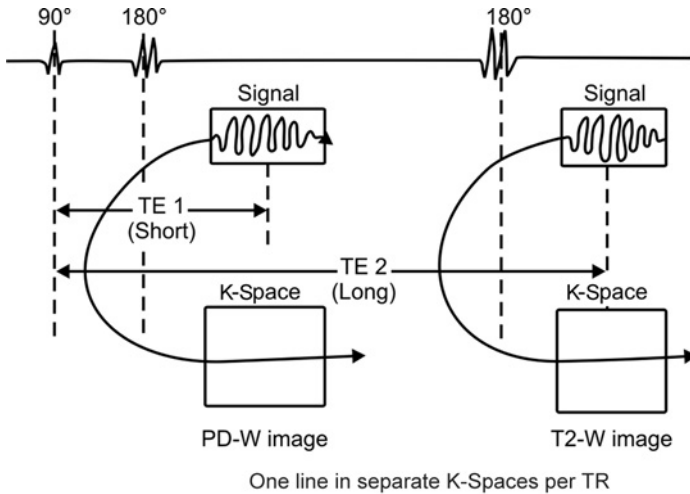


Fig. 5.3: Double Echo sequence

2. FAST (TURBO) SPIN-ECHO Sequence

In fast SE sequence, multiple 180 degree rephasing pulses are sent after each 90 degree pulse. It is also called as multi spin-echo or Turbo spin-echo sequence (Fig. 5.4). In this sequence, multiple echoes are obtained per TR, one echo with each 180 degree pulse. All echoes are used to fill a single K-Space. Since K-Space is filled much faster with multiple echoes in a single TR the scanning speed increases considerably.

Turbo factor: turbo factor is the number of 180 degree pulses sent after each 90 degree pulse. It is also called as **echo train length**. The amplitude of signal (echo) generated from the multiple refocusing 180 degree pulses varies since the TE goes on increasing. The TE at which the center of the K-Space is filled is called as '*TE effective*'. The amplitude of the signal is maximum at the TE effective. Short turbo factor decreases effective TE and increases T1 weighting. However, it increases scan time. Long turbo factor increases effective TE, increases T2 weighting and reduces scan time. Image blurring increases with turbo factor because more number of echoes obtained at different TE form the same image.

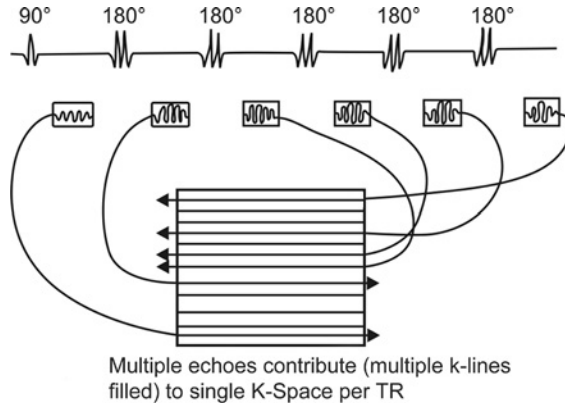


Fig. 5.4: Fast/Turbo spin echo sequence

When a negative 90 degree pulse is sent at the end of the echo train, the magnetization for tissues with high T2 flips quickly back in the longitudinal plane at the end of each TR. This makes fast SE sequences even faster. The fast SE sequences using this 90 degree flip-back pulse at the end of each TR are called fast recovery (FRFSE, GE), driven equilibrium (DRIVE, Philips) or RESTORE (Siemens) sequences.

3. SINGLE-SHOT FAST SPIN-ECHO Sequence

This is a fast SE sequence in which all the echoes required to form an image are acquired in a single TR. Hence it is called 'single-shot' sequence. In this sequence, not only all K-Space lines are acquired in a single excitation but also just over a half of the K-Space is filled reducing the scan time further by half (Fig. 5.5). The other half of the K-Space is mathematically calculated with half-Fourier transformation. Thus, for example, to acquire an image with matrix of 128 x 128 it is sufficient to acquire only 72 K-Space lines. This number can be further reduced by use of parallel imaging, greatly reducing blurring.

Gradient Echo (GRE) Sequence

There are basic three differences between SE and GRE sequences.

1. There is no 180 degree pulse in GRE. Rephasing of TM in GRE is done by gradients; particularly by reversal of the frequency encoding

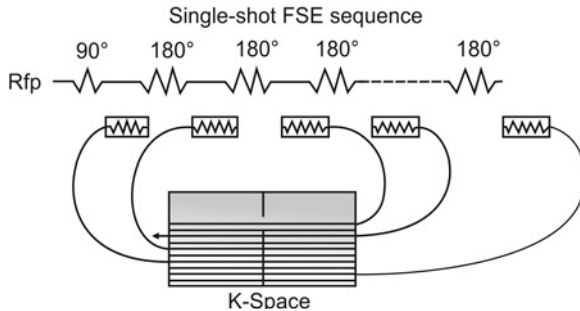


Fig. 5.5: Single-shot fast spin-echo sequence

gradient. Since rephasing by gradient gives signal this sequence is called as Gradient echo sequence.

2. The flip angle in GRE is smaller, usually less than 90 degree. Since flip angle is smaller there will be early recovery of longitudinal magnetization (LM) such that TR can be reduced, hence the scanning time.
3. Transverse relaxation can be caused by combination of two mechanisms—
 - A. Irreversible dephasing of TM resulting from nuclear, molecular and macromolecular magnetic interactions with proton.
 - B. Dephasing caused by magnetic field inhomogeneity.

In SE sequence, the dephasing caused by magnetic field inhomogeneity is eliminated by 180 degree pulse. Hence there is 'true' transverse relaxation in SE sequence. In GRE sequence, dephasing effects of magnetic field inhomogeneity are not compensated, as there is no 180 degree pulse. T₂ relaxation in GRE is called as T₂^{*} (T₂ star) relaxation.

$$1/T_2^* = 1/T_2 + 1/\text{relaxation by inhomogeneity}$$

Usually $T_2^* < T_2$.

So the basic GRE sequence is as shown in the diagram (Fig. 5.6).

Types of GRE Sequences

GRE sequences can be divided into two types depending on what is done with the residual transverse magnetization (TM) after reception of the signal in each TR. If the residual TM is destroyed by RF pulse or

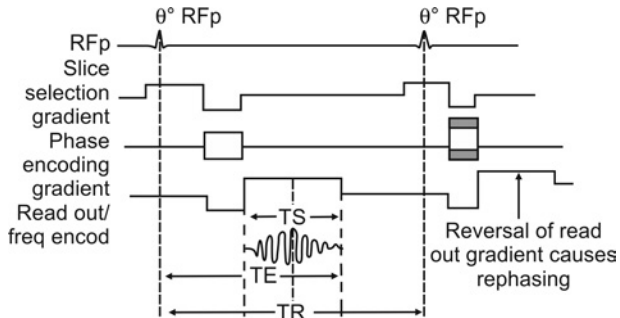


Fig. 5.6: Gradient Echo sequence (GRE). Reversal of frequency encoding gradient (instead of 180 degree pulse) causes rephasing of protons after RFp is switched off. TS = time to signal

gradient such that it will not interfere with next TR, the sequences are called spoiled or incoherent GRE sequences. In the second type of the GRE sequences, the residual TM is not destroyed. In fact, it is refocused such that after a few TRs steady magnitude of LM and TM is reached. These sequences are called steady-state or coherent GRE sequences.

SPOILED/INCOHERENT GRE Sequences

These sequences usually provide T1-weighted GRE images (FLASH/SPGR/T1-FFE). These sequences can be acquired with echo times when water and fat protons are in-phase and out-of-phase with each other. This 'in- and out-of-phase imaging' is used to detect fat in the lesion or organs and is discussed in chapters 6 and 7. Spoiled GRE sequences are modified to have time-of-flight MR Angiographic sequences. The 3D versions of these sequences can be used for dynamic multiphase post contrast T1-weighted imaging. Examples include 3D FLASH and VIBE (Siemens), LAVA and FAME (GE), and THRIVE (Philips).

STEADY STATE (SS) Sequences

When residual transverse magnetization is refocused keeping TR shorter than T2 of the tissues, a steady magnitude of LM and TM is established after a few TRs. Once the steady state is reached, two signals are produced in each TR: FID (S+) and spine-echo (S-). Depending

on what signal is used to form the images, SS sequences are divided into 3 types.

1. *Post-excitation refocused steady-state sequences.*
Only FID (S+) component is sampled. Since S+ echo is formed after RF excitation (pulse), it is called post-excitation refocused.
e.g. FISP/GRASS/FFE/FAST.
 2. *Pre-excitation refocused steady-state sequences.*
Only spin echo (S-) component is used for image formation. S- echo is formed just before next excitation hence the name pre-excitation refocused.
e.g. PSIF (reversed FISP)/SSFP/T2-FFE/CE-FAST.
 3. *Fully refocused steady-state sequences.*
Both FID (S+) and Spin echo (S-) components are used for the image formation. These are also called 'balanced-SSFP' sequences as gradients in all three axes are balanced making them motion insensitive.
e.g. True FISP/FIESTA/Balanced FFE
- SS sequences have very short TR and TE making them fast sequences that can be acquired with breath-hold. They can be used to study rapid physiologic processes (e.g. events during a cardiac cycle) because of their speed. Balanced-SSFP sequences have highest possible SNR among all MR sequences and show tissues or structures with high T2 (e.g. fluid) more bright than usual T2-weighted images. However, they lack internal spatial resolution and do not demonstrate gray-white differentiation in the brain or corticomedullary differentiation in the kidneys.

Inversion Recovery (IR) Sequence

IR sequence consists of an inverting 180 degree pulse before the usual spin-echo or gradient echo sequence. In practice, it is commonly used with SE sequences (Fig. 5.7).

The inverting 180 degree pulse flips LM from positive side of Z-axis to negative side of Z-axis. This saturates all the tissues. LM then gradually recovers and builds back along positive side of Z-axis. This LM recovery is different for different tissues depending on their T1 values. Protons in fat recover faster than the protons in water. After a certain time, the usual sequence of 90-180 degree pulses is applied. Tissues will have

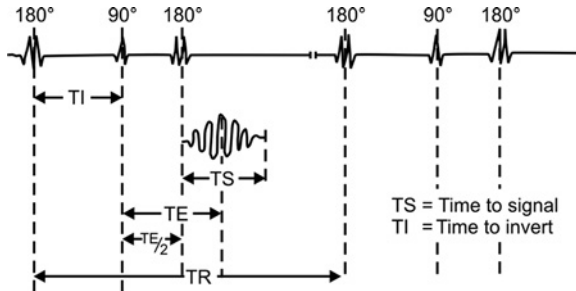


Fig. 5.7: Inversion recovery (IR) sequence

different degree of LM recovery depending on their T_1 values. This is reflected in increased T_1 contrast in the images.

The time between inversion 180 degree and excitatory 90 degree pulses is called as 'time to invert or T_I '. T_I is the main determinant of contrast in IR sequences.

Why is the inverting 180 degree pulse used? What is achieved?

The inversion 180 degree pulse flips LM along negative side of the Z-axis. This saturates fat and water completely at the beginning. When 90 degree excitatory pulse is applied after LM has relaxed through the transverse plane, contrast in the image depends on the amount of longitudinal recovery of the tissues with different T_1 . An IR image is more heavily T_1 -weighted with large contrast difference between fat and water. Apart from getting heavily T_1 -weighted images to demonstrate anatomy, IR sequence also used to suppress particular tissue using different T_I .

Tissue Suppression

At the halfway stage during recovery after 180 degree inversion pulse, the magnetization will be at zero level with no LM available to flip into the transverse plane. At this stage, if the excitatory 90 degree pulse is applied, TM will not be formed and no signal will be received. If the T_I corresponds with the time a particular tissue takes to recover till halfway stage there will not be any signal from that tissue. IR sequences are thus used to suppress certain tissues by using different T_I . The T_I

42 MRI Made Easy (For Beginners)

required to null the signal from a tissue is 0.69 times T1 relaxation time of that tissue.

Types of IR Sequences

IR sequences are divided based on the value of T1 used. IR sequences can be of short, medium or long T1.

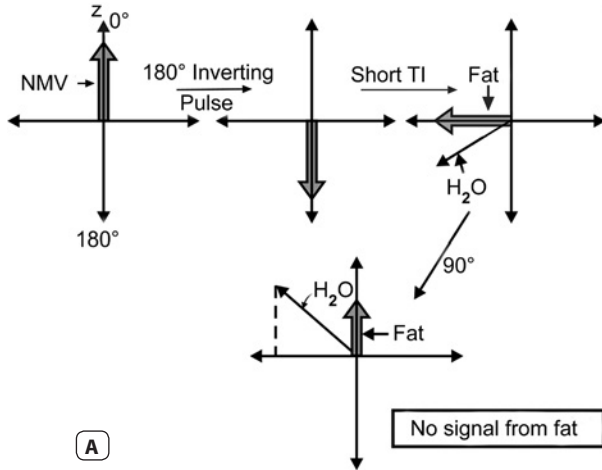
Short T1 IR sequences use T1 in the range of 80-150 ms and example is STIR. In Medium T1 IR sequences, T1 ranges from 300 to 1200 ms, and example is MPRAGE (Siemens). Long T1 ranges from 1500 to 2500 ms and example is FLAIR.

SHORT T1 (tau) IR Sequence (STIR)

When 90 degree pulse is applied at short T1, LM for all or virtually all tissues is still on negative side. The tissues with short T1 have near zero magnetization, so don't have much signal. Most pathologic tissues have increased T1 as well as T2. Moderately high TE used in STIR allows tissues with high T2 to retain signals while tissues with short T2 will have reduced signal. This results in increased contrast between tissues with short T1-T2 and tissues with long T1-T2. In short T1 IR sequences fat is suppressed since fat has short T1 (Fig. 5.8). Most pathology appear bright on STIR making them easier to pick up.

Table 5.1: STIR versus FLAIR

STIR	Vs	FLAIR
Short T1 of 80-150 ms used.	1.	Long T1 of 1500-2500 ms is used
Combined T1 and T2 weighting is obtained	2.	Heavily T2 weighted images are obtained
Fat and white matter are suppressed	3.	CSF and water is suppressed
Mainly used in body imaging	4.	Used in neuroimaging
Cannot be used in postcontrast imaging as short T1 tissue are suppressed and contrast shortens T1 of tissues that uptake the contrast	5.	Can be used in postcontrast imaging



Figs 5.8A and B: STIR sequence. (A) When excitatory 90° pulse is applied after a short TI the magnetization vector of fat reaches zero degrees (along positive side of Z-axis). As the signal cannot be detected when the vector is vertical along Z-axis, there is no signal from fat and fat is saturated. (B) STIR coronal image of the pelvis: note there is suppression of subcutaneous fat

LONG TI IR Sequence

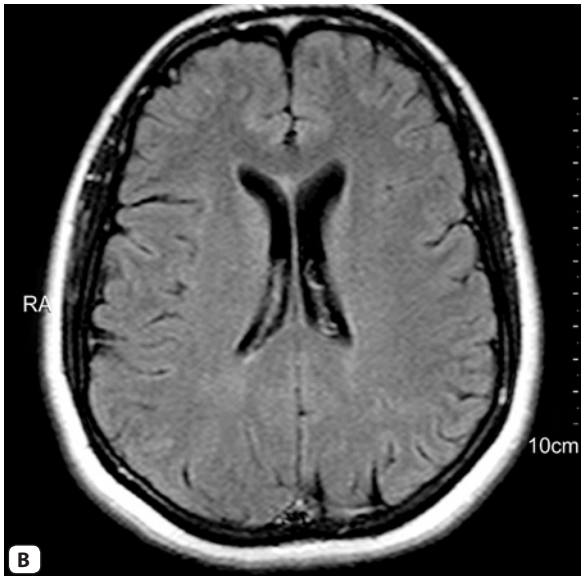
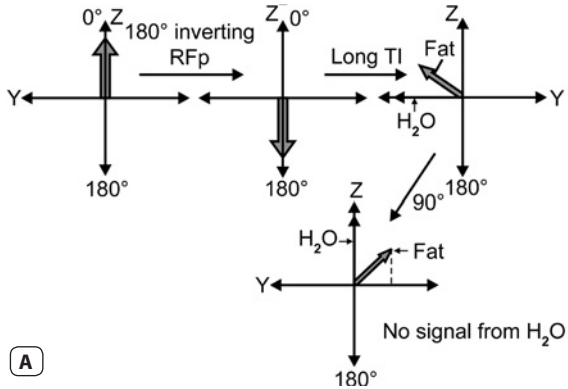
When 90 degree pulse is applied at long TI, LM of most tissues is almost fully recovered. Since water has long T1, its LM recovery is at halfway stage at long TI. This results in no signal from fluid such as CSF. The sequence is called fluid-attenuated inversion recovery sequences (**FLAIR**). In FLAIR, long TE can be used to get heavily T2-weighted without problems from CSF partial volume effects and artifacts as it is nulled (Fig. 5.9). As in STIR, most of the pathologies appear bright on FLAIR.

Echo Planar Imaging (EPI)

Scanning time can be reduced by filling multiple lines of K-Space in a single TR. EPI takes this concept to the extreme. All the lines of K-Space, required to form an image, are filled in a single TR. Since entire 2D raw data set (i.e. a plane of data or echo) could be filled in single echo decay, the term 'Echo Planar Imaging' was given to this technique by Sir Peter Mansfield in 1977.

Multiple echoes generated in single TR in EPI are phase encoded by different slopes of gradient. These multiple echoes are either generated by 180 degree rephasing pulses or by gradient. Therefore, EPI can be Spin Echo EPI (SE-EPI) or Gradient echo EPI (GRE-EPI). However, in SE-EPI multiple 180 degree RF pulses cause excessive energy deposition in patient tissues and long train of 180 degree pulses would take so long time that most of the signal would be lost before satisfactory data could be acquired. Hence SE-EPI is not routinely used. In GRE-EPI, rephasing is done by rapidly switching read out and phase encoding gradients on and off. This requires gradient strength higher than 20 mT/m.

GRE-EPI is very sensitive to susceptibility artifacts because T2* decay is not compensated in GRE sequences. Signal-to-noise ratio (SNR) is poor in single shot EPI. These problems can be overcome to certain extent by the hybrid sequence. Hybrid sequence combines advantages of gradient (speed) and RF pulses (compensation of T2* effects). SNR can be improved by use of multi-shot EPI. In multi-shot EPI, only a portion of K-Space is filled in each TR. Multi-shot EPI improves SNR and spatial resolution, and gives better PD and T1-weighting at the cost of slight increase in time.



Figs 5.9A and B: FLAIR sequence. (A) Magnetization vector of water reaches zero degree when 90° pulse is applied after a long TI. Hence no signal is received from water and it is nulled. (B) FLAIR axial image of brain: CSF is suppressed and is dark. Note scalp fat is not suppressed and is bright

EPI has revolutionized MR imaging with its speed. EPI has potential for interventional and real time MRI. Presently it is used in diffusion imaging, perfusion imaging, functional imaging with BOLD, cardiac imaging and abdominal imaging.

Table 5.2: Summary of Sequences

	Sequences	Siemens*	GE *	Philips*
1.	Spin Echo sequences			
	Conventional SE (90°-180° RF pulses)	SE	SE	SE
	Double SE (90° followed by two 180° RF pulses)	PD/T2	PD/T2	PD/T2
	Multi SE (90° followed by multiple 180° RF pulses)	Turbo SE	Fast SE	Turbo SE
	Multi SE with flip-back 90° pulse	RESTORE	FRFSE	DRIVE
	Single-shot Multi SE (Multi SE with half K-Space filling)	HASTE	Single Shot FSE	Ultrafast SE
	Radial K-Space filling	BLADE	PROPELLER	MultiVane
2.	Gradient Echo Sequences			
	A. Incoherent spoiled TM	FLASH	SPGR	T1-FFE
	3D versions	3D FLASH VIBE	LAVA FAME	THRIVE
	B. Coherent/Rephased TM			
	1. Post-excitation refocused (FID sampled)	FISP	GRASS	FFE
	2. Pre-excitation refocused (Spin echo sampled)	PSIF	SSFP	T2-FFE
	3. Fully refocused (both FID & spin echo sampled)	True FISP	FIESTA	Balanced FFE
3.	Inversion Recovery Sequences Short TI (80-150 ms) e.g. STIR Medium TI (300-1200 ms) e.g. MPRAGE Long TI (1500-2500 ms) e.g. FLAIR			
4.	Hybrid Combination of SE and GRE	TGSE	GRASE	GRASE
5.	EPI Single shot Multishot-segmented			
*Vendor nomenclatures for sequences are taken from References—1. Nitz WR. MR Imaging: Acronyms and clinical applications. Eur Radiol. 1999; 9:979-997. and 2. Brown MA, Semelka RC. MR Imaging Abbreviations, Definitions, and Descriptions: A Review. Radiology 1999; 213:647-662.				

Sequences II: Accessory Techniques

CHAPTER 6

In this chapter some accessory techniques or concepts used in combination with the sequences will be discussed. These techniques include fat suppression, parallel imaging, motion compensation techniques, magnetization transfer, key-hole imaging and saturation bands.

Fat Suppression

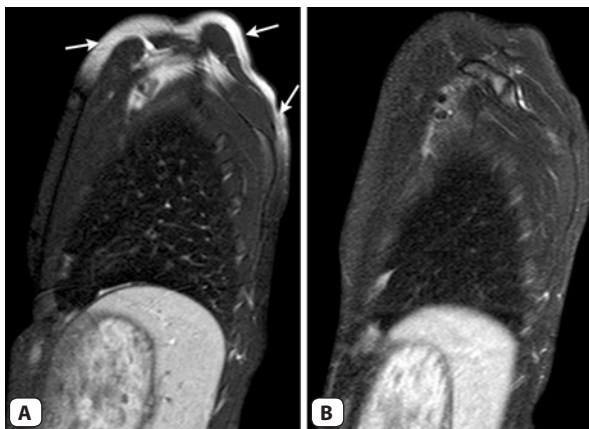
Fat suppression, i.e. nulling signal from the adipose tissues, is used to differentiate other short T1 tissues (e.g. enhancing lesion) from fat in any lesion or structure, to detect presence of fat in any lesion or organ, and to minimize the deleterious effects of fat such as reducing artifacts. There are 5 basic techniques of fat suppression including 1. Frequency-selective fat suppression, 2. STIR, 3. Out-phase imaging, 4. Dixon method and 5. Selective water excitation. The first three methods are compared in Table 6.1 and illustrated in Figs 6.1-6.3.

1. Frequency-selective fat suppression:

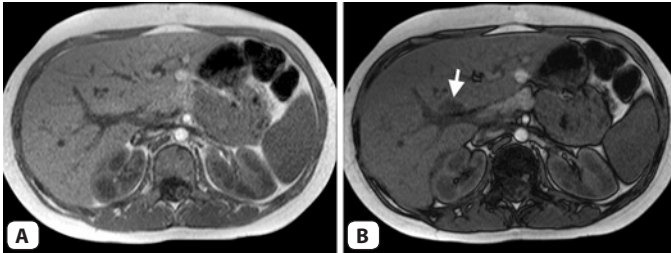
In this method, a frequency-selective RF pulse with same resonance frequency as lipids is applied to each slice-selection RF pulse. This is followed by homogeneity spoiling gradient pulse to dephase the lipid signal. The signal received after subsequent slice-selection pulse contains no lipid signals. In general, the technique is called CHESS (chemical shift selective) and can be used to suppress or selectively excite fat or water protons. A fat-selective CHESS RF pulse can be used as a preparation pulse. After a delay, proper



Figs 6.1A and B: Fat saturation versus non-fat saturation T1-w imaging. T1-w sagittal images of the leg acquired after intravenous contrast administration, without (A) and with (B) fat saturation, show an enhancing linear lesion (arrows). On the fat saturated image (B), the lesion is easily and well appreciated



Figs 6.2A and B: Frequency-selective fat saturation versus STIR. Sagittal T2-w fat suppressed (A) and STIR (B) images of the chest do not show any abnormality. There is inhomogeneous and incomplete fat suppression on the T2-w image (arrows on A). The STIR image shows homogeneous fat suppression



Figs 6.3A and B: In and out-of-phase imaging. Axial T1-w GRE images of the liver in in-phase (A) and out-of-phase (B) show a focal area of fatty infiltration (arrow on out-of-phase). The fatty area is only seen on the out-of-phase image as it turns dark as compared to surrounding liver parenchyma

sequence is run that does not have signal from the fat. Versions of this preparation pulse include FAT SAT, SPECIAL (spectral inversion at lipid), SPIR (spectral presaturation with inversion recovery) and SPAIR (spectral attenuated inversion recovery).

2. Short tau inversion recovery (STIR):

Principle of inversion recovery and how fat gets suppressed in STIR sequence is discussed in chapter 5.

3. Out-of-phase Imaging:

Protons in a water environment precess faster than protons in fat environment. This difference in precessional frequency of protons in water and fat environment is called *chemical shift*. Because of this differential precessional frequency they are in-phase at certain echo time (TE) and they are in opposite phase (180 degrees to each other) at the certain TE. At 1.5 Tesla, fat and water protons are in phase at TE of 4.45 ms, 8.9 ms and so on while they are out-of-phase at TE of 2.23 ms, 6.69 ms and so on. The images acquired at in-phase TE will have signal from water and fat protons added together while images at out-of-phase will be have signal from water and fat protons subtracted. On out-of-phase images, the fat containing lesions or structures will appear darker as compared to in-phase images. On out-of-phase imaging; the fat will appear darker only if it is present in a voxel that contains both fat and water. Voxels containing only water or only fat will not change in signal

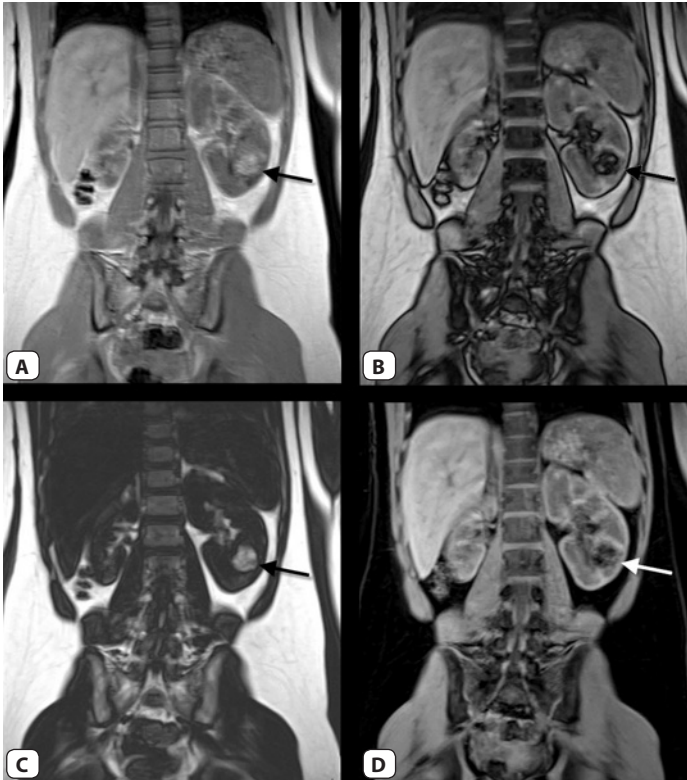
Table 6.1: Fat suppression techniques

Frequency-Selective	STIR	Out-of-phase Imaging
1. Only adipose tissue is suppressed	1. Suppresses whole adipose tissue including water and fat fractions within it. Also suppresses tissues with short T1 like mucoid, gadolinium, melanin and some proteinaceous material.	1. Best suited for suppression of tissues with similar amount of water and fat or microscopic fat.
2. Small amount of fat may not be detectable	---	2. Good for detection of small amount of fat.
3. Affected by inhomogeneity (causes inhomogeneous fat suppression)	3. Insensitive to field inhomogeneity	3. Usually unaffected by static field inhomogeneity
4. SNR of adipose tissue is reduced but overall SNR is maintained	4. Overall SNR is poor as compared to other methods	4. SNR is maintained
5. Generally good for post-contrast T1-w images and T2-w images with short FOV	5. Good for large FOV images, low field-strength. Cannot be used post contrast.	5. Generally used for detection of small amount of fat such as in liver lesions or adrenal adenomas and also for detection of fatty liver.

on in and out-of-phase imaging. Hence subcutaneous fat does not become darker on out-of-phase images.

4. Dixon method:

This is based on in and out-of-phase imaging. In this method, two sets of images are acquired, one at in-phase TE and other at out-of-phase TE. Addition of these two sets of images gives 'water-only' image while subtraction gives 'fat-only' image (Fig. 6.4). Dixon method can be very effective in areas of high magnetic susceptibility but requires good homogeneity of magnetic field.



Figs 6.4A to D: Dixon method. Coronal images of the abdomen show a fatty lesion in the lower pole of the kidney (arrow) in keeping with angiomyolipoma. Four sets of images are available with Dixon method in a single acquisition including in-phase (A), out-of-phase (B), fat-only (C), and water-only (D) images

5. Water selective excitation:

Combination of series of short RF pulses can be used to excite only water protons. Fat protons are not excited and are left in equilibrium hence do not produce any signal on the water selective excitation images. This method is susceptible to field inhomogeneity. Examples include ProSet and WATS.

Parallel Imaging

It is a technique that takes advantage of the spatial information inherent in phased-array RF coils to reduce scan time. Multiple coil elements in the phased-array coil receive signal simultaneously from the area they are covering. The information from each coil element is then combined to get a single large FOV and image. The acquisition time of any sequence is proportional to the number of phase encoding lines in K-Space. In parallel imaging, a significantly shortened scan time is possible by reducing the number of K-Space lines sampled (typically by a factor of 2 or more). This under sampling of K-Space maintains spatial resolution but reduces the field of view (FOV), thereby producing aliasing, or wrap-around artifacts. This aliasing is corrected by reconstruction algorithms that use spatial information from individual elements of the phased-array coil.

SNR in parallel imaging is always less compared to an unaccelerated study obtained with the same coil array. However, within constraints of available SNR, parallel imaging improves speed (by factors of 1.5 to 3), spatial and temporal resolution, and overall image quality. Instead of decreasing the acquisition time, the reduced speed can be used to improve spatial resolution in the same amount of time. The image blur in fast spin-echo (SE) and single shot fast SE sequences can be improved by reducing echo train lengths. Susceptibility artifacts seen in diffusion weighted imaging can be reduced significantly by use of parallel imaging.

Coil sensitivity calibration is a fast low resolution acquisition (typically a gradient echo sequence) that generates spatial information based on the different physical locations of the independent coil elements (four to 32 elements). This spatial sensitivity is subsequently used during image reconstruction in parallel imaging techniques including sensitivity encoding (SENSE, Philips). Other parallel imaging techniques include array spatial sensitivity encoding technique (ASSET, GE), Integrated parallel acquisition technique (iPAT, Siemens), Generalized autocalibrating partially parallel acquisition (GRAPPA, Siemens) and simultaneous acquisition of spatial harmonics (SMASH).

Apart from reduced SNR with higher acceleration factors (called as iPAT factor or SENSE factor), limitations of parallel imaging include

artifacts such as uncorrected aliasing, central aliasing, ghosting and area of low SNR in the center of FOV.

Respiratory Compensation Techniques

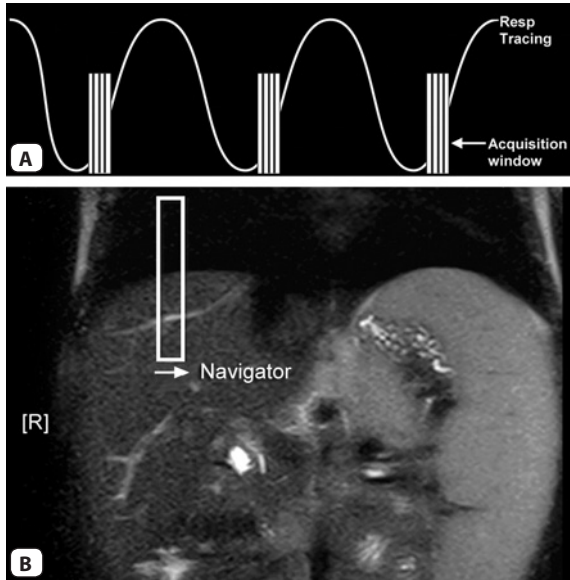
Respiratory motion compensation can be done by: 1. respiratory gating in which the image data is acquired during a particular portion of the respiratory cycle or 2. respiratory ordered phase encoding (ROPE) in which the K-Space is filled in a particular way.

Respiratory gating can be performed in two ways (Fig. 6.5). In the first method, respiratory tracings are obtained by tying a *bellows* around the chest. Images are acquired in a designated phase of respiration with each respiratory cycle. The second method for respiratory triggering is *navigator technique*. In this technique, the position of the diaphragm is detected by a navigator pre-pulse and signal acquisition is prospectively or retrospectively gated to the most stable portion of the respiratory cycle, typically end-expiration.

In ROPE also respiratory tracings are obtained either by tying a bellows or by navigator pre-pulse. However, the image data is acquired at regular times independent of the respiratory cycle. The central portion of K-Space is then filled with the echoes with minimal inspiration and expiration while peripheral portion is filled with echoes where expiration was greatest. Center of K-Space is responsible for SNR and is filled with shallow phase encoding gradient slope. Shallow slope of phase encoding gradient results in good signal amplitude. When gradient slope is shallow the phase shift caused by movement is less resulting in less ghosting. Periphery of K-Space is filled with steep slope of phase encoding gradient when movement is the maximum (Fig. 6.6).

Gradient Moment Rephasing (GMR)

Flow in the vessels can cause additional phase shift and artifacts in the image. When gradients are applied the additional phase shift caused by the flow is called gradient moment. Gradient moment caused by constant velocity is called first-order gradient moment; by acceleration, a second-order; and moment by change in the acceleration, a



Figs 6.5A and B: Respiratory compensation techniques. (A) Respiratory gating with tracings obtained by tying a bellows. (B) Navigator (white rectangle) is placed over the diaphragm to track its position. Images are acquired during most stable phase of the respiration

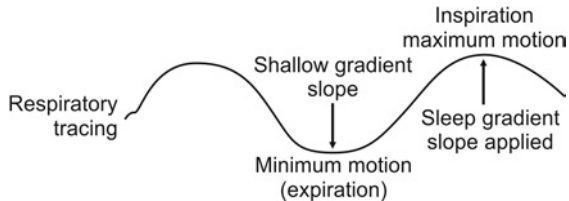


Fig. 6.6: Respiratory ordered phase encoding (ROPE)

third-order gradient moment. GMR is a technique in which additional gradient pulses are applied to eliminate phase shift produced by moving protons. GMR reduces flow artifacts from vessel and CSF pulsations.

Magnetization Transfer

Magnetization transfer (MT) is a technique which selectively alters tissue contrast on the basis of micromolecular environment. Tissues normally have three pools of hydrogen protons that are responsible for MR signals. These are—

1. Free water protons
2. Bound or restricted water protons in macromolecules
3. Hydration layer water protons adjacent to macromolecules.

In routine imaging protons from free water pool are responsible for most of MR signals in an image because of their long longitudinal relaxation time (T_2). Protons from other two pools have very short T_2 , hence contribute little to MR signal.

Range of resonance frequency or spectral bandwidth of free pool is narrow while restricted pool has wide spectral bandwidth.

Restricted pool can be saturated by applying RF pulse at anywhere its spectral width. Once saturated, protons of restricted pool exchange their magnetization with protons of free pool via hydration layer protons. This occurs through a process called ‘dipolar coupling’. This results into reduction of T_2 of restricted pool or macromolecules and reduction in their signal intensity. The increase in image contrast thus achieved is called MT contrast (MTC). Amount of signal loss on MT images reflect amount of macromolecules in given tissue.

MT pulse is applied as off resonant RF pulse to water peak. It is usually applied as a presaturation pulse, at +1000Hz, opposite side of fat saturation pulse (at -220Hz) (Fig. 6.7).

Applications of MTC:

1. Contrast enhanced MRI—MT suppresses background tissue signals while affecting negligibly to enhancing lesion or structure. Thus improves visualization of the lesion (Fig. 6.8).

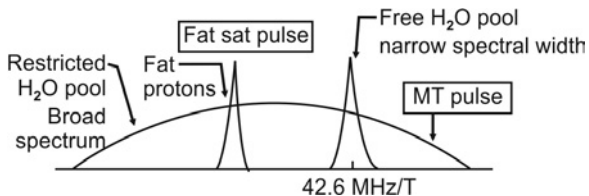
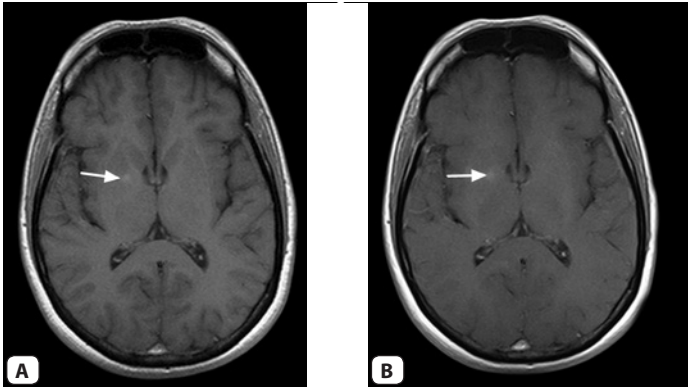


Fig. 6.7: Magnetization transfer diagram



Figs 6.8A and B: Magnetization transfer. T1-w post contrast axial image (A) of the brain shows an enhancing lesion in the right globus pallidus (arrow). With magnetization transfer on (B) the conspicuity of the lesion increases (arrow) while background signal reduces with reduction in gray-white differentiation

2. MR Angiography—MT suppresses background tissue while preserves signal from blood vessels resulting into improved small vessel visualization.
3. Pathology characterization—Apart from increasing conspicuity of enhancing lesion MT is also being studied to characterize lesions into benign and malignant depending on their macromolecular environment and high molecular weight nuclear proteins.

Keyhole Imaging

The K-Space is completely filled only for the first image. For the subsequent images, only central (approximately 20%) K-Space is filled. Rest 80% is filled from the first image. This results in significant reduction in scanning time. This technique is mainly used in contrast enhanced MR angiography (Fig. 6.9).

Saturation Band

It is also called REST slab or SAT band and is used to suppress the signal from a part of the FOV (Fig. 6.10). A 90 degrees RF pulse is sent

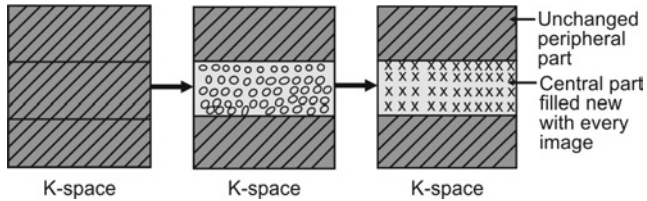


Fig. 6.9: Key-hole imaging

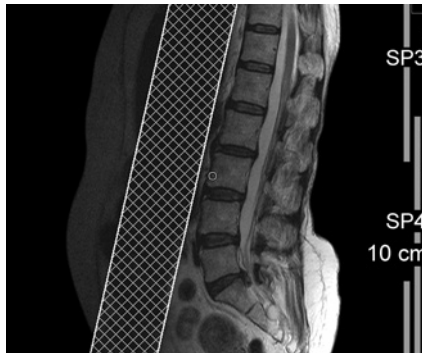


Fig. 6.10: Image showing saturation band anterior to the spine

immediately prior to proper sequence tilting the magnetization in transverse plane in the region of the band. When proper excitation pulse follows there is no longitudinal magnetization in this region to be tilted. Hence this region will not have any signal. Sat bands can be used to reduce aliasing signal into region-of-interest, to reduce the fat signal wrapping in the region of interest, and in MR spectroscopy to define the region of interest by suppressing surrounding signals. Penalty for using sat band include increased specific absorption rate (SAR) and reduction in the number of slices that can be obtained per TR.

Sequences III: When to Use What Sequences

CHAPTER 7

This chapter discusses and compares contrast, resolution and speed of acquisition offered by various sequences. Clinical applications of common sequences are illustrated with reason to use a sequence in particular situation.

T1- Weighted Sequences

Three types of T1-w images are commonly used in practice. These include T1-w spin-echo (SE) or fast spin-echo (FSE), T1-w 2D gradient echo (GRE) and T1-w 3D GRE sequences. These sequences are compared in Fig. 7.1.

T1-w FSE is used when good resolution and T1-contrast is desired. However, this sequence takes long-time to acquire and may be affected by motion artifacts. T1-w 2D GRE sequences (FLASH/SPGR/T1-TFE) are slightly faster but have inferior T1 contrast and resolution as compared to its FSE counterpart.

In and Out-of-Phase Imaging

A special version of T1-w 2D GRE sequences is called '***In and out-of-phase***' imaging. This is used to detect fat in an organ (Fig. 7.2) or a lesion (Fig. 7.3) and its principles are discussed in chapter 6 in the fat suppression section.

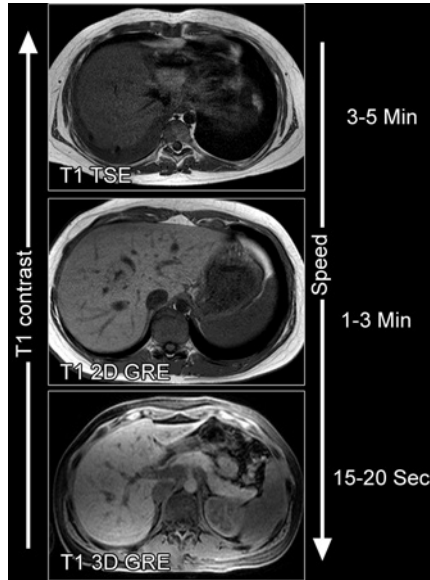
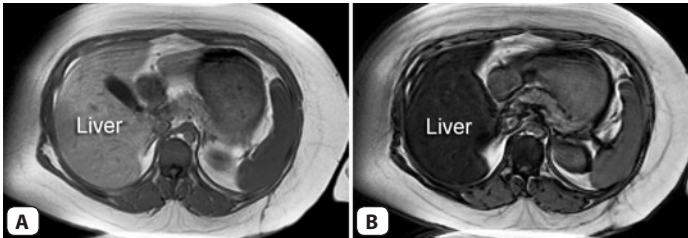
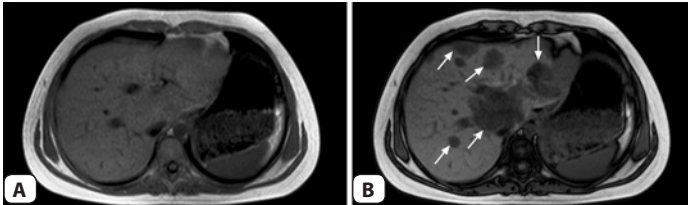


Fig. 7.1: Comparison of T1-w sequences. The speed of acquisition increases from TSE to 3D GRE, however, T1 contrast (ability to differentiate structures based on their T1 relaxation time) is best for TSE and less for GRE sequences



Figs 7.2A and B: In and out-of-phase imaging in fatty liver. Axial T1-w GRE images at in-phase TE of 4.5 ms (A) and out-of-phase TE of 2.3 ms (B) at 1.5T machine show liver turning dark on the out-of-phase image suggestive of fatty infiltration



Figs 7.3A and B: In and out-of-phase imaging in fat containing lesion. Axial T1-w GRE images at in-phase TE of 4.5 ms (A) and out-of-phase TE of 2.3 ms (B) at 1.5T machine show multiple dark lesions in the liver only on the out-of-phase images (arrows) suggestive of fatty lesions. These lesions turned out to be multiple adenomas

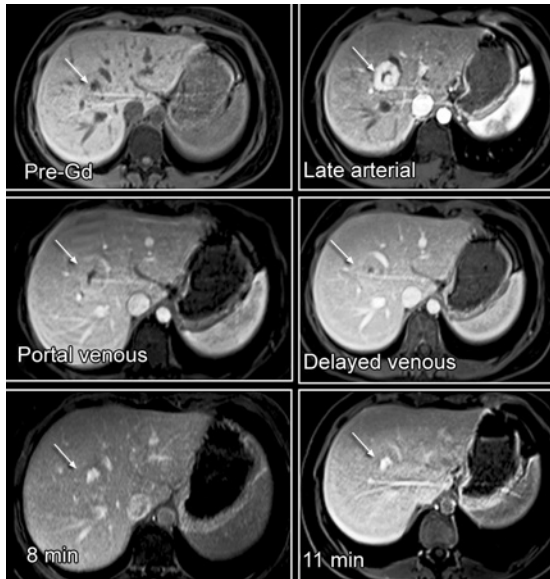


Fig. 7.4: Multi-phase post-contrast imaging with 3D T1-w GRE sequence in liver focal nodular hyperplasia (FNH). The liver lesion (arrows on the images) is isointense on pre-gadolinium T1-w VIBE image, enhances avidly in arterial phase and become isointense to liver parenchyma in portal venous and equilibrium phases. The central scar does not enhance in early phases but enhances on delayed phase images at 8 and 11 minutes. The findings are in keeping with FNH

T1-w 3D GRE (VIBE/3D-FLASH/LAVA/THRIVE)

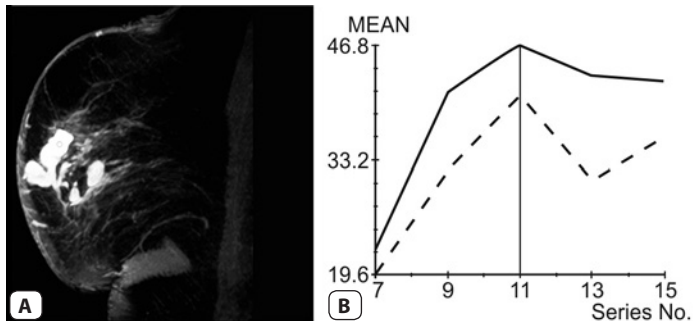
These are fastest amongst T1-w sequences and can be acquired in breath-hold time. Hence they are used for multiphasic or dynamic studies where images can be obtained in arterial, portal venous and delayed phases after contrast injection (Fig. 7.4) or pattern of enhancement of a lesion can be assessed (Fig. 7.5).

Medium Ti Inversion Recovery Sequence

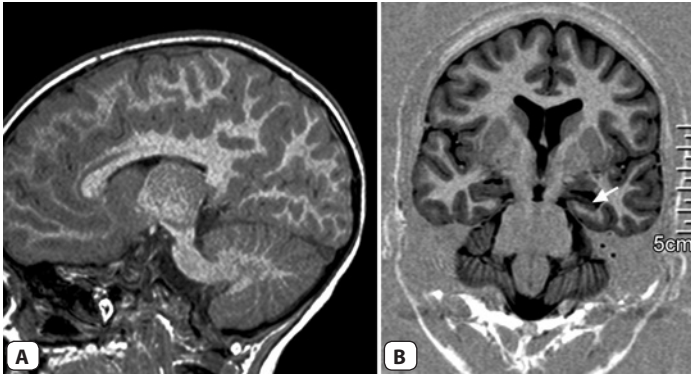
Sequences like MPRAGE (Siemens) and T1-FLAIR (Philips) are T1-w sequences that use inversion pre-pulse with medium inversion time (TI) in the range of 600-1200 ms. This increases contrast between gray and white matter (Fig. 7.6A). Because of their good gray-white differentiation ability they are used in the epilepsy protocol for the evaluation of mesial temporal sclerosis (Fig. 7.6B) and detection of cortical dysplasia.

T2-Weighted Sequences

T2-w sequences come in more variety than T1-w sequences. Commonly used T2-w sequences from SE group include T2 FSE, T2 fast recovery FSE and T2 single shot sequences. T2-w sequences provided by inversion recovery group are STIR and FLAIR. Even though STIR has combined T1



Figs 7.5A and B: Enhancement pattern with T1-w GRE sequence. Sagittal T1-w 3D FLASH image (A) Shows two enhancing lesions (with tiny circle in their center) in the breast. (B) The graph of degree of enhancement over time shows that there is rapid uptake-rapid washout of contrast suggestive of probably malignant lesions



Figs 7.6A and B: (A) MPRAGE sagittal image of the brain. Appreciate the gray-white differentiation ability of the sequence. (B) Medium T1 Inversion recovery oblique coronal image of the brain shows atrophic left hippocampus (arrow) in a patient with epilepsy

and T2-weighting, for all practical purposes, it is used as a T2-w fat sat sequence. T2-w sequence from GRE group is balanced SSFP (TruFisp/FIESTA/bTFE) and its modifications. Diffusion b-value = 0 can be considered T2-w image from the EPI group. All these T2-w sequences are compared in Fig. 7.7. Heavily T2-w images with high TE are used for fluid imaging such as MRCP, myelography and urography. Principles of this technique are discussed in the chapter on MRCP. Some common applications of T2-w sequences are illustrated below.

Single Shot Fast Spine Echo (SSFSE/HASTE)

The distinct advantage of this sequence is the speed of acquisition. It can be acquired in seconds as a breath-hold sequence or with respiratory triggering. Not only the overall time of acquisition is short, each echo is acquired very fast so that moving structures can be imaged with this sequence. It is used for imaging of heart (Fig. 7.8A), bowel (Fig. 7.8B), fetal imaging (Fig. 7.8C) and uncooperative patients and children (Fig. 7.8D). This is also an important sequence for MRCP, MR urography and MR myelography where it can be acquired as a slab of a few centimeter thickness with high TE, usually more than 700-800 ms

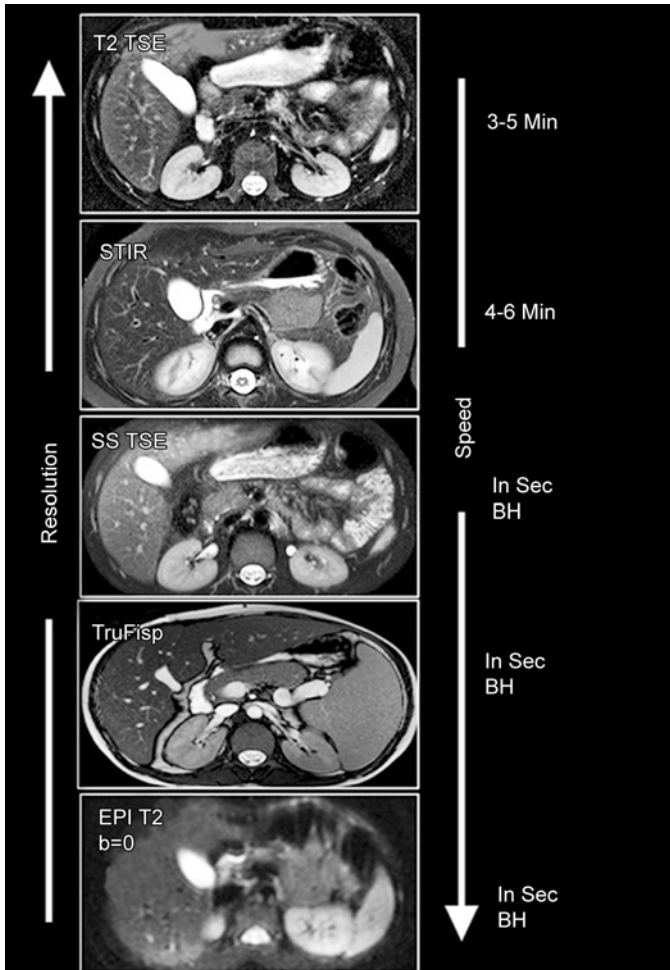
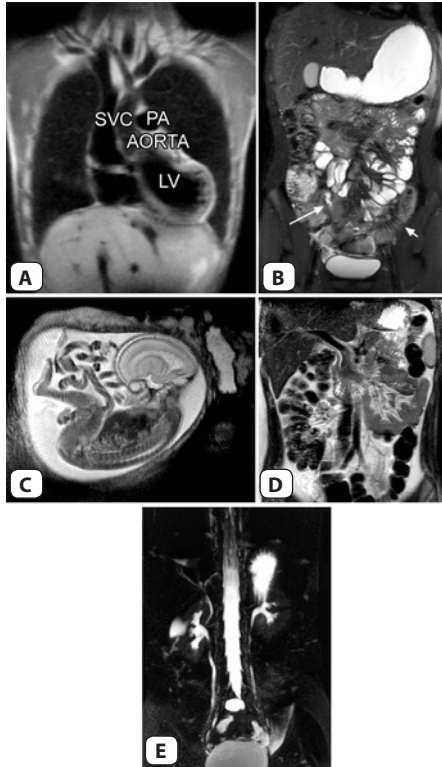


Fig. 7.7: Comparison of T2-w images. The resolution and speed of acquisition is as shown. Signal-to-noise ratio (SNR) is best for T2 TSE, less for STIR and single-shot (SS TSE) sequences and very poor for EPI T2-w image. Even though TruFISP has highest SNR it does not necessarily have high resolution (note it does not have corticomedullary differentiation in the kidneys)

(Fig. 7.8E). It has less SNR and resolution as compared to the proper T2-w FSE sequence. For this reason, T2-w FSE sequence should be preferred, whenever possible, in solid organ imaging.



Figs 7.8A to E: Clinical applications of single-shot TSE. (A) HASTE in cardiac imaging. HASTE is a spin echo sequence hence the flowing blood in the vessels and cardiac chambers is dark. PA-pulmonary artery, LV- left ventricle, SVC-superior vena cava. (B) SSFSE in MR Enterography. There is thickening of the terminal ileum (long arrow) and descending colon (short arrow) in this patient with Crohn's disease. (C) SSFSE in fetal imaging. (D) SSFSE in abdominal imaging in an uncooperative patient can produce relatively motion artifact free images. (E) A 40 mm HASTE slab with TE of 800 ms shows pelvicalyceal systems, biliary tree and thecal sac. Background soft tissues are suppressed because of high TE

Short Tau Inversion Recovery (STIR)

Even though STIR has combined T1 and T2-weighting, for all practical purposes, it is used as a T2-w fat sat sequence. It is easy to pick up lesions on STIR as most pathologic tissues are proton rich and have prolonged T1 and T2 relaxation times resulting in high signal intensity on STIR images. Fat suppression on STIR images is more robust and homogenous as compared to T2-weighted fat saturated images. Hence STIR is used all most everywhere in the body imaging. STIR has lower SNR than T2-w FSE sequence. Few common uses are—

1. Bone marrow imaging: STIR shows marrow edema very well (Fig. 7.9A). It is very useful detecting multiple lesions in bones (Fig. 7.9B) and is used for bone metastases screening in whole-body MRI.
2. It is used in orbital imaging especially for optic nerves (Fig. 7.9C).
3. It is used in SI joint imaging and shows marrow edema earlier than erosions seen on CT scan in arthropathies (Fig. 7.9D).

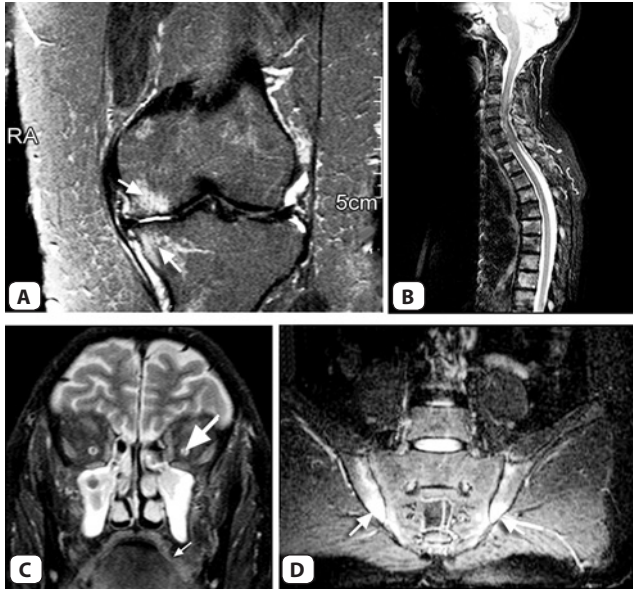
Fluid Attenuated Inversion Recovery (FLAIR)

This is a long TI (1500-2500 ms) inversion recovery sequence used for T2-w imaging with suppression of fluid. It is mainly used in neuroimaging where CSF is effectively suppressed and heavily T2-weighted images can be obtained without problems from CSF partial volume effects and artifacts. It can also be acquired after contrast injection. Some of the common uses include:

1. Extent of perilesional edema can be determined easily (Fig. 7.10A).
2. Brain infarctions are well seen on FLAIR (Fig. 7.10B).
3. Bright lesions of multiple sclerosis are better seen on FLAIR (Fig. 7.10C).
4. Increased signal in mesial temporal sclerosis is better appreciated on FLAIR (Fig. 7.10D).
5. Fast FLAIR shows subarachnoid haemorrhage (Fig. 7.10E).
6. Syrinx/cysts in spinal cord are well seen on FLAIR.

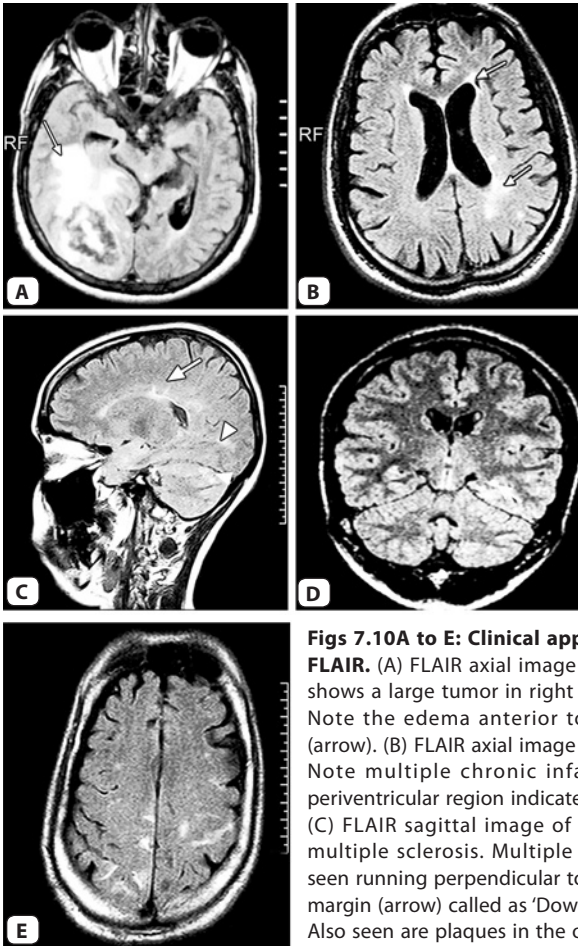
Balanced SSFP (TRUFISP/FIESTA/Balanced TFE)

These are sequences from second type of GRE sequences, called steady state sequences, in which residual transverse magnetization is rephased. These are very fast sequences that can be acquired in breath-hold



Figs 7.9A to D: Clinical applications of STIR. (A) STIR coronal image of the knee. Bright signals are seen in the medial condyle of tibia and femur (arrows) suggestive of marrow edema in this case of osteoarthritis. (B) STIR sagittal image of the cervico-dorsal spine. Multiple bright spots are seen in vertebral bodies as well as posterior elements suggestive of metastases in this patient with known primary tumor. (C) STIR coronal image of the orbit. The left optic nerve is atrophic with prominent CSF space around it (arrow). (D) STIR coronal image of sacroiliac joints in ankylosing spondylitis. Early inflammatory changes in the form of edema are seen as bright signals bilaterally (arrows)

time and have highest possible SNR amongst all sequences. They are motion insensitive as gradients in all three axes are balanced. The speed, motion insensitivity and high SNR make these sequences, the sequence of choice in cardiac (Fig. 7.11A), bowel (Fig. 7.11B) and fetal imaging (Fig. 7.11C). They are also commonly used in abdominal imaging (Fig. 7.11D). Even though they have a very high SNR, they lack internal spatial resolution. This can be understood with the fact that gray-white

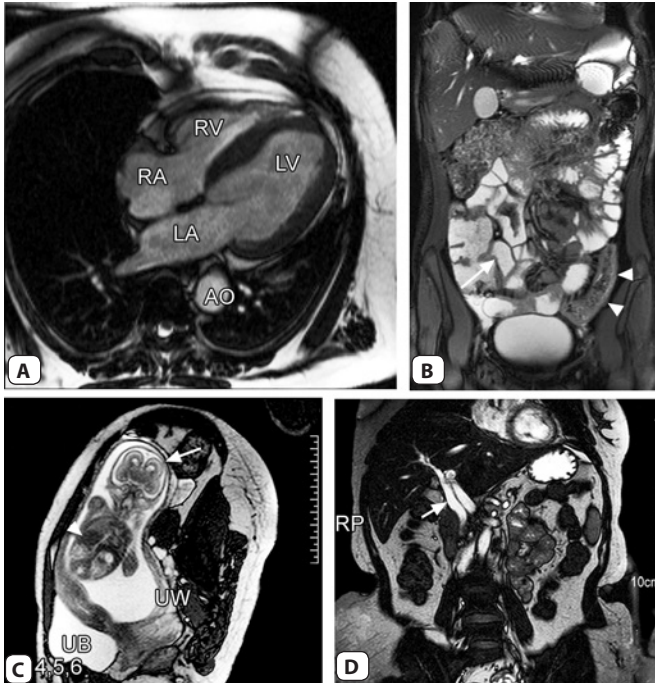


Figs 7.10A to E: Clinical applications of FLAIR.

(A) FLAIR axial image of the brain shows a large tumor in right hemisphere. Note the edema anterior to the lesion (arrow). (B) FLAIR axial image of the brain. Note multiple chronic infarcts in left periventricular region indicated by arrows. (C) FLAIR sagittal image of the brain in multiple sclerosis. Multiple plaques are seen running perpendicular to the callosal margin (arrow) called as 'Dawson's fingers'. Also seen are plaques in the occipital lobe and the cerebellum (arrowheads). (D)

FLAIR oblique coronal image of the brain shows hippocampi in cross section. The left hippocampus is atrophic and bright (arrow) in this patient with epilepsy. (E) FLAIR axial image of the brain. Bright signals suggestive of subarachnoid hemorrhage (SAH) are seen in cortical sulci

differentiation in the brain and corticomedullary differentiation in the kidney is almost absent on these sequences. Hence they are not suitable for solid organ imaging. Another very important use of these sequences is vessel assessment. But care should be taken about vessel patency on



Figs 7.11A to D: Clinical applications of balanced SSFP. (A) True FISP four chamber view of the normal heart. Myocardium and valves are seen as dark signal structures against bright blood in the chambers. LA- left atrium, LV-left ventricle, RA-right atrium, RV-right ventricle. (B) Coronal bTFE in MR Enterography shows thickened terminal ileum (arrow) and descending colon (arrowheads) in this patient with Crohn's disease. (C) True FISP image of the gravid uterus. Appreciate the head of the fetus (arrow), fetal liver (arrowhead), maternal urinary bladder (UB) and uterine wall (UW). (D) True FISP coronal image of the abdomen shows dilated common bile duct (arrow). Note the bright vessels, biliary ducts, fluid and fat

these sequences as they may not be reliable to detect filling defects in the vessels. It should be used for anatomic vessel imaging only. Arteries, veins, fluid and fat all are bright on these sequences.

Constructive Interference at Steady State (CISS)/ FIESTA-C

CISS is the slower and 3D version of TruFISP in which two true FISP runs are combined to eliminate banding artifacts. This T2-w 3D sequence can provide thin slice high resolution images of posterior cranial fossa showing cranial nerves dark against the background of bright CSF (Fig. 7.12). CISS is routinely performed for suspected internal auditory canal and cerebello-pontine angle cistern pathology. CISS can also be used to visualize spinal nerve roots and optic nerve.

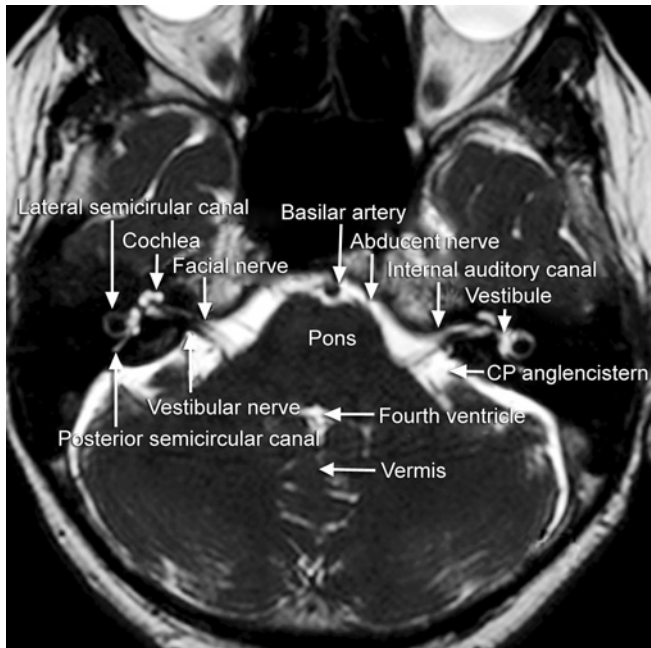


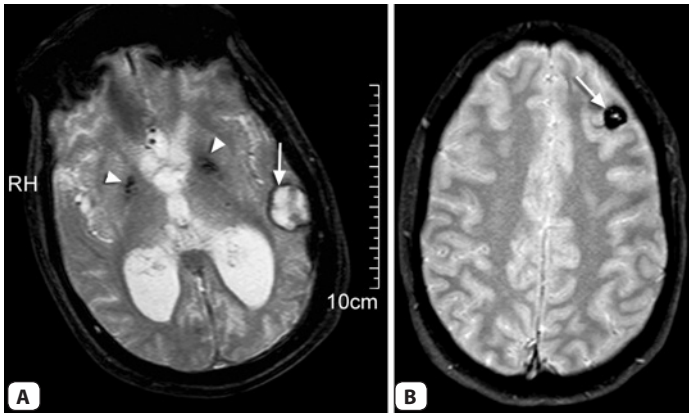
Fig. 7.12: CISS axial image of the posterior cranial fossa. Cranial nerves are seen as dark linear structures against the background of bright CSF

T2* Weighted Sequences

Most of the clinically used T2*-w sequences are related to or modifications of spoiled GRE (e.g. FLASH) and post excitation refocused GRE (e.g. FISP) sequences. The third type of T2*-w images are provided by the EPI group. The GRE sequences can be made T2*-w (i.e. more sensitivity to susceptibility effects) by using low flip angle, long TE and long TR. Common T2*-w sequences include Gradient hemo (Siemens), MPGR (GE) and T2 FFE (Philips). These sequences are used to detect hemorrhage (Fig 7.13), hemosiderin deposition and calcification.

Cartilage Sensitive Sequences

These are GRE sequences with variable T2* susceptibility depending on the particular sequence. On these images, bone appears dark because of susceptibility amongst trabeculae and cartilage appears brighter because of T2-weighting of the sequences. This results in a good contrast between the bone and the cartilage. Following are commonly used cartilage sensitive sequences:



Figs 7.13A and B: (A) Gradient Hemo axial image of brain. A bright area with dark rim (arrow) is noted in the left temporoparietal region suggestive of hemorrhage. Bilateral basal ganglion calcifications are also seen (arrowheads). (B) T2 FFE image of the brain shows a cavernoma in the left frontal lobe (arrow). Blood products such as hemosiderin deposition from chronic bleeding in the lesion are causing darkening

Dual Echo at Steady State (DESS) (Siemens)

DESS combines two images formed separately from FISP and PSIF signals (as against the TruFISP sequence in which these two signals are combined before and then the image is formed). DESS has both T1 and T2 contrast hence anatomy as well as fluid is seen very well. DESS with water excitation pre-pulse is used in joint imaging, where it shows articular cartilage, bone and synovial fluid very well (Fig 7.14). Data can be post processed using MIP and MPR.

Multi Echo Data Image Combination (MEDIC) (Siemens)

It is a RF spoiled GRE sequence that combines images with different T2-weighting. It has minimal flow artifacts and less sensitivity to susceptibility and chemical shift effects. It can be used in imaging of any joint. It is mainly used in cervical spine imaging with flow compensation to avoid artifacts from neck vessels (Fig. 7.15).

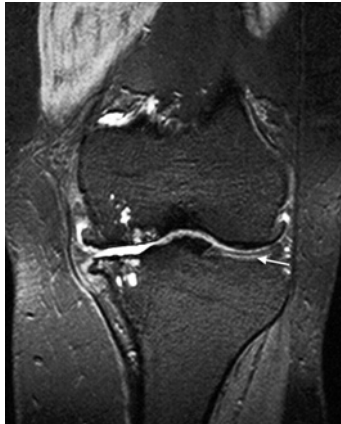


Fig. 7.14: DESS coronal image of the knee. Medial compartment osteoarthritis is seen with subchondral (bright) cysts and osteophytes. Note the normal articular cartilage (arrow) in the lateral compartment seen as moderately high intensity structure

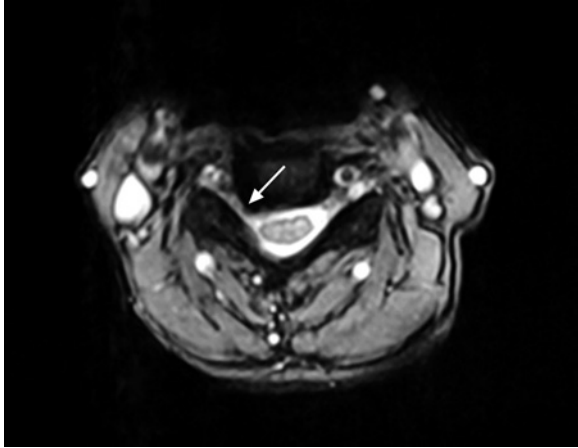


Fig. 7.15: MEDIC axial image of the cervical spine. Right posterolateral disk herniation is seen as dark structure (arrow) encroaching on the neural foramen

MPGR (GE)/T2 FFE (Philips)

These T2*-w sequences do not have exactly same design on GE and Philips. However, they are equivalent and have similar clinical applications. They are used for detection of hemorrhages, hemosiderin deposition and calcification as well as cartilage evaluation in joint imaging (Fig. 7.16).

In summary, different sequences offer different contrast, resolution and speed of acquisition. We need to use them depending upon the need and clinical query to be answered. More about the use of a sequence in a particular situation is discussed in the chapters on principles of interpretation in neuroimaging and body imaging.



Fig. 7.16: Coronal T2 FFE image of the knee shows the articular cartilage as intermediate signal intensity structure (arrows)

Magnetic Resonance Imaging Artifacts

CHAPTER 8

Magnetic resonance imaging also suffers from artifacts as other radiological modalities. Artifacts can cause significant image degradation and can lead to misinterpretation. It is impossible to eliminate all artifacts though they can be reduced to acceptable level. With newer techniques coming up newer artifacts are added. In this chapter we will discuss few common artifacts, their causes and measures to reduce them. Most artifacts tend to occur along a particular axis of the gradients hence axis along which the artifact occurs is given with each artifact.

Ghosts/Motion Artifacts

Ghosts are replica of something in the image. Ghosts are produced by body part moving along a gradient during pulse sequence resulting into phase mismapping. Ghosts can originate from any structure that moves during the acquisition of data (Fig. 8.1). Periodic movement such as respiratory, cardiac and vessel pulsation causes coherent ghosts while nonperiodic movement causes a smearing of the image. *N/2 ghost* is a type of ghost seen on single-shot echo-planar images in which ghost appears as an additional image with reduced intensity that is shifted by half the field of view.

Axis: ghosts almost always seen along phase encoding axis.

Corrective Measures

1. *Phase encoding axis swap*—Phase encoding direction is changed. For example—in sagittal image of the spine with phase encoding

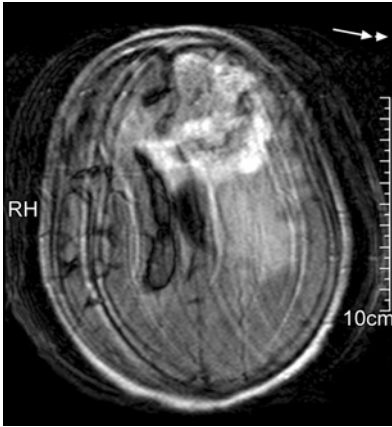


Fig. 8.1: Ghosting/
 Movement artifacts occurring along the phase encoding direction (side to side in this case). The phase direction is indicated by the arrow on some machines

in anterior to posterior direction pulsation of aorta causes ghosting over the spinal cord. If phase encoding gradient is applied in head to foot direction, this artifact will not overlap over the spinal cord.

2. **Saturation band**—The area producing motion artifacts is saturated with RF pulses before start of proper pulse sequence such that all signals from this area are eliminated.
 For example—in sagittal image of the cervical spine swallowing produces ghosts along phase axis (anterior-posterior) and obscures the spinal cord. Application of saturation band anterior to the cervical spine over esophagus eliminates this artifact.
3. **Respiratory compensation**—Effect of respiratory motion can be eliminated by breath-hold sequences. Respiratory motion can be reduced by respiratory triggering by tying a bellows or by using navigator pre-pulse. Respiratory motion can also be reduced by respiratory ordered phase encoding. All these techniques are discussed in chapter 6.
4. **ECG gating for cardiac motion**—Data acquisition is done in a particular phase of cardiac cycle in every cycle.
5. **Gradient Moment Nulling/Rephasing**—Reduces ghosts caused by flowing nuclei moving along gradients by adjusting the gradient (discussed in chapter 6).

Aliasing/ Wraparound

In aliasing, anatomy that exists outside the FOV appears within the image and on the opposite side (Fig. 8.2). When the imaging field of view is smaller than the anatomy being imaged, aliasing occurs. The body part outside the selected FOV produces signal if it is in close proximity to the receiver coil. During signal encoding, signals from the anatomy outside the FOV are also allocated pixel positions. If frequencies of these signals are higher than the limit that can be sampled, these frequencies are given pixel positions within FOV on lower frequency side. Hence there is wraparound of structures outside the FOV into the image.

Axis: aliasing can occur along any axis. Aliasing along frequency encoding axis is called frequency wrap and along phase encoding axis is called phase wrap. Aliasing can occur along slice selection axis in 3D imaging.

Corrective Measures

1. Frequency wrap—Frequency wrap is easier to correct. Low pass-filters are used to cut-off the frequencies originating from outside FOV.
2. Phase wrap—Phase wrap can be corrected by increasing FOV along phase encoding direction, by phase oversampling, phase-frequency axis swap and using surface coils.

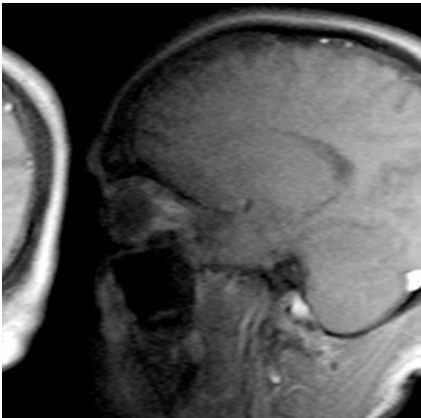


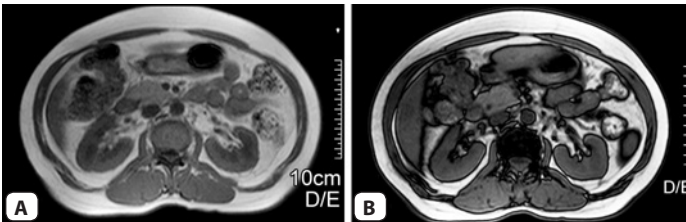
Fig. 8.2: Aliasing artifact: T1-w sagittal image of the brain shows posterior part of the head wrapped around and seen anteriorly

Chemical Shift Related Artifacts

Because of different chemical environment protons in water and fat precess at different frequencies. This difference in precessional frequencies of protons in water and fat is called 'chemical shift'. It is expressed in parts per million (ppm). The frequency of water protons is about 3.5 ppm greater than that of fat protons. This chemical shift of 3.5 ppm causes water protons to precess at a frequency 220 Hz higher than that of fat proton at 1.5 Tesla. Chemical shift forms the basis for



Fig. 8.3: Chemical shift artifact: T2-w sagittal image of the brain shows a tectal lipoma with dark edge on its superior aspect (arrow) and bright edge on its inferior aspect (arrowhead) in keeping with chemical shift type 1



Figs 8.4A and B: Normal in-phase image with TE of 5 ms (A) and out-of-phase image with TE of 2.4 ms (B) at 1.5T MRI scanner. Note dark edges around the kidneys, liver and muscles on the out-of-phase image from dephasing occurring in the voxels at the interface containing both water and fat protons

MR Spectroscopy. However, same chemical shift becomes source of artifacts in MR imaging.

There are two types of artifacts related to chemical shift- 1. Chemical shift misregistration artifact (Fig. 8.3) and 2. Interference from chemical shift (in-phase/out-phase) (Fig. 8.4). These are discussed in table format below.

	Chemical shift misregistration	Interference from chemical shift
1. Mechanism	Receive bandwidth is the range of frequencies that must be mapped across FOV. If bandwidth is ± 16 kHz i.e. 32000 Hz and frequency encoding steps are 256 then each pixel has an individual frequency range of 125Hz/pixel (3200/256). At 1.5T chemical shift between water and fat is 220 Hz. Therefore, water and fat protons existing adjacent to one other are mapped 1.76 pixels apart (220/125). This pixel shift of fat relative to water results into artifacts	Since water protons precess about 220 Hz faster than fat protons at 1.5 T, they complete an extra-revolution every 4.5 ms. So fat and water protons are in phase at certain times and out of phase at others. At TE times that are multiples of 4.5 ms at 1.5 T, they are in phase. They are out of phase at TE times halfway between the in-phase TE times. When they are in-phase their signals add together. When out of phase their signals cancel each other out. This results in artifacts
2. Axis	Along frequency encoding axis	Phase encoding axis since caused by phase difference.
3. Artifact	Subcutaneous fat is projected within the organs Dark edge at the interface between fat and water Dark edge on one side and bright edge on other side of a fatty structure or lesion	Dark edge around certain organs where fat and water interfaces occur within same voxel (also called India ink artifact)
4. Corrective Measures	1. Fat suppression 2. Increase bandwidth	1. Using Spin-echo sequence- since 180 degree rephasing pulses compensate for phase difference between fat and water. So the artifact is reduced in SE sequence 2. Selecting TE that is multiple of 4.5 ms at 1.5 T. So that water and fat are in phase
5. Good effects	Chemical shift along frequency encoding axis forms the basis of MR spectroscopy	In-phase and out-phase imaging is used to detect fat in the organs or lesion such as adrenal adenoma

Truncation Artifact

Truncation artifacts are also called as edge, Gibbs' and ringing artifacts.

Truncation artifacts produce low intensity band running through high intensity area (Fig. 8.5). The artifact is caused by under sampling of the data so that interfaces of high and low signal are incorrectly represented on the image. Truncation artifacts can be misleading in long narrow structures, such as spinal cord or intervertebral disk. For example in T1-weighted sagittal image of the cervical spine CSF in central canal appears dark as compared to spinal cord and might be misinterpreted as syringomyelia. This is specifically called as Gibbs' artifact. Truncation artifacts are also seen as bright or dark lines parallel with and adjacent to the borders of an area of abrupt signal intensity change.

Axis: Phase encoding.

Corrective Measures: Increase the number of phase encoding steps. For example—256 x 256 matrix instead of 256 x 128.

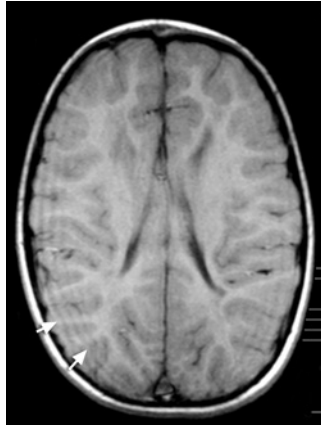


Fig. 8.5: Truncation artifacts: T1-weighted axial image of the brain shows dark linear artifacts along the periphery of the brain (arrows). These lines disappeared with increased matrix

Magnetic Susceptibility Artifact

Magnetic susceptibility is the ability of a substance to become magnetized. Some tissues magnetize to different degree than other, resulting into differences in precessional frequency and phase. This causes dephasing at the interface of these tissues and signal loss. For example, magnetic susceptibility difference between soft tissues and air is about 10 ppm. This causes signal loss and distortion of the boundaries of the brain near air sinuses. Other common causes of magnetic susceptibility artifacts include metal and iron content of hemorrhage.

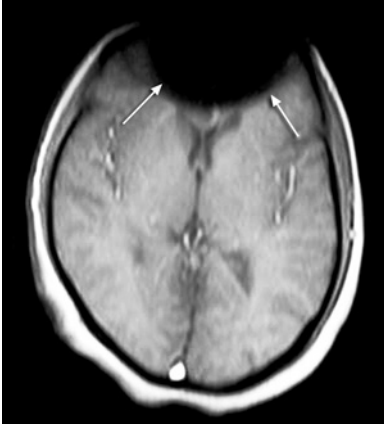


Fig. 8.6: Susceptibility artifact: This dark artifact (arrows) in the axial localizer image of the brain is because of the magnetic susceptibility effect caused by some metallic components in the *bindi* (a small sticker routinely applied on forehead by Indian women). Similar artifacts may be caused by mascara

Magnetic susceptibility is more prominent in GRE sequence than SE sequence (Fig. 8.6). In SE sequences compensation for the phase differences occurs because there is refocusing of the dephasing caused by magnetic field inhomogeneities by 180 pulses.

Axis: Frequency encoding and phase encoding.

Corrective Measures

1. Use of SE sequence.
2. Remove all metals.
3. In cases with metallic hardware, susceptibility artifacts can be reduced to certain extent by increasing bandwidth, reducing TE, using thin slices and higher matrix.
4. Susceptibility artifacts can also be reduced by use of parallel imaging and use of sequences with radial K-Space sampling like BLADE/PROPELLER.

Good Effects

Magnetic susceptibility also has good effects apart from artifacts and can be useful in following ways.

1. Used to diagnose hemorrhage, hemosiderin deposition and calcification (Fig. 8.7).



Fig. 8.7: Magnetic susceptibility effect: Gradient hemo axial image of the brain shows bleed in the right perisylvian region as dark areas (arrows)

2. Forms the basis of post-contrast T2* weighted MR perfusion studies.
3. Used to quantify myocardial and liver Iron overload.

Straight Lines and Zipper Artifacts

Straight lines—Regularly spaced straight lines through MR image is caused by spike in the K-Space, i.e. bad data point in the K-Space (Fig. 8.8). Spike can result from loose electrical connectivity and breakdown of interconnections in an RF coil. RF interfering sources inside the room could be monitoring devices or flickering light bulb. The location of the spike and its distance from the center of K-Space determine the angulation of the lines and the distance between them.

Zipper like artifact—It is a line with alternating bright and dark pixels propagating along the frequency encoding direction. It is caused by stimulated echo that have missed phase encoding. It is caused by RF leakage. All MR scanner rooms are shielded (faraday cage) to prevent any RF from local radio broadcasting stations or from electronic equipment entering the room. Leakage can be caused by any equipment brought into the room or defective faraday cage.

Axis: Zipper artifact is seen along frequency encoding axis.

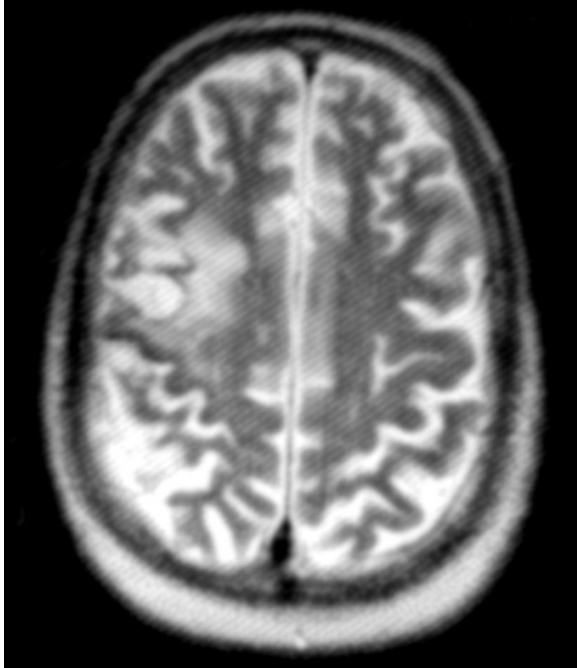


Fig. 8.8: Straight lines: T2-w axial image of the brain shows oblique straight lines through out the image related to a spike in the K-Space

Corrective Measures

For the RF interference, the site of RF leak should be located and corrected. Sources of RF inside the room should be removed. Zipper artifact can be eliminated by spoiler gradients arranged in special pattern to remove stimulated echoes.

Shading Artifacts

In shading artifact image has uneven contrast with loss of signal intensity in one part of the image (Fig. 8.9). The causes include uneven excitation of nuclei within the patient due to RF pulses applied at flip angles other than 90 and 180 degree, abnormal loading of coil

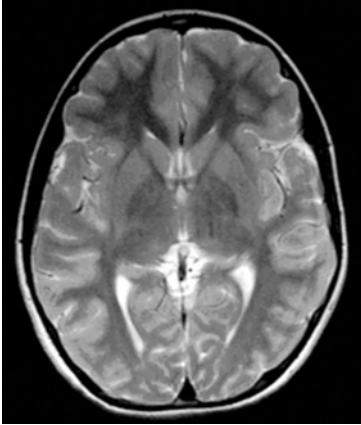


Fig. 8.9: Shading artifact: T2-w axial image of the brain shows comparatively less signal in the frontal regions. This was because of the improper loading (connection) of the coil in the anterior part

or coupling of coil, inhomogeneity of magnetic field and overflow of analog-to-digital converter (ADC).

Axis: Frequency and phase encoding.

Corrective Measures

1. Load the coil correctly.
2. Shimming to reduce the inhomogeneity of the magnetic field.
3. To avoid ADC overflow, images are acquired with less amplification.

Cross Excitation and Cross Talk

An RF excitation pulse is not exactly square. As a result, nuclei in slices adjacent to the one excited by RF pulse may also receive energy and be excited. This energy flips NMV of these nuclei into transverse plane. When they are excited by their own RF excitation pulse they do not have enough longitudinal magnetization to be tilted. This results in reduced signal intensity in the adjacent slices. This phenomenon is called *cross excitation* (Fig. 8.10).

The same effect is produced when RF pulse is switched off. The energy is dissipated to the nuclei from neighbouring slice when nuclei within the selected slice relax after RF pulse is switched off. This is called as *cross talk*.

Axis: Slice selection gradient

Corrective Measures

Cross talk can not be corrected.

To minimize the cross excitation—

1. Increase interslice gap.
2. Scanning with interleaved slices. First slice numbers 1, 3, 5, 7 are excited and then slices 2, 4, 6, 8 are excited. So that nuclei have time to relax.

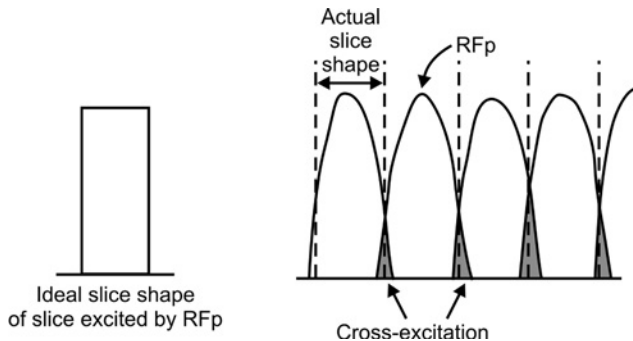


Fig. 8.10: Cross Excitation: Diagram shows excitation of nuclei in the adjacent slices because of parabolic shape of the slice excitation



Fig. 8.11: Parallel imaging artifact: Coronal T1-w image of the brain obtained with parallel imaging shows graininess in the center of the image (arrows) related to the higher acceleration (sense) factor

Parallel Imaging Artifact

Graininess in the center of the image can be caused by high acceleration factor used in parallel imaging or using too small FOV with parallel imaging (Fig. 8.11). This artifact can be reduced by using lower acceleration factor and increasing the FOV.

Magnetic Resonance Safety

CHAPTER 9

In spite of no proven hazards yet, MR has potentials for bioeffects. Safety precautions should be followed strictly as failure to do so can lead to life threatening incidences. This chapter is intended to make the readers aware of some potential bioeffects of MR and some safety precautions to be strictly followed to avoid any untoward effects. These safety precautions are based on recommendations in “American College of Radiology White Paper on MR Safety” published in AJR 2002;178:1335-47 and later updated in AJR 2004;182:1111-14 and AJR 2007;188:1-27.

Please note that safety issues discussed in this chapter are just viewpoints based on ACR white paper on MR safety and some text books. These are not recommendations or guidelines given by any authorised body. Therefore, author will not be responsible for any decision about scanning patients with safety issues, based on views expressed in this chapter.

MR Bioeffects

Patients undergoing MR examination is exposed to three different forms of electromagnetic fields—

1. Static magnetic field.
2. Gradient magnetic field.
3. RF electromagnetic field.

Static magnetic field can raise the skin temperature. It can cause electrical induction and cardiac effects with elevation of T-wave

amplitude. It also has potential effects on neurons. All these bioeffects are not proved to be hazardous at field strength <3 Tesla. Scanning at field strength >2 Tesla may cause vertigo, headache and peripheral nerve stimulation.

Gradient field related possible effects include ventricular fibrillation, epileptogenic potentials and visual flashes. It also has thermal effects. All these effects have not been significant in presently used clinical MR systems.

RF magnetic field can result into energy deposition and tissue heating. SAR (specific absorption rate) is measure of tissue energy deposition and its unit is Watt/Kg. FDA limit for clinical examination is $SAR < 0.4$ W/Kg. However, no clinically hazardous effects or increased skin and body temperature were seen with SAR up to 4W/Kg in experiments. SAR increases with increasing field strength. There is four-fold increase in SAR at 3T as compared to 1.5T. Testes and eyes are more temperature sensitive organs.

Acoustic Noise

It is caused by vibrations of gradient coils. Noise increases with heavy duty cycles and sharper pulse transition. Noise also increases with thin slices, small FOV, less TR and TE. Ear plugs and ear phones should be provided to patients and accompanying person.

Safety Related Issues

1. MR Personnel/Non-MR Personnel
MR Personnel are those who have been trained and educated about MR safety and approved by the MR Medical Director of the institution or the center. Level 1 MR Personnel has education about their own safety while level 2 MR Personnel are trained in broader MR safety issues. Only MR Personnel should have free access to zones III and IV.
2. Site access restriction
ACR white paper recommends that MR site should be divided into four zones to restrict the free access to the Non-MR Personnel. Only zone I has free access to the general public. Zone II is for patient history and preparation. Patients can move in Zone II only under

supervision of MR Personnel. Zone III should be physically restricted from general public access. Only MR personnel will have free access to zone III. Zone IV is the MR scanner room itself and should be located within the zone III. Non-MR Personnel are not allowed to enter zones III and IV without prior screening.

3. Screening of patient and Non-MR Personnel

MR-Personnel should screen patients and relatives for any metallic or ferromagnetic objects before allowing entry into zone III and IV. They should be asked to remove metallic personal belongings and devices such as watches, jewelry, pagers, mobiles phones, body piercings, contraceptive diaphragms, metallic drug delivery patches, clothing items that may contain fasteners, hooks, zippers, loose metallic components or metallic threads and cosmetic containing metallic particles such as eye makeups. Metallic devices can be screened with hand held magnet (>1000 gauss). Any person with suspected metallic foreign body in the orbit or near vital organs should be investigated with plain radiographs and if required CT scan. Intraocular foreign body is an absolute contraindication for undergoing MR examination. With metallic implants, materials and foreign body, the possible adverse effect include displacement, induction of electric current in the object, excessive heating causing burns and misinterpretation because of artifacts. Patients should be changed in site-specific gowns.

4. Pregnancy related issues

Electromagnetic fields used for MRI may have the potential to produce developmental abnormalities. It may affect cell undergoing divisions, as in developing fetus. However, there is little data available at present on this issue.

a. Pregnant Health Care Practitioner:

Pregnant MR Personnel can be permitted to work in and around the MR environment through out all stages of pregnancy. However, they should be requested not to remain inside scanner room during actual data acquisition (when sequence is running).

b. Pregnant patient:

ACR white paper permits scanning of pregnant patient in any stage of pregnancy. It also suggests case-by-case

analysis to decide whether data obtained by MR examination will significantly affect the patient management, whether postponing MRI till end of the pregnancy is feasible and whether this data can be obtained by any other modality. Written and informed consent should be obtained from the patient.

c. Contrast media during pregnancy:

Gadolinium is known to cross the placenta. It is then excreted by fetal kidney and can re-circulate through amniotic fluid several times. Gadolinium can dissociate from its chelate if it stays longer in the amniotic fluid. ACR white paper recommends that MR contrast medium should not be injected in pregnant patient. However, a case-by-case basis decision can be done with risk-benefit analysis.

d. Contrast media in lactating patients:

Gadolinium is excreted in human milk. Breast milk should be expressed after injection and thrown away. Baby should not be breast fed for 36–48 hours.

5. Aneurysm and hemostatic clips

Many of these clips in use are ferromagnetic and they are absolute contraindication for MR examination. Only those aneurysm clips that are tested prior to placement to be non-ferromagnetic and that are made up of titanium, and this is documented in writing by referring physician can undergo MR examination. Having safely undergone a prior MR examination with an aneurysm clip or other implant in place at any given static magnetic field strength is not in and of itself sufficient evidence of its MR safety or compatibility. Variation in static and gradient magnetic field can result into untoward effects next time.

6. Dental devices and materials

Lesser chances of displacement with these devices hence they are not contraindication. However, artifacts caused by them can be problematic.

7. Heart valves

Majority of prosthetic valves show measurable deflection forces. However, the deflection forces were relatively insignificant compared with the forces exerted by the beating heart. Therefore, patients with prosthetic heart valves may safely undergo MRI.

8. Intravascular coils, filters and stents
These devices are usually attached firmly into the vessel wall approximately 4–6 weeks after deployment, therefore unlikely to be dislodged after 6 weeks. Patient may undergo MRI safely.
9. Ocular implants
There is possibility of discomfort and minor injury with ocular implants. Risk-benefit analysis should be done.
10. Orthopedic implants, materials and devices
Most of these devices used in present practice are made from non-ferromagnetic materials, therefore may be safely imaged by MRI. However, artifacts caused by them can be a problem, if they are in region of interest.
11. Otologic implants
Cochlear implant is an absolute contraindication to undergo MR examination.
12. Pellets, bullets and sharpnels
Decision should be taken on individual basis with respect to position of the object near a vital neural, vascular or soft tissue structure. Assessment should be done by taking proper history and plain radiographs.
13. Penile implants and artificial sphincters
Penile implants are relative contraindication for MR examination as they can cause patient discomfort. Artificial sphincters are absolute contraindication.
14. Pacemakers
Cardiac pacemakers are absolute contraindication for undergoing MR examination. There is possibility of displacement and damage of pacemaker, programing change, electromagnetic interference and fibrillation when patient with cardiac pacemaker undergoes MR examination. Even though there are recent reports of patients with pacemaker being safely scanned the data and experience is still scarce.
15. Vascular access ports
Insignificant displacement of simple ports, hence not a contraindication. However, ports with electronic activation and programing are strict contraindication.

16. Patient monitoring and emergency

Monitoring devices like pulse oxymeter, ventilators are now available as MR compatible devices that can be used safely in scanner room. These should be kept as away from magnet bore as possible. In spite of availability of these devices the first approach in case of emergency must be shifting the patient out of the scanning room as early as possible and start resuscitation.

PRECAUTIONS

1. Always screen the patient and accompanying person for any metallic objects. Metallic objects can form projectile because of strong magnetic attraction. This can lead to life threatening consequences.
2. Always see to it that wires and coils are well insulated and are not touching patient's body. It can cause burns. Patient's body part should also not be touching magnet bore.
3. Avoid loop formation:
Wires of pulse oxymeter, ECG leads, etc. should never form a loop. Loop formation can lead to induction of current and burns. Even loop formation of body parts for example crossed arms or legs can form a large conductive loop and can result into induction of current.
4. In case of emergency first approach must be to remove the patient out of scanner room as early as possible and start resuscitation.
5. Doors of scanner room should have label with pictures of object that are strictly prohibited to take inside scanner room.

ABSOLUTE CONTRAINDICATIONS

1. Internal cardiac pacemaker
2. Implantable cardiac defibrillator
3. Cochlear implants
4. Neurostimulators
5. Bone growth stimulators
6. Electrically programmed drug infusion pumps, vascular access ports
7. Intraocular foreign body
8. Non-titanium aneurysm clips.

Magnetic Resonance Contrast Media

CHAPTER 10

In the beginning years of MR imaging, it was thought that MR may not need any contrast medium injection because of its inherent tissue contrast. Soon it was found that the contrast enhancement improves detection, delineation and characterization, and increases confidence in the interpretation. Now with combination of fast sequences and contrast media, it is possible to assess rapid physiologic processes such as perfusion and dynamic studies to assess enhancement pattern. In this chapter, types of MR contrast media, their mechanism of action, special characteristics and safety issues including NSF are discussed.

Classification of MR contrast media

1. Parenteral
2. Oral

Parenteral contrast agents can be classified based on relaxivity and susceptibility.

Depending on Relaxivity

1. Positive relaxation agents (T1 agents)

These agents affect T1 relaxation of the tissues. T1 of the tissue in which contrast media is accumulated is reduced. Reduction in T1 results into increase in the signal intensity on T1-W images hence these agents are called positive relaxation agents.

Examples: Gadolinium, Mn-DPDP.

2. Negative relaxation agents (T2 agents)
They affect T2 relaxation and reduce T2 of the tissue where they accumulate. This results in reduction in the signal intensity of the tissue on T2-W images.
Examples: Iron oxide particles, Gadolinium (high doses).

Depending on Susceptibility

1. Paramagnetic agents
Gadolinium is a paramagnetic agent. They are usually positive agents but at higher doses can cause T2 shortening resulting into decreased signal on T2-W images. When paramagnetic agents initially pass through the vascular bed of brain, they cause local T2 shortening and decrease in the signal on T2-W images. This effect is used in perfusion studies.
2. Superparamagnetic agents
They are negative contrast agents. They cause proton dephasing leading to T2 shortening and signal loss. Example: Iron oxide (Fe_3O_4) like superparamagnetic iron oxides (SPIOs) and ultrasmall SPIO (USPIOs).

Mechanism of MR Contrast Enhancement

In X-ray based modalities like fluoroscopy and CT scan, contrast is mainly related to one factor, i.e. degree of X-ray attenuation caused by the electron density of the tissues or contrast agent. In MR imaging, the contrast mechanism is multi-factorial and includes spin density, relaxivity (T1, T2), magnetic susceptibility, diffusion and perfusion of contrast agent.

Relaxivity: Paramagnetic ions increase relaxation of water protons by a dipole-dipole relaxation. This phenomenon, in which excited protons are affected by nearby excited protons or electrons, is called '*dipole-dipole interaction*'. The dipole-dipole interaction affects the rotational and translational diffusion of water molecules leading to their relaxation. The more and closer the water molecules approach the paramagnetic ions, greater will be the relaxation.

Gadolinium

Gadolinium (Gd) is a rare earth metal of lanthanide group with atomic number 64. Free Gd ions tend to accumulate in the body and do not get excreted. Free Gd ions are toxic. Therefore, Gd ions are combined with chelates such as DTPA that cause their rapid and total renal excretion.

Gadolinium (Gd) causes both T1 and T2 relaxation of the tissues in which it is accumulated. Increased T1 relaxation leads to bright signal on T1-W images (Fig. 10.1). If gadolinium chelates accumulate in excess amount after a threshold, there could be darkening on T1-w images (Fig. 10.2). T1 effects of Gd are used more commonly in clinical practice. A T2 effect of Gd leading to reduction in signal on T2-w images is generally insignificant and clinically not relevant. However, the susceptibility

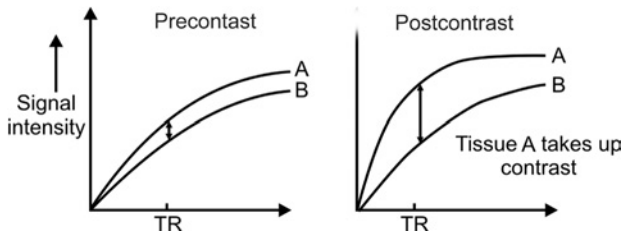


Fig. 10.1: T1 curves- pre and postcontrast: Tissue A takes up Gadolinium leading to reduction in its T1 and increased signal intensity. At short TR, the signal intensity difference between A and B increases resulting into increased contrast

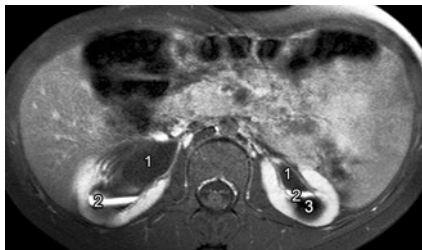


Fig. 10.2: T1-w postcontrast axial image of the abdomen shows bilateral dilated renal pelvis with triple layering of the excreted contrast. 1 = urine with little amount of gadolinium; 2 = moderate amount of gadolinium; 3 = marked amount of gadolinium in the dependant part causing darkening

effect (not the relaxivity) of Gd, as it initially passes through the vascular bed leading to decreased signal on T2-w images, is used in the MR perfusion.

Gadolinium

Atomic Number-64

Paramagnetic agent

Reduces T1 and T2 of the tissues where it accumulates

Increased signal on T1-w and reduced signals (negligible) on T2-w images

Usual dose: 0.1 mmol/Kg

Median Lethal dose (LD50): 6–30 mmol/kg

Overall adverse reaction rate: 3–5%

Osmolality:

Ionic: Magnevist- 1960 mmol/kg

Nonionic: Omniscan - 789 mmol/kg

Prohance - 620 mmol/kg

Gadolinium Chelates

Chelates are substances that have high affinity for metal ions. They bind with metal ions and make them less toxic and facilitate their excretion from the body. Gadolinium is combined with various chelates such as DTPA, DOTA and BOPTA to make it nontoxic and facilitate its excretion from the body. These gadolinium-based compounds/contrast media can have linear or macrocyclic (ring) structure. In general, macrocyclic compounds have more stability, i.e. gadolinium and chelates stay together for longer time. Ionic gadolinium-based contrast media have more stability than nonionic contrast media.

Some of the gadolinium chelates like gadobenate (Multihance) and gadoxetate (Primovist/Eovist) are excreted in part by hepatobiliary system. These agents can be used to assess hepatobiliary pathology and are called as hepatobiliary specific contrast agents.

Gadolinium based contrast agents				
Type	Compound name	Trade Name (Vendor)	T1-relaxation time at 1.5T (L/mmol*s)	Excretion
Linear, nonionic	Gadodiamide (Gd-DTPA-BMA)	Omniscan (GE)	4.6	Renal
	Gadoversetamide (Gd-DTPA-BMEA)	Optimark (Mallinckrodt)	5.2	Renal
Linear, ionic	Gadopentetate (Gd-DTPA)	Magnevist (Bayer)	4.3	Renal
	Gadobenate (Gd-BOPTA)	Multihance (Bracco)	6.7	96% Renal; 4% biliary
	Gadoxetate (Gd-EOB-DTPA)	Eovist (Bayer)	6.9	50% Renal; 50% biliary
	Gadofosveset	Vasovist	19.0	95% Renal; 5% biliary
Macrocylic, nonionic	Gadobutrol (Gd-BT-DO3A)	Gadovist (Bayer)	5.2	Renal
	Gadoteridol (Gd-HP-DO3A)	Prohance (Bracco)	4.4	Renal
Macrocylic, ionic	Gadoterate (Gd-DOTA)	Dotarem (Guebert)	3.6	Renal
Data from: Juluru K, et al. <i>Radiographics</i> 2009; 29:9-22.				

Adverse Reactions

Majority of adverse reactions to Gd are mild and transient. Overall reaction rate is approximately 3–5% and includes nausea, headache and injection site symptoms. Anaphylaxis is very rare. Patient with history of allergy, asthma, and previous reaction to drugs, iodinated contrast and Gd are more prone for the adverse reactions. Precautions should be taken in these cases. Reversible increase in serum iron may be seen

with Magnevist and Omniscan. Increase in bilirubin has been shown with Magnevist in some cases. Ionic versus nonionic MR contrast is not as significant clinically as in iodinated contrast. Their safety profile does not differ significantly.

Nephrogenic Systemic Fibrosis (NSF)

This rare but potentially fatal disease, likely related to gadolinium-based contrast media administration in patients with renal failure, has grabbed much more attention than advances in the field of MR imaging in last few years. Its prevalence is approximately 4–5% in renal failure patients who received gadolinium-based contrast media in series reported so far. 90% of the cases reported were already on dialysis. It has not been reported in patients with normal renal function so far.

The NSF involves deposition of collagen and fibrosis in the skin resulting in thickening, tightening, induration and erythematous changes in the skin. The involvement is predominant in dependant areas with lower extremities and lower thighs involved more than trunk and upper extremities. Systemic involvement including skeletal muscle, heart, lungs, kidneys and diaphragm is also seen, giving the name ‘nephrogenic systemic fibrosis’ to this condition. The disease typically develops from a few days to 3 months after exposure.

For the specific recommendations on administration of gadolinium-based contrast media in patient with impaired renal function, readers can check ACR white paper that is updated time to time. Many institutions have their own policies on this issue. In general, risk benefit analysis should be done for patient with $\text{GFR} < 60 \text{ ml/min/1.73 m}^2$ and gadolinium administration should be avoided. In case the decision is made to inject gadolinium in patients with GFR between 30 and 60 ml/min/1.73 m^2 , only half dose should be used and written informed consent should be obtained. In patients with $\text{GFR} < 30 \text{ ml/min/1.73 m}^2$, gadolinium should not be injected.

Safety Issues

1. Renal failure

This is discussed under NSF. Gd chelates can be dialysed. In chronic renal disease with $\text{GFR} > 60 \text{ ml/min/1.73 m}^2$, no special precautions are needed.

2. History of allergy/asthma
Precautions should be taken in these patients and constant monitoring should be performed. Premedications with hydrocortisone and antihistaminic drugs may be given as clinically warranted.
3. Pregnancy
Gadolinium is known to cross the placenta. It is then excreted by fetal kidney and can re-circulate through amniotic fluid several times. Gadolinium can dissociate from its chelate if it stays long in the amniotic fluid. ACR white paper recommends that MR contrast medium should not be routinely injected in pregnant patient. However, a case-by-case basis decision can be done with risk-benefit analysis.
4. Lactation
Gadolinium is excreted in human milk. Breast milk should be expressed after injection and thrown away. Baby should not be breast fed for 36–48 hours.

Other MR Contrast Agents

1. Iron Oxide (Fe_3O_4)-

It is a superparamagnetic agent. It is phagocytosed by reticulo-endothelial system (RES) with prominent uptake in liver and spleen. Normal liver tissue takes up Iron oxide and becomes dark on T2-w images. Focal lesions such as metastases do not have RES cells within them, so they remain same and appear relatively bright.

2. Mn-DPDP (Mangafodipir trisodium)

This is a hepatobiliary specific contrast agent as 50% of the administered amount is excreted through the biliary system and other 50% by the kidneys. It causes positive contrast enhancement of the normal liver parenchyma and lesions containing hepatocytes on T1-W images. The lesions without hepatocytes like metastasis will not show enhancement and remain relatively darker.

3. Dysprosium Chelates: Dy-HP-DO3A

These were found to be more superior to Gd chelates in perfusion studies (not in routine T1-W images) because of more T2 relaxivity and susceptibility effects.

Oral Contrast Agents

1. Positive Contrast

Example: Manganese chloride, Gd-DTPA, oil emulsions

Image degradation can occur with peristaltic movements of bowel. For MR Enterography, sorbitol (3%) with or without barium or polyethylene glycol solutions can be used as oral contrast.

2. Negative contrast

They decrease signal from bowel lumen reducing the motion related image degradation. They are also used in MRCP.

Example: Superparamagnetic iron oxide particle reduce signal by susceptibility effects. Barium, blue-berry or pineapple juice (contain manganese) and perfluorochemicals are also used to reduce signals from bowel.

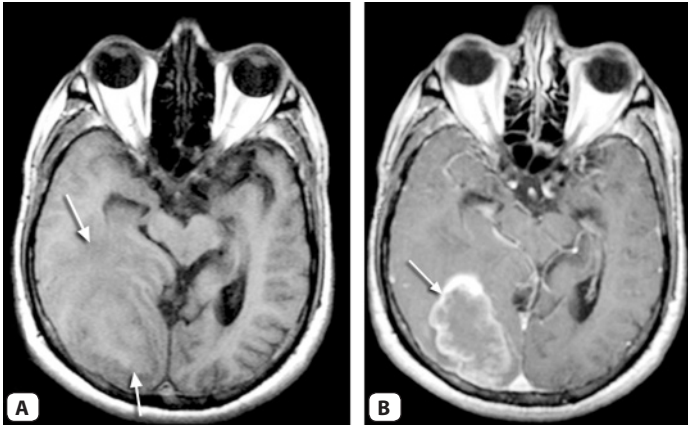
Role of Contrast in MRI

It has been shown that there is substantial improvement in lesion identification and characterization with Gd.

CNS Neoplasm: Contrast improves identification, margin delineation and invasion in brain tumors (Fig. 10.3). It is most in patients undergoing surgery. Metastases and meningiomas can appear isointense on plain scan. Contrast injection makes them more conspicuous. Contrast is very useful in post-treatment tumors to differentiate recurrence from necrosis, especially with MR perfusion.

CNS Infection: Contrast enables lesion characterization and assessment of lesion activity (Fig. 10.4). Acute lesions may be differentiated from chronic lesions (gliosis). Disease progression/regression can be monitored. Enhanced MRI is superior to enhanced CT especially in meningeal enhancement (Fig. 10.5) because of beam hardening artifacts in CT.

Ischemic CNS diseases: Gd is not routinely indicated in ischemic diseases. However, it can be useful for temporal dating and characterization. Intravascular enhancement is seen in first week after infarction, with parenchymal enhancement seen after that up to 8 weeks. Intravascular and gyriiform enhancement may help differentiating infarct from other conditions.



Figs 10.3A and B: Brain tumor: (A) Non-contrast T1-w axial image of the brain shows a large ill-defined space occupative lesion in the right occipito-temporal region (arrows). (B) Postcontrast image shows predominantly peripheral enhancement of the tumor (arrow)

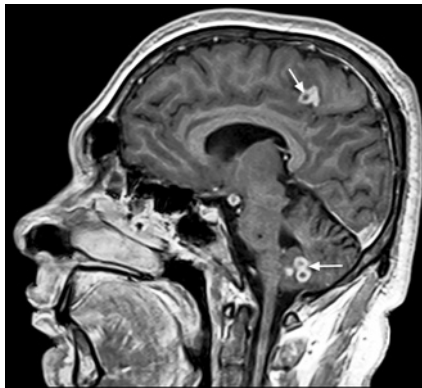


Fig. 10.4: Contrast-enhanced T1-w sagittal image of the brain shows multiple ring enhancing lesions (arrows) suggestive of tuberculomas

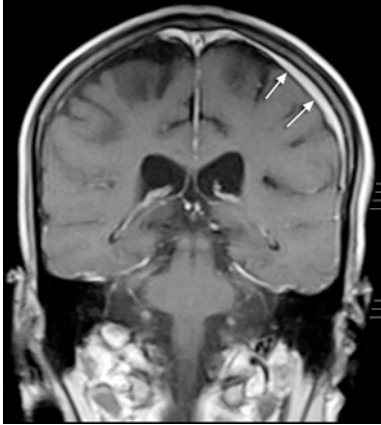


Fig. 10.5: Contrast-enhanced T1-w coronal image of the brain shows thick asymmetric enhancement of the meninges over the left parietal convexity (arrows)



Figs 10.6A and B: Postoperative spine. (A) T2-w sagittal image of the spine shows prominent disk herniation at L4-5 level (arrow). Note evidence of laminectomy at the same level. (B) Contrast-enhanced T1-w sagittal image of the spine shows non-enhancement of the disk at L4-5 level (arrow), confirming the disk rather than a scar. A scar will show enhancement

Spine: Contrast injection is indicated in postoperative spine to differentiate between scar and disk. Scar being a vascular structure will enhance while disk usually will not enhance (Fig. 10.6). Gd increases visualization of leptomeningeal metastases and may differentiate tumor syrinx from congenital/traumatic syrinx. In vertebral body metastases Gd injection can be avoided as it does not improve the lesion characterization.

Body Imaging: Even though body MR imaging has high intrinsic tissue contrast, Gd is useful in viable versus necrotic lesion, for identification of active infection and in recurrent neoplasm. It may help in differentiating benign from malignant lesions. Gd is used in breast, liver, spleen, kidney and musculoskeletal pathology, especially neoplastic. Dynamic imaging during gadolinium injection can be performed to characterize liver and breast lesions. Gd is used in stress perfusion and myocardial viability in cardiac MRI.

Principles of Interpretation: Neuroimaging

CHAPTER 11

To be able to interpret MR images, apart from detail anatomical and pathological knowledge, knowing basics of pulse sequences and signal intensities of various tissues on different sequences is essential. In this chapter, signal intensities of various normal structures and choices of sequences for various clinical situations in neuroimaging will be discussed.

Normal Signal Intensity

Signal intensity of any structure depends on density of protons (hydrogen ions) in that structure, longitudinal relaxation time (T1), transverse relaxation time (T2), and flow and diffusion effects. Most intense signals are received from tissues with short T1 and long T2 and high proton concentration. Conversely, lowest signal intensity is seen in tissues with long T1, short T2 and low proton concentration. All these factors decide appearance of the tissue, structure or lesion on particular sequence. Water has long T1 and long T2 and it appears dark on T1-weighted and bright on T2-weighted images. Fat has short T1 and short T2 and it appears bright on T1-weighted and less bright on T2-weighted images. In spite of its short T2, fat does not turn dark on T2-weighted images because of its high proton content.

Air is dark on all sequences because of very low hydrogen proton concentration. Cortical bone is also dark on both T1 and T2-weighted images because of very low mobile protons. Appearance of medullary bone depends on the degree of fat replacement. Circulating blood in

the vessels will be seen as flow void (dark) on spin echo sequences and bright on gradient echo sequences (for the mechanism, refer to chapter 14 on MR angiography).

Calcifications are usually dark on both T1 and T2-weighted images with some exceptions. Lesions having high content of proteinaceous material, methemoglobin (subacute hemorrhage) and cholesterol debris appear bright on T1-weighted images. Some lesions of basal ganglia that are bright on T1-weighted images include hyperintense globi palladi in hepatocellular degeneration, manganese deposition in parenteral nutrition, some calcifications and foci of abnormal signal intensity (FASI) in neurofibromatosis 1.

The normal white matter (WM) is bright on T1-weighted images as compared to gray matter (GM) because of myelin (lipid) content of WM. On T2-weighted images, GM has high signal intensity than WM because of its higher water content. Posterior pituitary has bright signal on T1-weighted images because of neurosecretory granules (Fig. 11.1). Presence of the bright posterior pituitary on T1-weighted images is related to the functional status of the hypothalmo-neurohypophyseal axis. In adult patients, clivus should be seen as homogeneous high signal intensity on T1-w images because of its fatty marrow content.

Signal	On T1-w images	On T2-w images
<i>Dark</i>	Air, cortical bone, stones, some calcifications, flow voids in blood vessels, ligaments, tendons, scar	Air, cortical bone, stones, some calcifications, flow voids in blood vessels, ligaments, tendons, scar
<i>Intermediate</i>	Water (intermediate to low), muscles, gonads, spleen, liver	Muscles, liver, pancreas, hyaline cartilage
<i>Bright</i>	Fat, fatty marrow, proteinaceous material like complex cysts, blood products (methemoglobin), melanin, contrast enhancing tissue	Water, fat, red marrow, proteinaceous material, blood products (oxyhemoglobin and extracellular methemoglobin)

Sequence Selection

Conventionally, T1-weighted images are used to see anatomy and T2-weighted images to see pathology. Majority of diseases are associated with increased T1 and T2 relaxation times with edema hence appear



Fig. 11.1: T1-w sagittal image of the brain. Posterior pituitary is seen as a bright spot in the sella (arrow). Note the bright homogenous clivus (arrowhead) as it contains fatty marrow. Also appreciate the white matter has higher signal intensity than the gray matter

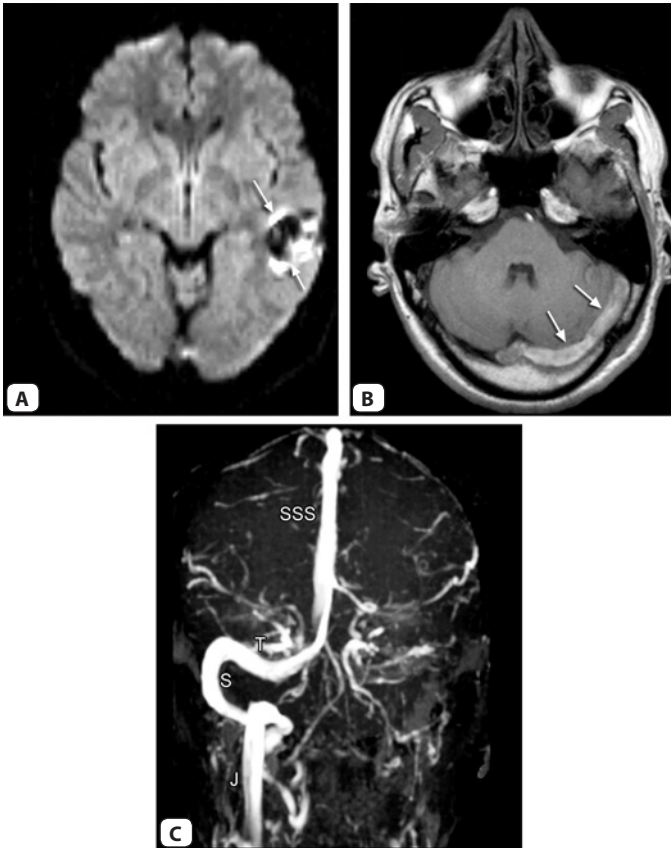
bright on T2-w images. Whatever the reason for scanning, a few basic sequences need to be acquired in all brain examinations. Generally, these sequences include T2-w axial, Diffusion, T1-w sagittal, gradient-echo sequence to detect hemorrhage, T2-w FLAIR axial, and T2-w coronal sequences. Examination usually starts with T2-w images and can be tailored depending on what is seen on it.

Stroke Imaging

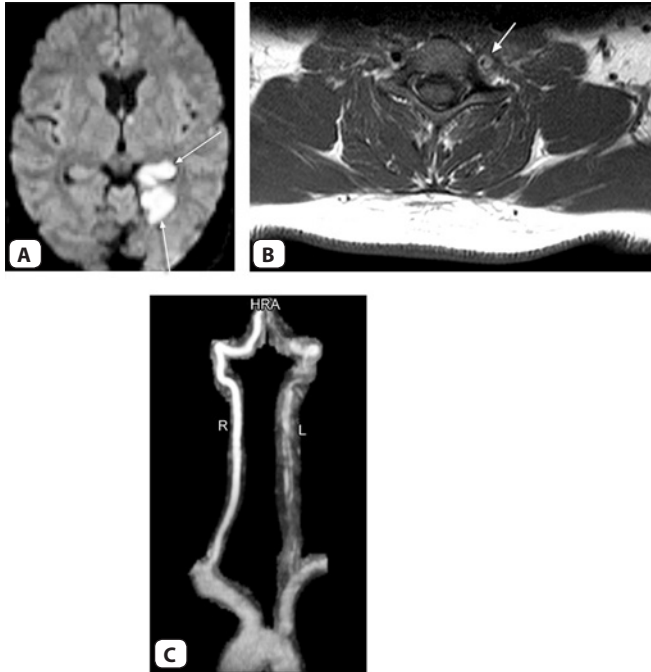
Examination should start with diffusion weighted images that will show acute infarct. Gradient-echo sequence to detect acute bleed should be done next followed by fast FLAIR that shows subarachnoid hemorrhage. Time of flight MR angiography can be done to look for obstruction/stenosis in the vessels. If infarcts are peripheral and hemorrhagic, then phase contrast MR venograms are useful to rule out venous sinus thrombosis (Fig. 11.2). In case of posterior circulation stroke, T1-w fat saturated axial sections of the neck are acquired to look for vertebral artery dissection or thrombosis (Fig. 11.3).

Tumors

MR is the best modality to evaluate brain tumors because of its excellent soft tissue contrast and multiplanar capability. Intravenous

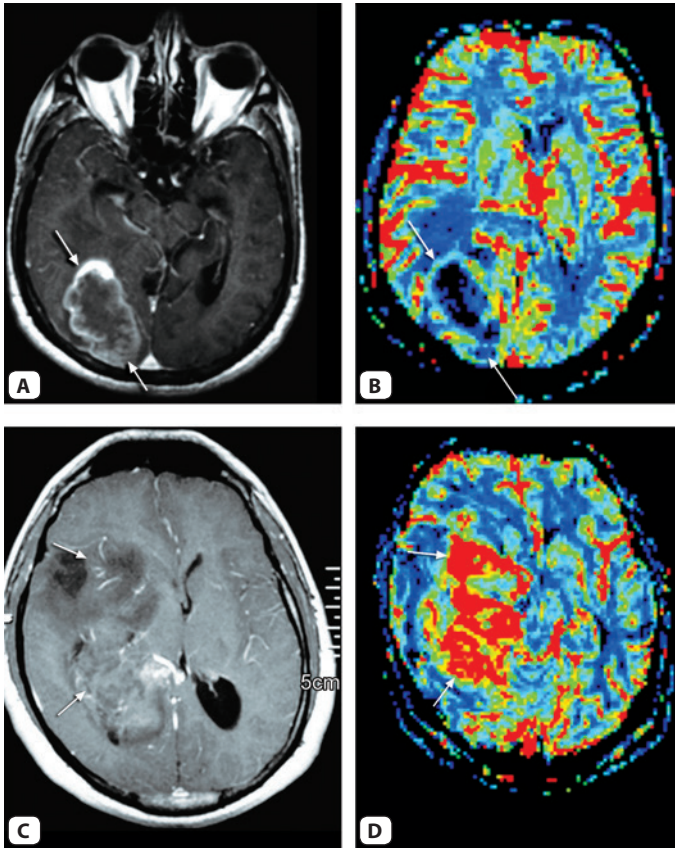


Figs 11.2A to C: Venous infarct. (A) Diffusion weighted axial image of the brain shows haemorrhagic infarct (arrows) in the left temporal region. (B) T1-w axial image of the brain shows hyperintense left transverse sinus (arrows) suggestive of thrombosis. (C) Time of flight (TOF) MR venogram coronal view shows normal right transverse (T), sigmoid sinus (S) and Jugular vein (J) as well as the superior sagittal sinus (SSS). Left sided transverse, sigmoid sinuses and jugular vein are not visualized in keeping with thrombosis



Figs 11.3A to C: Posterior circulation stroke. (A) Axial diffusion weighted image shows an acute infarct (arrows) in the left PCA territory. (B) Axial T1-w image of the neck shows vertebral artery dissection on the left side (arrow). (C) TOF MR Angiogram shows dissection in the left vertebral artery (L)

gadolinium injection is essential for the evaluation of brain tumors. Tumor enhancement suggests break in the blood-brain barrier and does not necessarily represent tumor vascularity (Fig. 11.4). Tumor vascularity is evaluated with MR perfusion. MR perfusion and spectroscopy can be helpful in: 1. differentiating neoplastic from nonneoplastic lesions, 2. grading tumors and 3. guiding the appropriate biopsy site. Spinal cord screening should be done in tumors like ependymoma, medulloblastoma, hemangioblastoma, choroids plexus tumors to rule out 'drop metastases' in the spinal canal.



Figs 11.4A to D: Tumor vascularity. (A) T1-w postcontrast axial image of the brain shows enhancing tumor in the right occipital lobe (arrows). (B) MR Perfusion CCBV map (in the same patient shown in A) shows the lesion to be hypovascular (arrows). Red color corresponds with high perfusion while blue or dark color is suggestive of least perfusion. (C) T1-w postcontrast axial image of the brain in another patient shows predominantly non-enhancing tumor in the right cerebral hemisphere (arrows) causing mass effect and midline shift. (D) MR Perfusion CCBV map (in the same patient shown in C) shows the tumor to be hypervascular (red area marked by arrows)

Infection

As in tumor, intravenous gadolinium injection is helpful in the evaluation of CNS infection. Contrast enhanced MR is superior to the contrast enhanced CT in CNS infection because it shows dural enhancement and thickening better (Fig. 11.5). However, MR is inferior to CT in chronic and congenital infectious processes in which presence of calcifications is a major finding.

Epilepsy

Imaging is performed in epilepsy patients to rule out tumors or cortical dysplasia as a cause of epilepsy. Apart from this, the areas of focus in epilepsy, especially partial complex seizure (associated with loss of consciousness), are temporal lobes and the hippocampus. The imaging of hippocampus should involve oblique coronal sections that are roughly parallel to the anterior surface of the pons such that bilateral hippocampi are seen in true cross section. Side-to-side symmetry of the hippocampus for comparison is judged by cochlea appearing symmetrical on a single image. Oblique coronal sequences (Fig. 11.6) include T2-w, FLAIR, medium T1 inversion recovery and T1-w 3D GRE. FLAIR images show small epileptogenic foci in the cortex and signal abnormalities in the mesial temporal sclerosis. Medium T1 inversion

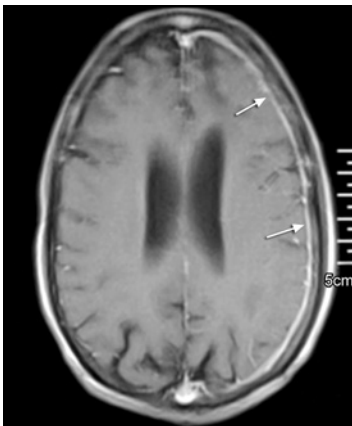
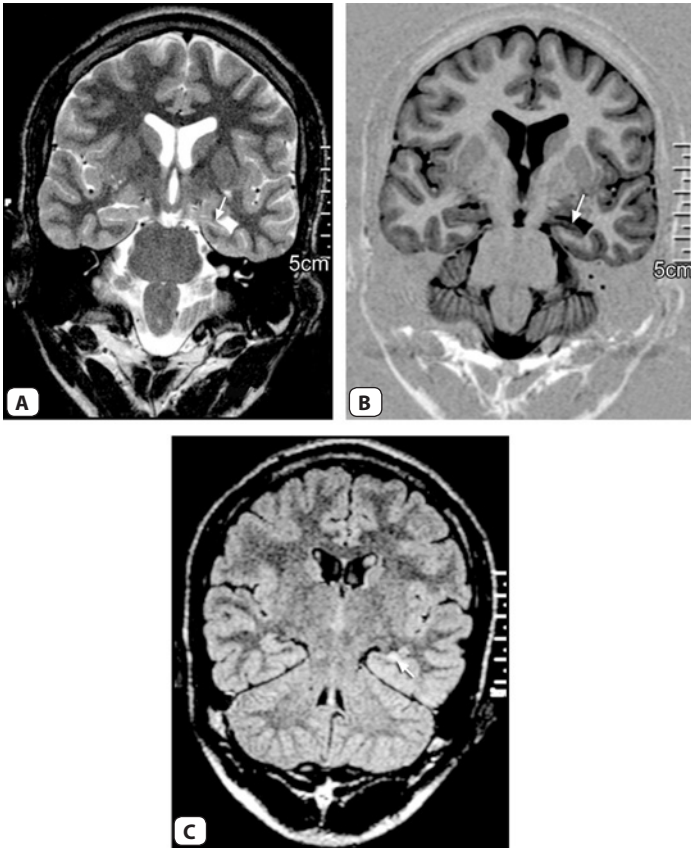


Fig. 11.5: T1-w postcontrast axial image of the brain shows enhancing meninges over the left cerebral hemisphere (arrows)



Figs 11.6A to C: Epilepsy protocol. (A) T2-w oblique coronal image of the temporal lobes shows the left hippocampus to be atrophic (arrow). Note increased size of the left temporal horn of the lateral ventricle. (B) Medium TI inversion recovery (IR) oblique coronal image of the temporal lobes shows the atrophic left hippocampus (arrow). Note excellent gray white differentiation in this image. (C) FLAIR oblique coronal image of the temporal lobes shows the atrophic as well as hyperintense left hippocampus (arrow). These findings are suggestive of left mesial temporal sclerosis

recovery images show cortical dysplasia and migrational abnormalities well because of their superior gray-white differentiation. They are also good for evaluation of hippocampal architecture. T2-weighted gradient-echo sequence should be included to see any subtle hemorrhage associated with small vascular malformations and trauma. MR findings of mesial temporal sclerosis include hippocampal atrophy, increased signals on T2-w or FLAIR images and loss of internal architecture.

CP Angle Lesions

All patients presenting with tinnitus, hearing loss and vertigo should have a highly T2-w steady-state sequence called CISS/FIESTA-C that shows dark cranial nerves in the bright CSF. Study should also include MR angiogram to rule out any vascular loop as a cause of tinnitus. Intravenous gadolinium is injected to rule out labyrinthitis and any small enhancing tumor like acoustic neuroma in the internal auditory canal (Fig. 11.7).

Demyelinating Lesions

T2-w images are mainstay for demyelinating lesions and should be acquired in all three orthogonal planes. The lesions near ventricular margin are better seen on FLAIR images as CSF gets suppressed. FLAIR

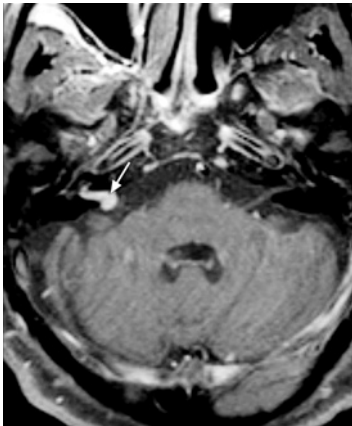
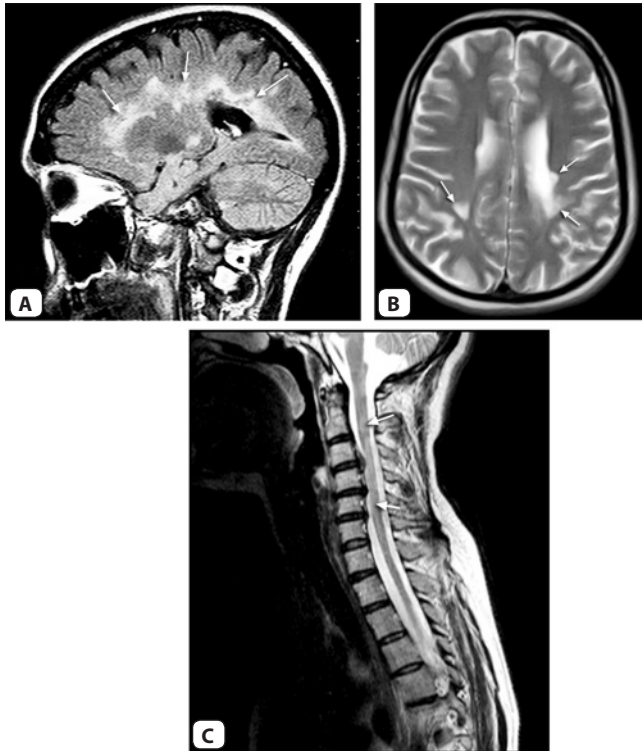


Fig. 11.7: T1-w postcontrast axial image of the brain shows small enhancing acoustic neuroma in the right internal auditory canal (arrow)



Figs 11.8A to C: Multiple sclerosis. (A) FLAIR sagittal image of the brain shows multiple hyperintense plaques running vertically from the corpus callosum margin (arrows) suggestive of 'Dowson's fingers'. (B) T2-w axial image of the brain shows multiple hyperintense plaques (arrows) in periventricular white matter. (C) T2-w sagittal image of the cervical spine shows hyperintense plaques in the spinal cord (arrows)

sagittal images best show callaso-septal lesions of the multiple sclerosis and 'Dowson's finger' running perpendicular to the ventricular margin (Fig. 11.8). The study should include optic nerve evaluation. Spinal cord should be screened in demyelinating lesions to rule cord involvement.

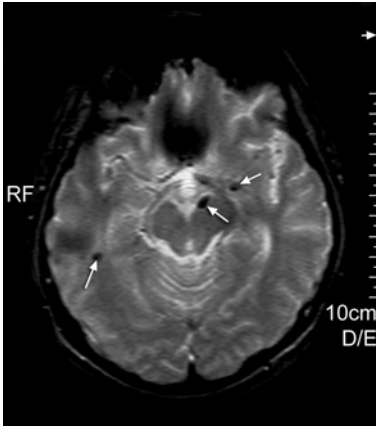


Fig. 11.9: Gradient hemo axial image of the brain shows small petechial hemorrhages (arrows) in this head injury patient suggestive of diffuse axonal injury (DAI)

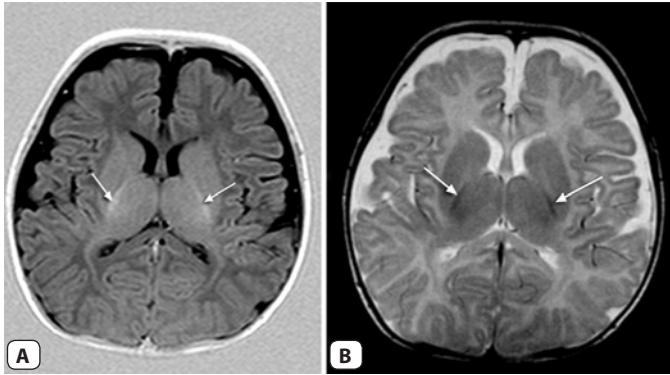
Contrast is given in multiple sclerosis to see the activity of the lesion. Enhancing lesions are usually active.

Trauma

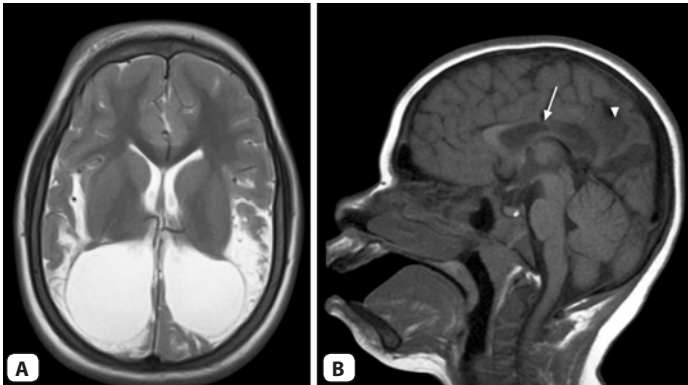
CT is still modality of choice for head injury. CT is convenient, less time consuming and available everywhere. It shows acute bleed and bony fractures easily. If MRI is performed, gradient-echo and T1-weighted images are important in showing acute bleed. MR is useful in evaluation of the diffuse axonal injury and sequelae of the head injury (Fig. 11.9). MR is also useful when CT is indeterminate in posterior fossa lesions.

MRI in Pediatric Brain

Knowledge of stages of normal myelination is important. Myelination progresses caudocranially, dorsoventrally and from center to the periphery. It is usually completed by two years of age. Myelinated white matter appears bright on T1-w and dark on T2-w images (Fig. 11.10). In general, TR of T1 and T2-w sequences should be increased in neonatal brain as it has longer T1 and T2 relaxation time because of its high water content. The sequence that shows the suspected pathology best should be run first, for example diffusion weighted sequence in neonates.



Figs 11.10A and B: Normal myelination in two months old infant. (A) T1-w medium T1 IR axial image of the brain shows myelination in the posterior limb of the internal capsule as bright linear signal (arrows). (B) T2-w axial image of the brain shows myelination in posterior limbs as dark signal (arrow)



Figs 11.11A and B: Perinatal HIE/Hypoglycemic insult. (A) T2-w axial image of the brain shows severe volume loss in occipito-parietal lobes with ex vacuo dilatation of the lateral ventricles. (B) T1-w sagittal image of the brain shows severe volume loss (arrowhead) in the occipital region with severe atrophy of posterior part of corpus callosum (arrow)

These features are suggestive of perinatal hypoglycemic/hypoxic-ischaemic insult

MRI is the modality of choice in pediatric brain tumors, congenital anomalies and hypoxic-ischemic injury (HIE) (Fig. 11.11). Correlation with perinatal and birth history is required as hypoxic-ischemic injury affects periventricular white matter in premature infants while gray matter and water-shed areas are affected in term infants. Diffusion weighted images are useful in showing acute HIE. Metabolic diseases can be evaluated with MR spectroscopy.

Principles of Interpretation: Body Imaging

CHAPTER 12

In this chapter basic concepts including normal signal intensity of various structures and organs, and choice of sequences in musculoskeletal and body imaging are discussed.

Sequences

For the normal signal intensity of various structures please refer to previous chapter 11. Apart from T1-w and T2-w images, one sequence that has made impact on body and musculoskeletal imaging is STIR. It is a short TI inversion recovery sequence in which fat gets suppressed. As majority of pathology have increased water content, they stand out (bright) on STIR sequence. It can be used almost anywhere in the body. Fast sequences like single shot fast spin-echo and balanced SSFP have greater role in body imaging and are important sequences for chest, abdomen, fetal and cardiac imaging. Fat suppression and compensation of motions like respiration, cardiac pulsation and peristalsis are important aspects of body imaging.

Spine Imaging

It is probably the most frequently performed MRI examination at most MR centers. Vertebrae in adult patient are bright on T1-w images because of fatty marrow and moderate to hypointense on T2-w images. Annulus fibrosus is dark on all sequences because of low mobile proton density and acellular nature of fibrous tissue (Fig. 12.1). Nucleus pulposus is low signal on T1-w images and bright on T2-w

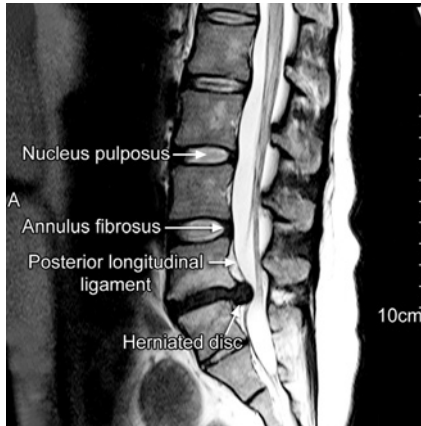


Fig. 12.1: T2-w sagittal image of the spine shows herniated disc at L4-5 level. Note other structures as labeled

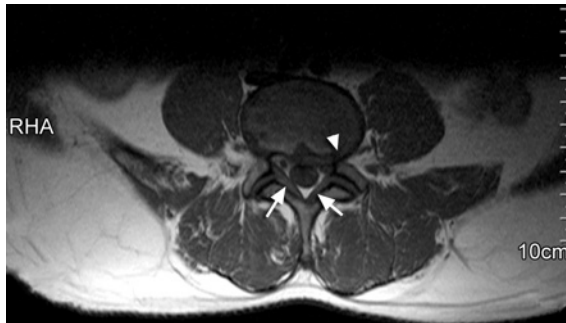


Fig. 12.2: T1-w axial image of the spine shows left posterolateral herniation of the disk encroaching on the neural foramina (arrowhead). There is also hypertrophy of the ligamentum flavum (arrows)

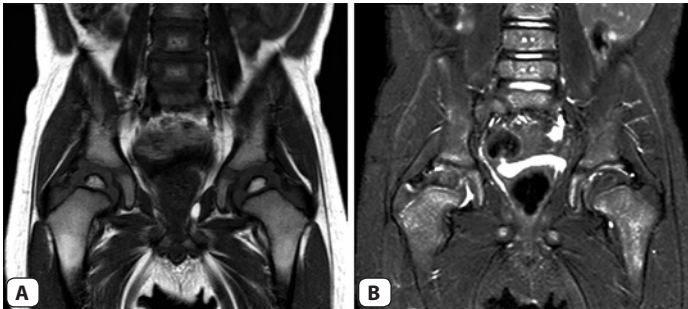
images because of its high water content. A central dark horizontal internuclear cleft seen in the nucleus pulposus on T2-w images is a normal finding in adults above 30 years of age. Ligaments are dark on all the sequences. The spinal cord has higher signal than CSF on T1-w images and lower signal than CSF on T2-w images. Apart from T1-w (Fig. 12.2) and T2-w axial and sagittal images, STIR should be acquired

in patients with vertebral focal lesion, trauma or marrow abnormalities. T2-w sagittal images of the whole spine should be acquired for counting vertebrae. In a patient with low backache if lumbosacral spine is normal then sacro-iliac joint screening should be done as the cause for the pain might be there. Single-shot FSE myelogram in lumbar spine gives gross idea of the thecal sac in a few seconds.

In postoperative spine, intravenous Gadolinium injection needs to be given as it helps differentiate scar from the recurrent disc prolapse. Scar being a vascular structure enhances in early phase while disc does not enhance in early phase (within 20–25 minutes). Some times though the scar and disc are mixed and disk can show enhancement because of infiltration by the granulation tissue.

Marrow Imaging

The MRI is the most sensitive method for marrow imaging. Yellow marrow is bright on T1-w images because of its fat content and moderate to iso-intense on T2-w images. Red marrow, which contains hematopoietic tissue, is iso to hypointense on T1 and bright on T2-w images (Fig. 12.3). As a child grows, there is gradual conversion of red marrow



Figs 12.3A and B: T1-w (A) and T2-w fat saturated (B) coronal images of the pelvis in a 2-year-old child. The femoral epiphyses are bright on T1-w and dark on T2-w fat sat images as they contain fatty marrow. The red marrow in the femoral metaphyses is iso-to-hypointense on the T1-w image and mildly hyperintense on T2-w image



Fig. 12.4: STIR coronal image of the SI joints in a patient of sacroiliitis. Arrows indicate marrow edema

into yellow marrow from appendicular to axial skeleton such that in adults red marrow is present only in the axial skeleton like vertebrae, rib cage, sternum, skull and pelvis, and proximal metaphyses of femora and humeri. Epiphyses and apophyses almost never have red marrow and are last to reconvert into red marrow in hematopoietic crisis. Therefore, dark epiphyses and apophyses on T1-w images suggest a severe hematopoietic disease. T1-w images are very useful in the marrow evaluation. The red marrow has lower signal intensity than fat but higher signal intensity than muscles on T1-w images. A marrow darker than that of muscle or intervertebral disks on T1-w images is always abnormal. Malignant lesions are either isointense or dark than red marrow on T1-w images. STIR and other fat suppressed T2-w images are also useful for marrow pathology. Marrow edema is best seen on STIR images (Fig. 12.4). Marrow involvement by neoplasm, infection or subtle trauma is earliest picked up by MRI especially with STIR sequence (Fig. 12.5). It requires more than 30% bone destruction by bone pathology to be visible on a plain radiograph. A metastatic lesion is seen as a hypointense lesion against the background of bright fatty marrow on T1-w images. This is, however, not a specific appearance because myeloma, lymphoma or infective lesions are also dark on T1-w images. Gradient-echo images should not be used for marrow imaging as marrow edema and pathology can get obscured by susceptibility amongst bony trabeculae (Fig. 12.6).

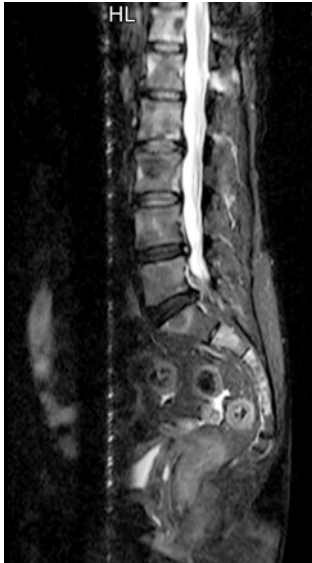
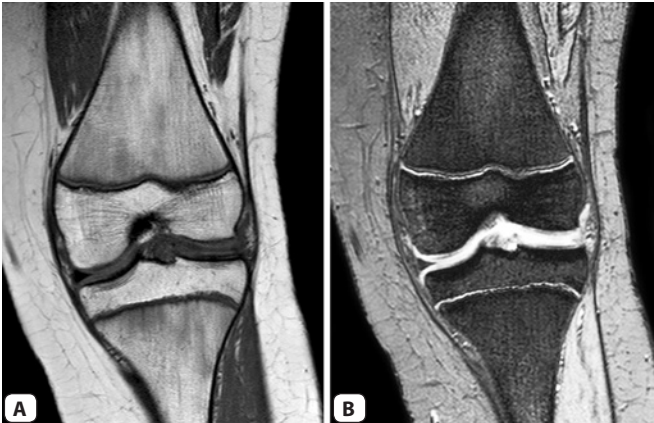


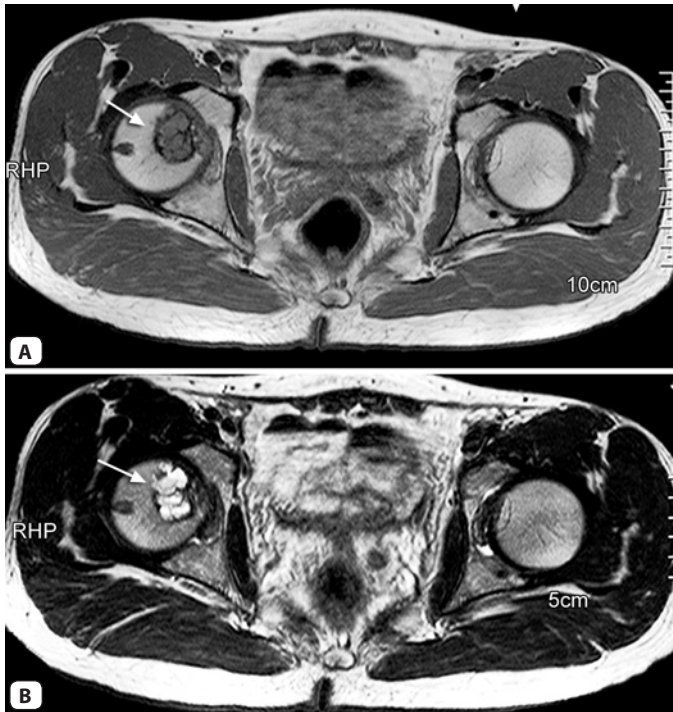
Fig. 12.5: STIR sagittal image of the lumbar spine shows multiple bright spots in vertebral bodies and posterior elements suggestive of metastases in this patient with known malignancy



Figs 12.6A and B: Coronal T1-w (A) and T2-FFE GRE (B) images of the knee joint in a teen-age boy. Patchy hypointense marrow changes in the metaphysis of the femur and tibia are only appreciated on the T1-w image. The marrow changes are not seen on the GRE image

Musculoskeletal Neoplasms

The MRI plays important role in evaluating extent, staging and treatment planning in MSK tumors. Cortical bone, ligament, tendon and fibrous tissue display low signal intensity on all sequences because of lack of mobile protons and relatively acellular matrix. Muscles have moderate signal intensity on T1-w and low signal intensity on T2-w images. Fat is bright on T1-w images and moderate signal intensity on T2-w images. Osteoid matrix is dark on all sequences while chondroid matrix shows



Figs 12.7A and B: Chondroid matrix in a patient with chondroblastoma. (A) T1-w axial image of the pelvis shows an intermediate signal intensity lesion in the head of the right femur (arrow). (B) T2-w axial image of the pelvis shows the same lesion as bright lesion (arrow) because of its chondroid matrix

moderate signal intensity on T1-w and high signal intensity on T2-w images (Fig. 12.7). Nonosseous tumors are usually low signal intensity on T1-w and high signal intensity on T2-w images. These signal intensity characteristics are used to differentiate tumors and for evaluating the extent and staging. Marrow involvement is better appreciated on T1-w and STIR images. The bone affected by the tumor should be imaged in its entire extent along with the joints it forms on both ends. This is important to rule out skip lesions as well as surgical planning. Intravenous contrast injection is essential in musculoskeletal tumors as it improves the depiction of lesion margin, presence of necrosis, cyst formation and tumor vascularity assessment.

Joint Imaging

The MRI is the best imaging modality for evaluation of joint pathology as it shows ligaments, cartilages and joint effusion very well. Infection, neoplasm, trauma and arthritis are best evaluated with MRI. Apart from T1 and T2-w images in orthogonal planes, PD, STIR and cartilage-sensitive GRE sequences are useful for the joint imaging. Marrow edema, fluid collections and bursal inflammation are best seen on STIR or T2-w fat suppressed images. Ligaments and menisci are best seen on proton-density images. Cartilage-sensitive gradient-echo sequences show articular cartilage as a moderate signal intensity structure (Fig. 12.8). MR arthrogram can be performed for recurrent dislocation of shoulder and perthes disease of the hip joint for detailed evaluation of labrum, ligaments, joint capsule and articular cartilages.



Fig. 12.8: Coronal T2 FFE image of the knee joint shows articular cartilage as an intermediate to high signal intensity structure (arrows)

Abdominal Imaging

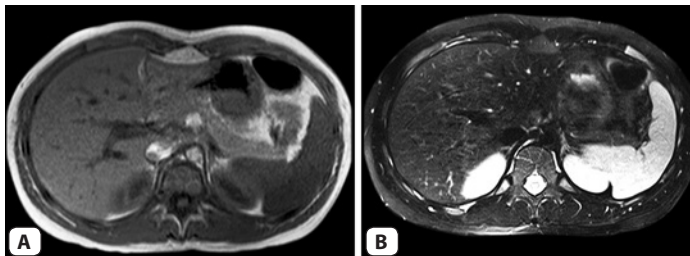
Liver has shorter T1 and T2 relaxation time than spleen hence it is brighter than the spleen on T1-w images and low in signal intensity than the spleen on T2-w images (Fig. 12.9). Iron or copper accumulation in the liver makes it dark, especially on T2 and T2*-w images.

Magnetic resonance cholangiopancreatography (MRCP) has become an important noninvasive method to evaluate biliary and pancreatic tree. Heavily T2-w sequences (with high TE above 700-800 ms) like single-shot FSE and 3D FSE sequences are used for the MRCP. These sequences can also be used to evaluate other slow moving or stable fluids like ureters in the MR urogram and thecal sac in MR myelogram.

For solid organ imaging, proper FSE sequences are preferred while for bowel imaging faster sequences like single-shot FSE and balanced SSFP are used. Gradient-echo steady state sequences such as balanced SSFP/True FISP are motion insensitive and can be acquired with breath-hold. They provide good quality images of abdomen for evaluation of gross anatomy of organs and vessels (Fig. 12.10). T1-w 3D GRE sequences like VIBE/THRIVE/LAVA images can be used for pre and post-contrast dynamic imaging of the abdominal organs. Images of the liver in arterial, portal venous and equilibrium phases during the intravenous injection of contrast can be acquired using these sequences.

Pelvic Imaging

The MRI is much superior to CT in the evaluation of pelvic pathology, both in male and female. It is the best modality to stage tumors of urinary bladder, prostate and uterus. Prostate zonal anatomy is well



Figs 12.9A and B: MR abdominal imaging. Axial T1-w GRE in-phase (A) and T2-w fat saturated (B) images of the abdomen show the signal intensity of the liver higher than spleen on the T1-w image and lower on the T2-w image



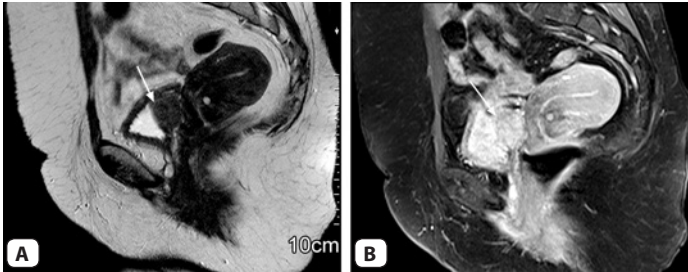
Fig. 12.10: Abdominal imaging. True FISP axial image shows vessels, fluid (CSF) and fat as bright structures. Note the lack of movement artifacts on the image as this sequence is intrinsically motion insensitive and very fast



Fig. 12.11: Prostate Imaging. T2-w axial image of the prostate shows dark central zone and bright peripheral zone

seen on T2-w images. Inner central zone is seen as lower signal intensity while the peripheral zone has hyperintense signal (Fig. 12.11). Any low signal intensity focus in the peripheral bright zone in an old patient may represent carcinoma of the prostate.

T2-w images are useful in depicting the anatomy of urinary bladder wall. Bladder wall is seen as low signal intensity smooth structure against high signal intensity of urine on T2-w images (Fig. 12.12). Visualization of the low signal intensity line between tumor and perivesical fat is an important feature in the tumor staging, differentiating T3a from T3b



Figs 12.12A and B: Bladder Imaging. (A) T2-w sagittal image of the pelvis shows a well defined mass along the posterior wall of the urinary bladder (arrow). (B) Post-contrast T1-w sagittal image shows enhancement in the mass (arrow) This mass turned out to be a leiomyoma of the bladder

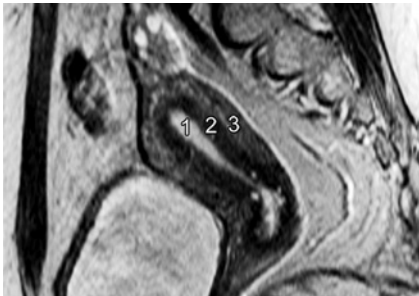


Fig. 12.13: Uterine Imaging. Trilaminar pattern. 1 = Endometrium; 2 = Junctional zone-inner myometrium and 3 = Outer myometrium

stage. Papillary intraluminal growth, however, is well seen as high signal intensity lesion in the low signal urine on T1-w images.

Characteristic trilaminar zonal architecture of the adult uterus seen on T2-w (Fig. 12.13) has helped to stage uterine carcinomas better. The normal endometrium and endometrial cavity are seen as high signal intensity central stripe. Intermediate low signal intensity junctional zone represents an inner layer of myometrium containing increased number of myometrial cells and increased density of compact muscle fibres. Peripheral zone is of intermediate signal intensity and represents outer myometrium. The same pattern continues into the cervix. However, an extra layer of low signal intensity may be seen surrounding bright endometrial stripe on high resolution images probably representing mucosa and infolded plica palmatae.

Section 2

CHAPTER

13

3-Tesla MRI

The 3T MRI has become more widespread in last few years and it is establishing its own role in imaging of various body areas. This chapter is overview of technical differences between 1.5 T and 3T, safety issues, artifacts and comparison of some of the clinical applications where 3T takes an edge over 1.5T.

Physics Differences

Technical differences between 1.5 and 3T are summarized in the Table.

Differences between 1.5T and 3T MRI		
Parameters	1.5 T	3T
Larmor frequency	63.9 MHz	127.8 MHz
Chemical shift	220 Hz	440 Hz
In and out-of-phase TEs in milliseconds	In-phase: 4.5, 9.5, 14.5, ... Out-phase: 2.3, 6.9, 12, ...	In-phase: 2.3, 4.5, 6.8, ... Out-phase: 1.1, 3.4, 5.7, ...
Susceptibility	Less compared to 3T	Increased compared to 1.5T
Field Inhomogeneity	Less	Difficult to achieve homogeneous magnetic field especially RF field (B1)

Contd...

Contd...

Differences between 1.5T and 3T MRI		
Parameters	1.5 T	3T
T1 relaxation time	Less as compared to 3T	T1 is increased by ~25% at 3T
T2 relaxation time	More as compared to 3T	T2 is reduced at 3T by ~10-15%
Specific Absorption rate (SAR)	Less as compared to 3T	SAR is increased fourfold at 3T
Signal-to-noise ratio (SNR)	Less as compared to 3T	SNR is doubled at 3T

Artifacts

Because of increased susceptibility, chemical shifts and difficulty to achieve homogeneous field at 3T, generally there are more artifacts at 3T as compared to 1.5T. Flow artifacts from vessels and CSF, movement artifacts, chemical shift-related artifacts and susceptibility artifacts (Fig. 13.1) are more commonly seen at 3T. Standing wave occurs at high field strength from reflection of RF waves at high conductivity gradient surfaces such as abdominal or chest wall resulting into artifactual signal reduction in the intermediate area between the center and the periphery of FOV. This artifact is called standing wave or dielectric artifact and it is increased in presence of metals, ascites and large abdomen. This artifact can be reduced by using dielectric cushions such as ultrasound gel and improving the magnetic field homogeneity.

Safety Issues

SAR is increased fourfold at 3T as compared to 1.5T. Some of the ways to reduce SAR include increasing TR, decreasing flip angle, use of parallel imaging, using bore fan to prevent excess heating and minimizing use of saturation band. There is increased potential of harmful effects from metal and implants in the body at 3T. Some of the implants and devices which are safe to scan at 1.5T may not be safe at 3T. It is important to check their compatibility at 3T.

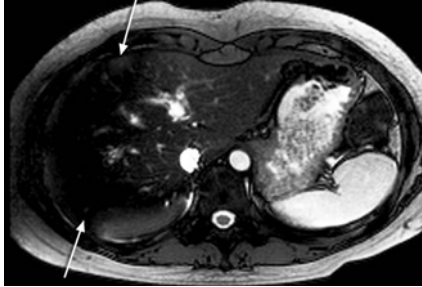
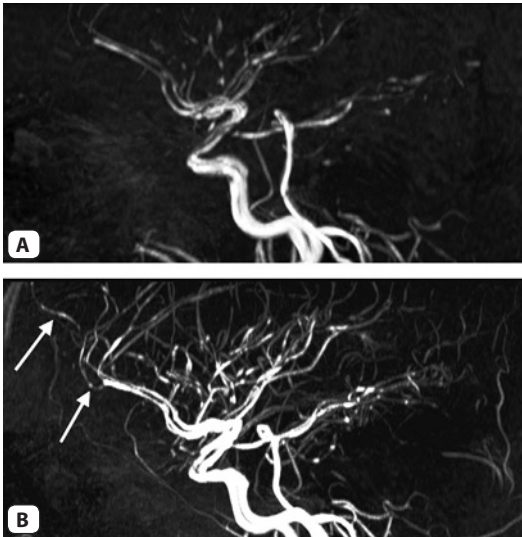


Fig. 13.1: Susceptibility artifact. The axial balanced SSFP image of the abdomen acquired at 3T shows large susceptibility artifact obscuring almost entire right lobe of the liver (arrows)



Figs 13.2A and B: MR angiography at 1.5T (A) versus at 3T (B) Time-of-flight MRA performed at 1.5T (A) and at 3T (B) in a patient with vasculitis on the same day show significantly more number of small vessels on the image acquired at 3T with 'beading' of vessels only appreciated on the 3T images (arrows)

Clinical Applications

Some of the advantages of 3T are countered by more artifacts. In general, T2-w images benefit most from high SNR. Because of increased T1, TR for T1-w images is longer resulting in slightly increased scan time. Gradient sequences have more susceptibility as expected. The double amount of SNR at 3T can be used to reduce the scan time or to get thin-section high resolution images in the same time.

In brain imaging, 3T is superior in epilepsy, inner ear and functional imaging. MR angiography is much superior at 3T with better visualization of small peripheral vessels (Fig. 13.2). High SNR also benefits MRCP with better visualization of small bile ducts. In MSK imaging, high SNR of 3T can be used to get thin-section high resolution images of joints to visualize cartilage and ligaments.

Magnetic Resonance Angiography

CHAPTER 14

MR angiography (MRA) is an attractive option for vascular assessment because of its non-invasiveness, lack of radiation and options to get MRA without contrast injection. In this chapter types of noncontrast MRA, their principles, advantages and limitations, and some newer noncontrast MRA techniques as well as contrast-enhanced MRA are discussed.

Types of MRA

MRA can be broadly divided into noncontrast and contrast-enhanced MRA (CEMRA). CEMRA still remains best method as far as its reliability and accuracy is concerned. However, in many clinical situations, for example evaluation of circle of Willis arteries, noncontrast MRA is sufficient to answer clinical queries. Also, because of concerns for complications of gadolinium-based contrast media especially nephrogenic systemic fibrosis (NSF) noncontrast MRA are gaining importance and more research is being done in this area.

Noncontrast MRA (NCMRA) can be broadly divided into black blood and bright blood imaging.

Black Blood Imaging: In these techniques blood appears black as these are spin-echo sequence based techniques (Fig. 14.1). In a spin-echo sequence protons that receive both 90° excitation pulse and 180° rephasing pulse produce signal. However, protons in the flowing blood usually do not receive either 90 or 180 degree pulse. Hence, signal is not produced and flowing blood appears dark. Slow flow and clot can

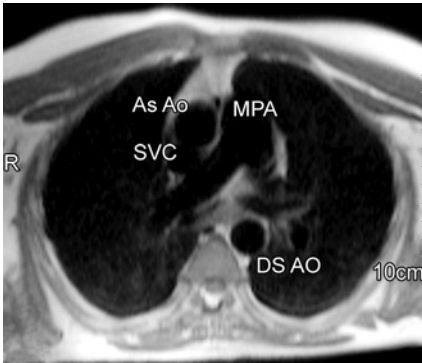


Fig. 14.1: Black blood imaging. All the vessels are dark on this axial HASTE (single-shot fast spin-echo) image of the chest. As Ao = ascending aorta; Ds Ao = descending aorta; MPA = main pulmonary artery and SVC = superior vena cava



Fig. 14.2: Bright blood imaging. All the vessels are bright on this axial TrueFISP image of abdomen, which is a gradient echo sequence

produce signal because they receive both 90 degree and 180 degree pulses.

Bright Blood Imaging: In these types of imaging blood appears bright as most of these are gradient echo based techniques (Fig. 14.2). In a gradient echo sequence excitation pulse is slice selective. But the rephasing, which is done by gradients rather than the 180 degree pulse, is not limited to the slice of interest and is applied to the whole imaging volume. Therefore, a flowing proton that receives an excitation pulse is rephased regardless of its slice position and produces a signal. Moreover, short TR is used in GRE sequences, which results in saturation of protons in the stationary tissues from repeated RF pulses. This increases contrast between the flowing blood and stationary tissues making GRE a more

flow sensitive sequence. There are also spin-echo based techniques that produce bright blood imaging, discussed later.

Noncontrast MRA Techniques

Basic two types of NCMRA commonly used in routine practice include:

1. Time of Flight MRA (TOF-MRA).
2. Phase contrast MRA (PC-MRA).

There are also several new techniques that are being increasingly used and include SSFP-based MRA and ECG-gated fast spin-echo (FSE) MRA.

Time of Flight MRA (Tof-MRA)

In a GRE sequence that uses short TR, protons in the blood flowing freshly into the slice or slab are not saturated (i.e. they have good magnitude of longitudinal magnetization) and produce good signal. On the other hand, the protons in the stationary tissue in the slice or slab get saturated because of repeated RF pulses and do not produce much signal. This results into increased contrast between blood vessels and stationary tissue with the vessels appearing bright. This phenomenon is called *inflow enhancement* and forms the basis for TOF MRA.

The base-sequence used for TOF-MRA is spoiled GRE sequence with gradient moment rephasing. TR is kept less than T1 of the stationary tissues. This saturates (beats down) stationary tissue protons, reducing signal from them.

Protons flowing along a gradient will change their phase because the magnetic field strength is altered along a gradient. If the phase of flowing protons is not maintained then signal will be altered from the flowing protons. To prevent this, gradients are adjusted in such a way that protons will not lose their phase. This technique is called as *gradient moment rephasing* or nulling (GMR).

For the evaluation of arteries protons in the veins are nulled or saturated by applying saturation pulses in the direction of venous flow. For example, for carotid MRA, saturation band is applied superior to the imaging volume.

Limitations of TOF MRA are flow saturation and T1 sensitivity. Protons may get saturated as they pass down the stream in the imaging

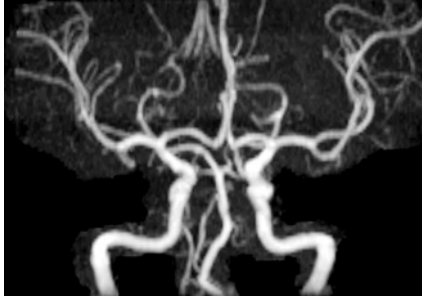


Fig. 14.3: Time of Flight MR Angiography of intracranial arteries, coronal projection

volume because they receive multiple RF pulses. This is more so if the vessel runs in the plane of slice or slab. This results in reduced signal from the vessel. Because of the sensitivity of this sequence to the short T1 tissues, bright signal from these tissues like fat may interfere with the vascular signal. Blood components with short T1 recovery time such as methemoglobin also appear bright on TOF-MRA and can make differentiation of subacute hemorrhage from flowing blood difficult.

TOF-MRA can be of three types—

1. 2D TOF
2. 3D TOF
3. MOTSA (Multiple Overlapping Thin Slab Acquisitions).

In 2D TOF, acquisition is slice by slice. 2D TOF is sensitive to slow flow and a large area can be covered. Hence it is used for slower velocity vessels like peripheral arteries and for venography. Resolution of 2D TOF is lower than that of 3D TOF.

In 3D TOF, acquisition is from whole volume of the tissue. It gives good resolution with better visualization of smaller vessels. It is usually used for high velocity flow. In 3D TOF, there is a higher risk of saturating protons within the volume.

MOTSA combines advantages of 2D (larger area of coverage) and 3D (high resolution). Imaging volume is divided into multiple thin overlapping slabs during the acquisition. These slabs are then combined to a single volume of data (Fig. 14.3) and (Fig. 14.4).

Reformation of angiography: Data from TOF MRA is reformatted by techniques like MIP (maximum intensity projection) or VRT (volume rendered technique) to get angiographic images. In MIP, pixels with maximum intensity are selected while other pixels are suppressed such that only vessels are visualized because they have pixels with maximum intensity. Disadvantage of this technique is overestimation of vessel stenosis. Hence, careful review of source images (axial images) is always recommended before commenting on stenosis.



Fig. 14.4: Time of flight MR angiography of carotid and vertebral arteries, coronal view

Phase Contrast MRA

PC-MRA uses change in the phase of transverse magnetization (TM) of the flowing blood to produce image of the flowing blood. The selective phase shift for the moving protons is produced as follows. The initial RF excitation pulse brings all the protons in phase. Gradient of a given strength is then applied to both stationary and flowing protons that causes phase shift in both stationary and flowing protons but at different rates. A second gradient pulse of the same amplitude and duration but of opposite polarity is applied. In the stationary tissue protons, reversal of the phase shift occurs of exact amount, canceling the effect of original phase shift and resulting into no net phase shift. However, since flowing protons have changed their position, the phase shift will not be corrected. This phase shift is directly proportional to the change in location or distance the protons travel between applications of first and second gradients. This phase shift is used by PC-MRA to create angiographic image and to measure flow velocity.

Velocity encoding gradients are applied in one or all three directions to acquire quantitative information. Velocity encoding technique compensates for projected flow velocity within the vessel by controlling the amplitude or strength of the bipolar gradient. If velocity encoding

(VENC) is selected lower than the velocity within the vessel, aliasing occurs. Aliasing results in low signal intensity in the center of the vessel and better delineation of the vessel wall. Typical values of the VENC are—

20–30 cm/s for venous flow

40–60 cm/s for higher velocity with some aliasing

60–80 cm/s to determine velocity and flow direction.

PC-MRA also provides information about flow direction. If flow is encoded from superior to inferior, flow from the head appears bright whereas flow from feet appears black. PC-MRA can be in 2D or 3D acquisition. 2D is more commonly used in routine practice because of its acceptable acquisition time of 1–3 minutes.

Time of flight MRA	Vs	Phase contrast
Inflow enhancement forms the basis for TOF MRA	1.	Selective phase shift in flowing protons by application of gradients forms the basis for PC MRA
Background signals are not completely suppressed	2.	Background signals are completely suppressed
Direction dependant, slice plane should be perpendicular to the vessel	3.	Independent of flow direction
Less effective with slow flow because of progressive saturation	4.	PC-MRA is good for slow flow because there is no saturation
Vessels flowing in the plane of slice show saturation hence poor signal from them	5.	No in-plane saturation, therefore, sensitive to flow within FOV. Images can be acquired in the plane of vessels
No quantification of flow	6.	Can quantify the flow
Useful for rapid blood flow like extracranial carotids	7.	Useful for studying small tortuous intracranial arteries and veins, especially when the blood flow is slow and in-plane (Fig. 14.5)
Less sensitive to flow turbulence	8.	More sensitive to turbulence
Sensitive to T1 effects hence intravascular contrast media like Gadolinium can be given	9.	Gadolinium cannot be used with the phase contrast MRA

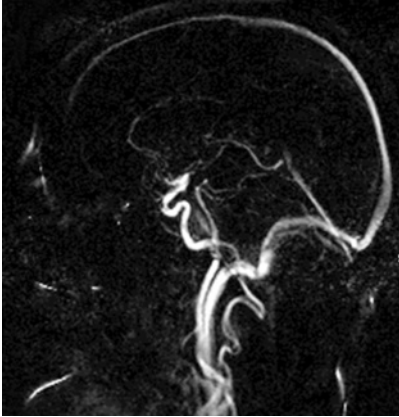


Fig. 14.5: Phase Contrast Venography of intracranial venous system, sagittal view

ECG-Gated FSE MRA

In this ECG-gated fast spin-echo technique, images of the vessels are acquired during diastole and systole. On the 'diastole' image both artery and vein are bright. On the 'systole' image the artery is dark due to fast flow while vein remains bright due to slow flow. The 'systole' images are subtracted from the 'diastole' images giving the bright blood arteriography. The vein and background are subtracted. Advantages of this technique include relatively short-time, sensitivity to slow flow and ability to acquire in coronal plane parallel to the vessels. It may not be suitable for patients with arrhythmia. It is mainly used for peripheral arteries and aorta. Examples include FBI (fresh blood imaging, Toshiba), NATIVE SPACE and NATIVE HASTE (Siemens), TRANCE (Philips) and Flow prep.

SSFP-Based MRA

Balanced SSFP sequences are gradient echo steady-state sequences with very high SNR and motion insensitivity due to balanced gradients in all three directions. These sequences are called TruFISP (Siemens), FIESTA (GE) and balanced-TFE (Philips). The contrast is determined by T2/T1 ration giving the blood very high signal without dependence on inflow. Veins, other fluid and fat are also bright on this sequence.

Hence some form of subtraction is required. Arterial spin labeling (ASL) or inversion recovery pulses are used for this purpose. Examples include Time SLIP (spatial labeling inversion pulse, Toshiba), NATIVE TrueFISP (Siemens) and IFIR (inflow inversion recovery, GE). These techniques can be used for renal arteries and other abdominal arteries. Limitations include relatively complex imaging and susceptibility to field inhomogeneities.

Contrast Enhanced MRA (CEMRA)

The sequence used for CEMRA is usually a modified T1-weighted spoiled gradient refocused GRE sequence (Fig. 14.6). Approximate T1 times of blood, muscle and enhanced blood are 1200 ms, 600 ms and 100 ms respectively. A dose of approximately 0.2 mmol/Kg of gadolinium is required to make T1 of blood shorter than that of fat and muscle, so that it will appear brighter than fat. The most important aspect in CEMRA is timing of peak arterial enhancement such that it will fill center of the K-Space that is responsible for contrast in the image. The time to fill the center of the K-Space is usually the initial 2–3 seconds of the typical 15–20 seconds run. It is important to match these 2–3 seconds with peak arterial enhancement to get good angiogram. Keyhole imaging (see chapter 6) can be applied to CEMRA to improve the temporal resolution. Examples of this time-resolved MRA technique include TRICKS (GE) and TWIST (Siemens).

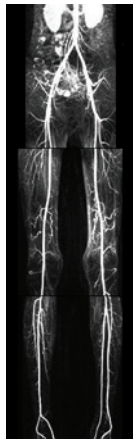


Fig. 14.6: Contrast Enhanced MR Angiography (CEMRA) of lower limb arteries

Magnetic Resonance Diffusion

CHAPTER 15

Diffusion weighted imaging (DWI) is an important imaging technique that is very useful in various diseases in all the body parts. It forms the integral part of brain imaging protocols and is expanding its role in the various areas of body imaging. Principles, technique and clinical applications of DWI are discussed. Also discussed are principles of diffusion tensor imaging (DTI).

What is Diffusion?

Diffusion means random movement of the water protons. The process by which water protons diffuse randomly in the space is called as *Brownian motion*. The water protons diffuse to dissipate their thermal energy. The difference in the mobility of water molecules between tissues gives the contrast in diffusion weighted imaging and helps to characterize tissues and pathology.

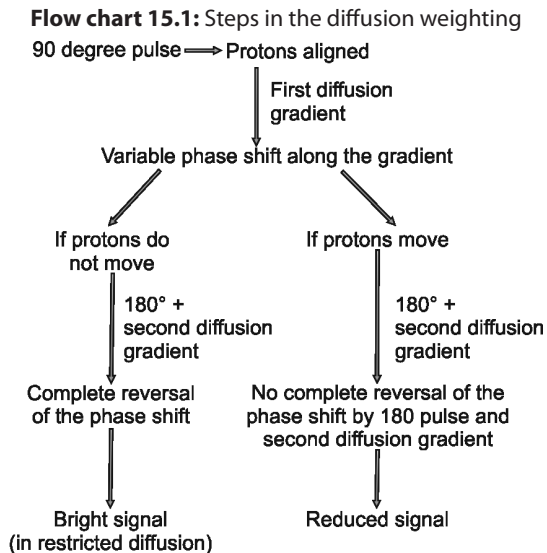
In the **Isotropic** diffusion, possibility of a water protons moving in any one particular direction is equal to the probability that it will move in any other direction (isotropy = uniformity in all directions).

In **Anisotropic** diffusion, water diffusion has preferred direction. Water protons move more easily in some direction than other.

Isotropic diffusion forms the basis for routine DWI while anisotropic diffusion forms the basis for diffusion tensor imaging (DTI) or tractography.

How do we Acquire Diffusion Weighted Images?

The “stejskal-Tanner pulsed gradient spin echo sequence” was the first experimental sequence described for the acquisition of DWI and forms the basis for all DWI performed today. It is a T2-w spin echo sequence with diffusion gradients applied before and after the 180 degree pulse (Fig.15.1). Currently diffusion gradients can be applied to various sequences but they are most commonly applied to the echo planar (EPI) sequence with infinite T2. Steps in the diffusion weighting are outlined in the Flow chart 15.1 below.



A few terms and concepts including b-value, diffusion trace, ADC and T2 shine through are discussed below.

The b-value

The b-value indicates the magnitude of diffusion weighting provided by the diffusion gradients. It also indicates sensitivity of the sequence to the diffusion. It is expressed in sec/mm^2 . It depends on amplitude,

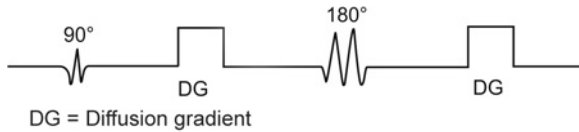


Fig. 15.1: Diagram of 'Stejskal-Tanner' sequence. DG = diffusion gradient

separation and duration of the diffusion gradients. The b-value increases with diffusion gradient strength, duration of their application and time between applications of the two gradients. As the b-value increases the signal from water molecules reduces. At high b-values (e.g. $b = 1000$) only tissues with very high T2 relaxation time or those with restricted motion of water molecules will have high signal.

Diffusion "trace"

Isotropic diffusion forms the basis for the routine diffusion imaging. However, there will be some anisotropy to the movement of water molecules in the tissue and especially in the brain from white matter tracts. To reduce this anisotropy, the image with higher b-value like $b = 1000$ is acquired in three directions along X, Y and Z axes. Diffusion changes along all three axes are then averaged to get a 'trace' diffusion image.

ADC: Apparent Diffusion Coefficient

Apparent diffusion coefficient is a measure of the diffusion. It is calculated mathematically from b-value = 0 and various higher b-value images. Signal attenuation of a tissue with increasing b-value is plotted on a graph with relative signal intensity on y-axis and b-values on x-axis. The slope of the line represents ADC. This is done pixel-by-pixel basis by the computer and is available at a click to the user as images called as 'ADC Map'. The ADC is independent of magnetic field strength. The area with reduced ADC (restricted diffusion) will manifest as a bright area on the diffusion weighted images (DWI) while the same area will turn dark on the ADC map. Quantitative information can also be derived from ADC maps. Drawing region of interest on ADC map gives ADC value of that particular area or tissue expressed in mm^2/sec .

T2 Shine through

The signal intensity of a tissue on DWI (higher b-value images) not only depends on ADC but also on T2 relaxation time of the tissue. The tissues with high T2 can appear bright on DWI even when they are not truly restricted. ADC map helps to differentiate T2 shine through from actual restricted diffusion. The area with true diffusion restriction will turn dark on the ADC map while the area with T2 shine through will remain bright on the ADC map. Another way to deal with T2 shine through is exponential images which are formed by the ratio of DWI images divided by T2-weighted ($b = 0$) images in the same series. These exponential images are called eADC by some vendors (Phillips). Truly restricted area is bright on eADC.

Images available to view

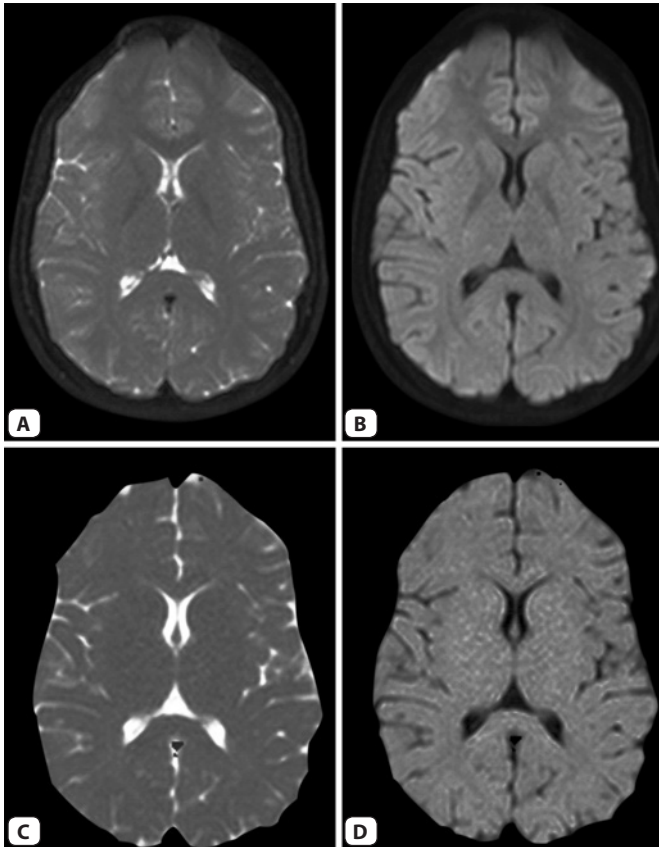
In routine practice, DWI is performed with EPI sequence and the acquisition time is typically less than a minute. With preset post-processing a few sets of images are available for viewing immediately after the acquisition. Depending on the number of b-values used these images typically include $b = 0$ image, higher b-values images and the ADC map. Highest b-value images are considered diffusion weighted images. Some vendors also provide exponential maps, eADC (Fig.15.2).

Clinical Applications of DWI

Neuroimaging Applications

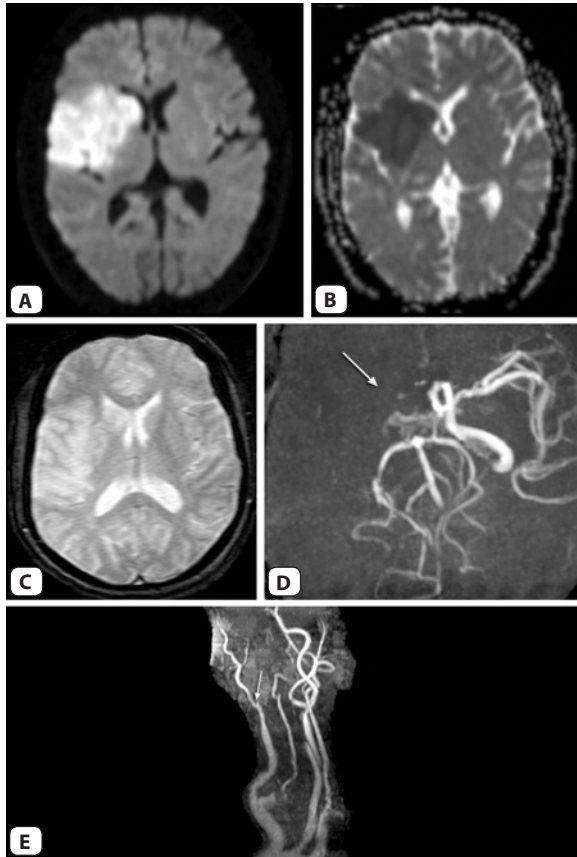
1. Stroke:

There is failure of Na-K ATPase pump in tissue ischemia, which results into influx of extracellular water into the cells. This is called as cytotoxic edema. Since there is a net shift of water molecules from extracellular into more restricted intracellular space, there is overall reduction in the diffusion of water molecules in that area. This will be manifested as bright signal on DWI and dark signal on ADC map. DWI can detect early ischemic tissue as early as minutes to hours. DWI shows the stroke lesion earliest when all other images including T2-weighted images are normal (Fig.15.3). It takes cerebral blood flow (CBF) to drop approximately below 15–20

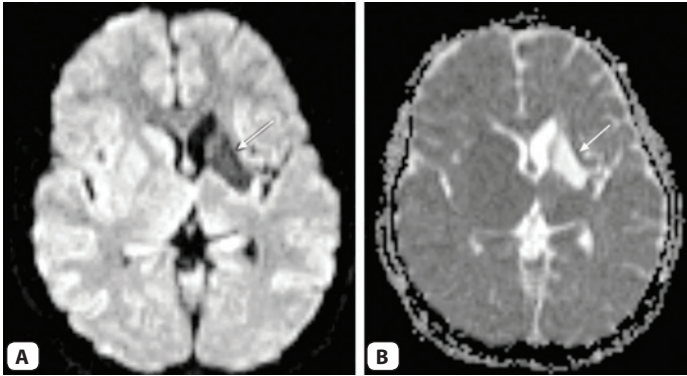


Figs 15.2A to D: Typical diffusion images in a normal brain. (A) b-value- zero image. (B) B-value-1000 image (diffusion weighted image). (C) ADC map (also called dADC). (D) Exponential map (also called eADC)

ml/100 gm of brain tissue/minute to be manifested as bright signal on DWI (reduced ADC). DWI is very useful in detecting hypoxic ischemic injury in newborns which also results in cytotoxic edema in early phase.



Figs 15.3A to E: A typical case of stroke. (A) DWI shows bright area in the right MCA territory. (B) On the ADC map the area turns dark suggestive of acute infarct. (C) On the Gradient Hemo image there is no evidence of any bleeding, making the infarct a non-hemorrhagic. (D) TOF MRA of the circle of Willis shows absence of the right ICA, MCA and ACA (arrow). (E) TOR MRA of carotid arteries shows complete occlusion of right ICA from its origin (arrow)



Figs 15.4A and B: Chronic infarct. A chronic infarct in the left basal ganglion region (arrows) is hypointense on DWI image (A) and bright on ADC map (B)

Contrary to the cytotoxic edema, vasogenic edema means increased fluid in the extracellular space. Since the extracellular space allows more mobility of water molecules there will be increased diffusion, seen as signal attenuation on DWI and increased signal on the ADC map. A chronic infarct is dark on DWI and bright on ADC map (Fig. 15.4).

2. Epidermoid versus Arachnoid cyst

Epidermoid is composed of keratin, debris and solid cholesterol, which provide barrier or hindrance to diffusion of the water molecules. Hence, the epidermoid is seen as a bright lesion on DWI. Since arachnoid cyst is a clear CSF containing cyst, it will not be bright on DWI and will be same as CSF in the signal intensity. DWI can detect a residual epidermoid.

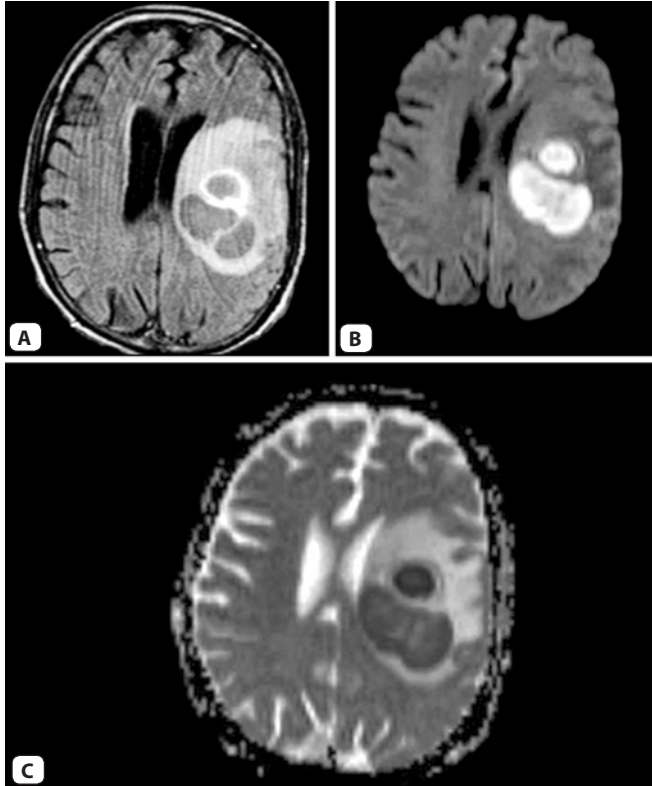
3. Abscess versus simple cystic lesion

An abscess contains thick fluid with hindrances to water diffusion. Hence it shows restricted diffusion, predominantly in the center (Fig. 15.5). Cystic lesion with relatively clear fluid does not show restricted diffusion.

4. DWI in brain tumors

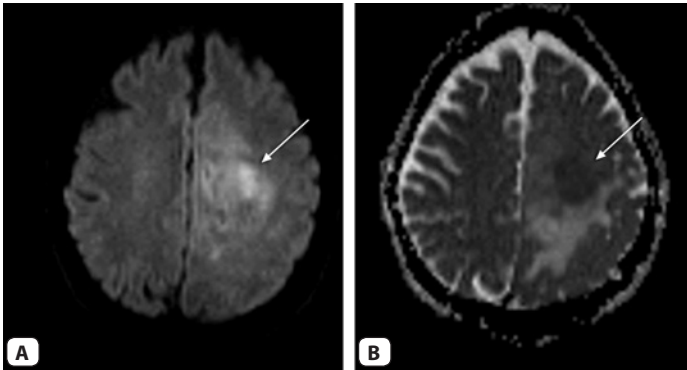
DWI can provide qualitative and quantitative information at cellular level such as cellularity and cell membrane integrity. A tumor with more number of cells and intact cell membranes

will not allow much motion of water molecules and will appear bright on DWI. On the hand, the tumor with less cells and broken cell membrane (for example from chemotherapy) will not be restricted on DWI. DWI can be used to detect, characterize and to assess chemotherapy response in tumors. Some tumors like

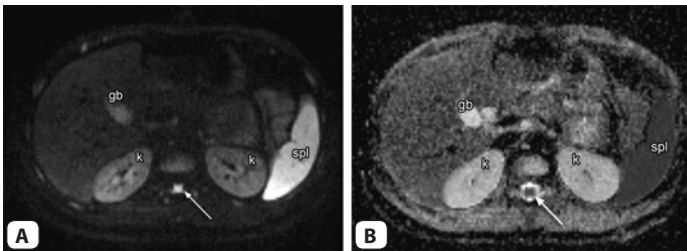


Figs 15.5A to C: Abscess. (A) Axial FLAIR image shows a large abscess in the left cerebral hemisphere. (B) DWI image shows central part of the abscess to be bright. (C) On the ADC map the central part of the abscess turns black suggestive of restricted diffusion. Surrounding edema, which is increased fluid in extracellular space, is bright on FLAIR, low on DWI and bright on the ADC map suggestive of increased diffusion

medulloblastoma, ependymoma and lymphoma (Fig. 15.6) are restricted (bright) on DWI. After chemotherapy, there is a sharp increase in the ADC value of some tumors within first two weeks of treatment. This increase in ADC value corresponds with volume of the tissue killed and can be used for assessing response to chemotherapy and prognostication.



Figs 15.6A and B: Lymphoma. Ill-defined areas of restricted diffusion (arrows) are seen in the left cerebral hemisphere, which are bright on DWI image (A) and dark on the ADC map (B). This turned out to be a primary CNS lymphoma. Lymphoma shows restricted diffusion due to its high cellularity



Figs 15.7A and B: DWI in abdomen. (A) Diffusion weighted image (b-value = 800) and (B) ADC map in a normal abdomen show T2-shine through in the gallbladder (gb) and kidneys (k), and true restriction of the spleen (spl) and the spinal cord (arrows). Other structures that can be normally restricted include lymph nodes, ovaries and testes

DWI in Body Imaging

Use of DWI in body imaging is relatively new. The two big obstacles to the application of DWI in the body imaging are motion from various causes and short T2 of various organs. With advances in the technology, DWI in the body can be performed with breath-hold, with respiratory triggering and even with free breathing (DWIBS). In general, lower b-values are used in body imaging than neuroimaging to counteract signal loss due to shorter T2. Presently DWI in body imaging is mainly focused in tumor imaging and assessing treatment response in tumors. Recently whole body DWI with background suppression and free breathing has been reported for staging of tumors and lymphoma with potential to replace presently used radiation involving techniques like PET. This technique is called DWIBS (diffusion-weighted whole-body imaging with background body signal suppression). The final DWIBS images show only the diffusion restricted structures and tissues (normal or abnormal).

Diffusion Tensor Imaging

Routine diffusion weighted imaging is based on the isotropic diffusion. DTI is based on the anisotropic diffusion of water molecules. Tensor is the mathematical formalism used to model anisotropic diffusion.

Technique: MR scanner axes X,Y and Z are never perfectly parallel to the white matter tracts at every point in the image. In DTI, images are acquired in at least six, usually 12–24 directions instead of three in the usual trace diffusion (Fig. 15.8). Pure apparent diffusion coefficient for each pixel is calculated from these images in multiple directions. This is called as '*principal eigen value*'. The principal eigen value is calculated along the true axis of diffusion called as '*eigen vector*'. The image formed with principal eigen value is called as diffusion tensor image that gives orientation of fiber tracts.

Uses: Diffusion tensor measures the magnitude of the ADC in the preferred direction of water diffusion and also perpendicular to the direction. The resultant image shows white matter tracts very well. Hence this technique also called as '*tractography*'. Various maps used to indicate orientation of fiber tracts include FA (fractional anisotropy), RA (regional anisotropy) and VA (volume ratio) maps. Tractography is

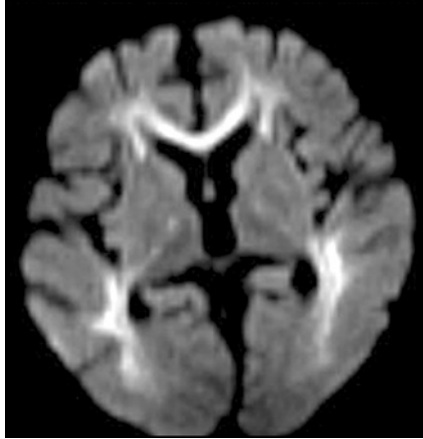


Fig. 15.8: DTI image (Fractional Analysis image) in one direction (anterior to posterior) shows bright genu of the corpus callosum and optic radiations because these fibers are perpendicular in this direction. Such images are obtained in 12 or 24 directions to get the tractography

useful for the assessment of relationship of tracts with tumor, tumor invasion of tracts and preoperative planning. It is also used to evaluate white matter tracts in various congenital anomalies and dysplasias.

Magnetic Resonance Perfusion

CHAPTER 16

Blood flow and metabolism of human tissues have been studied with tracers in nuclear medicine for many years and now being studied with positron emission tomography (PET). These techniques lack spatial and temporal resolution as well as specificity. Recent radiological methods include CT perfusion and MR perfusion. MR perfusion can be performed with exogenous contrast agent like Gadolinium or by endogenously without contrast agent administration. In this chapter, principles, technique and clinical applications of MR perfusion performed with exogenous contrast agent are discussed. Basic principles of arterial spin labeling (ASL) technique are also outlined.

Principles

Perfusion refers to the passage of blood from an arterial supply to venous drainage through the microcirculation. Perfusion is necessary for the nutritive supply to the tissues and for the clearance of products of metabolism. Perfusion can be affected by various disease processes affecting the particular tissue. Hence measuring changes in the perfusion can help in the diagnosis of certain diseases, monitoring and assessing the treatment response.

Paramagnetic agents like gadolinium cause shortening of both T1 and T2 of the tissue or region in which they go. Decrease in the T1 relaxation time on T1-weighted images results into increased signals or brightening. Decrease in the T2 relaxation time on T2 or T2* weighted images results into signal drop or blackening. As the

gadolinium-based contrast agent passes through the microvasculature in high concentration there is decrease in the signal in surrounding tissues from magnetic susceptibility induced shortening of T2* relaxation time. The signal drop is assumed to be proportional to the perfusion. Considering the concentration of contrast agent constant, more the number of small vessels per voxel of the tissue more will be the signal drop. Thus the microvasculature or relative perfusion of that region or tissue can be determined by the MR perfusion.

Technique of MR Perfusion with Exogenous Contrast Agent

A dose of 0.1 mmol/kg of gadolinium-based contrast media (Gd) is injected intravenously using power injector at the rate of 5 ml/second. Fast T2* weighted EPI sequence is run to catch the first pass of the contrast through the microcirculation. This sequence typically acquires 15–20 slices covering the entire brain in 1–2 seconds. About 60 such runs are acquired before, during and after dynamic injection of the contrast media.

From the raw data images various color coded maps are constructed using software. These are relative maps because the arterial input function is not typically measured. Hence true quantitative volumes (ml blood/ml tissue/time) are not routinely calculated. The maps include:

rCBV : relative Cerebral Blood Volume

CBF : Cerebral blood flow

TTP : Time to Peak

MTT : Mean Transit Time.

Permeability or Leakiness

Areas of severe blood-brain barrier break-down are frequently seen in the necrotic tumor and irradiated tumor beds. Increased permeability or leakiness because of break in the blood-brain barrier results in accumulation of gadolinium-based contrast (Gd) in the extravascular space. T1-enhancing effects of this extravascular Gd may predominate to counteract the T2 signal lowering effects of the intravascular Gd resulting in falsely low rCBV values. Some measures to reduce permeability induced effects on rCBV include mathematical

correction with calculation of permeability or K2 maps (Fig. 16.1) and use of dysprosium that has stronger T2* effects but negligible T1 effects instead of Gd.

Clinical Applications

MR perfusion has been studied for clinical utility in various conditions like stroke, brain tumors, dementia and psychiatric illnesses, migraine headaches, trauma, epilepsy and multiple sclerosis. Its role in stroke and tumor evaluation is discussed below, where it is commonly used in the clinical practice.

MR Perfusion in Stroke

With emerging concept of stroke as 'brain attack', and availability and acceptance of thrombolytic agents, it becomes very important to detect brain ischemia and salvageable tissue in early window period of 3–6 hours. DWI (diffusion weighted imaging) and PWI (perfusion weighted imaging) together are very effective in detection of early ischemia long before infarction or any abnormality seen on T2-weighted images. The mismatch between PW and DW represents potentially salvageable tissue (penumbra) (Fig. 16.2).

PW-DW mismatch may also indicate clinical outcome. Small mismatch has good clinical outcome. Large mismatch is associated with poor clinical outcome and larger vessel occlusion.



Fig. 16.1A: Permeability map. (A) An enhancing tumor is seen in the pons (arrow)

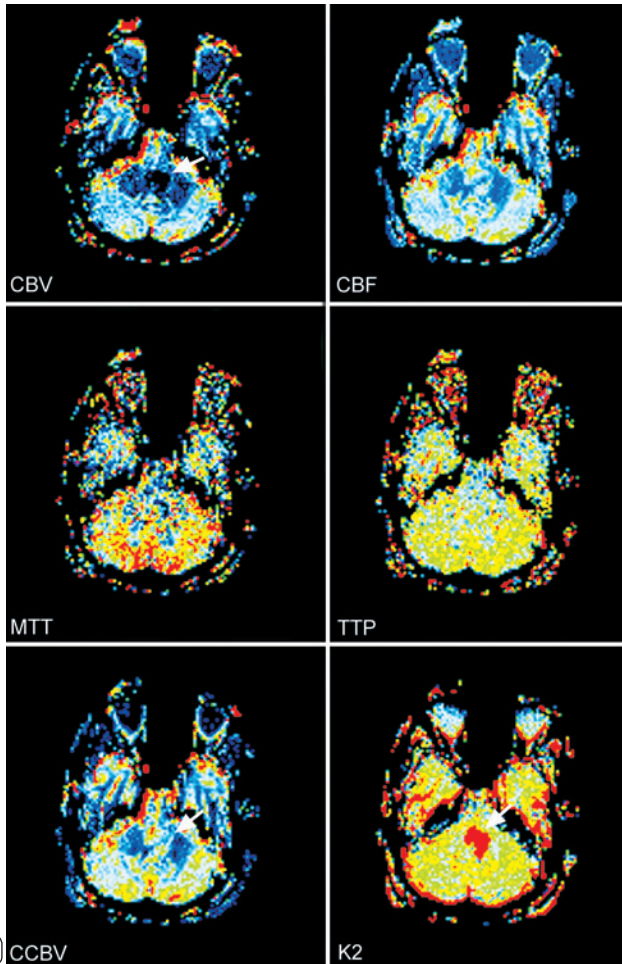
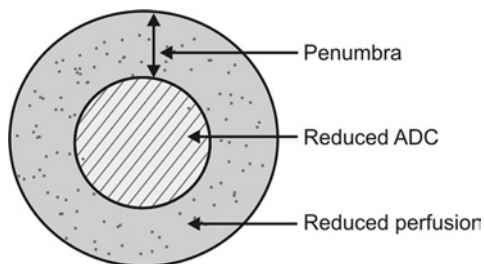


Fig. 16.1B: Permeability map. (B) Perfusion maps: On the CBV map the lesion is hypovascular (dark) but when K2 map (permeability map) and corrected CBV (CCBV) are calculated the lesion is hypervascular (green on CCBV map and red on K2 map). Redness of the lesion on K2 map is because of increased permeability due to break in the blood brain barrier

Table 16.1: Routine contrast enhancement versus perfusion imaging

	Routine contrast enhancement	Perfusion imaging
1. Sequence	T1-weighted imaging	T2*-weighted EPI sequence
2. Signal change	Increase in signal intensity	Drop in signal intensity
3. Mechanism	Gadolinium causes reduction in the T1 relaxation time	Gadolinium causes reduction in the T2 or T2* relaxation time and magnetic susceptibility
4. Detects	Break in the blood-brain barrier leading to leakage of gadolinium	Gadolinium in the microvasculature (capillaries) Thus gives information about number of small vessels (vascularity) and perfusion of the tissue

**Fig. 16.2:** Penumbra of salvageable tissue

PWI is more sensitive than DWI for detecting ischemia in early period after the onset of arterial occlusion. Restricted diffusion (reduced ADC) is always accompanied by total or near total perfusion deficit and there appears to be a threshold in humans before tissue becomes abnormal on DWI despite low rCBV. If decrease in the perfusion is mild ADC may be normal. The presence of perfusion delay (elevated MTT and TTP) is considered to represent tissue at risk whereas decreased ADC represents metabolic jeopardy.

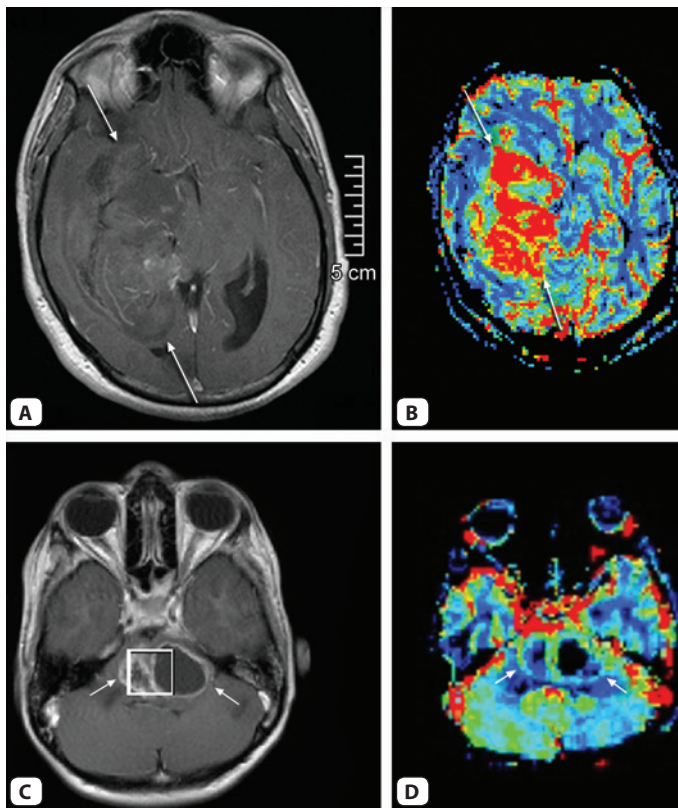
MR Perfusion in Brain Tumors

MR Perfusion can be useful in grading tumors like gliomas, in guiding biopsies and differentiating therapy induced necrosis from recurrent/residual tumor. It has been shown that rCBV correlates with both conventional angiographic assessment of tumor vascularity and histologic measurement of the tumor neovascularity. The rCBV can serve a surrogate marker of tumor angiogenesis and malignancy, and help grading gliomas (Fig. 16.3). The rCBV helps to guide biopsies. A tumor area with highest rCBV value yields good biopsy results and increases diagnostic confidence. The rCBV map can help differentiate between therapy induced necrosis (decreased rCBV or complete loss of rCBV) and recurrent/residual tumor (elevated rCBV) (Fig. 16.4).

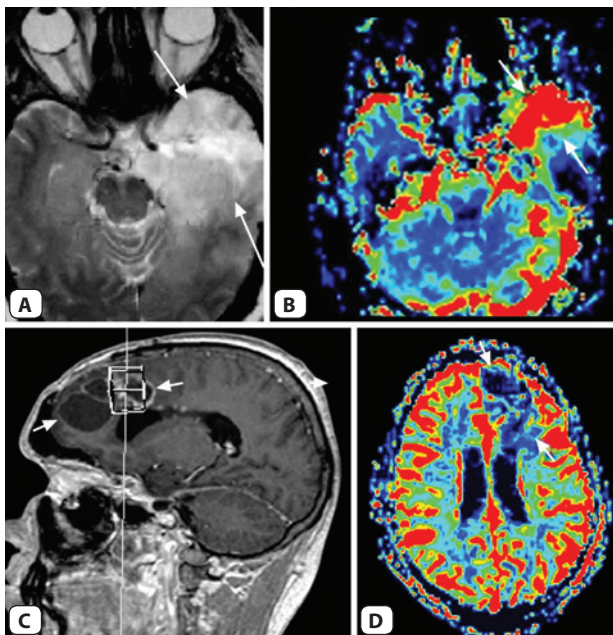
MR Perfusion may help in differentiating a solitary metastasis from glioma based on differences in the measurement of peritumoral rCBV. In metastasis, there is no histological evidence of tumor beyond the outer contrast enhancing margin. So peritumoral rCBV will not be elevated. On the other hand, the peritumoral region in high grade glioma usually represents a variable combination of vesogenic edema and tumor cells infiltrating along perivascular spaces and may show elevated peritumoral rCBV.

Some tumors like lymphoma and medulloblastoma may show reduced rCBV because of their high cellularity and high nuclear-cytoplasmic ratio. Others neoplasms like oligodendroglioma, meningioma and vascular metastases from renal cell carcinoma and melanoma usually show increased rCBV. However, a meningioma may show falsely high or falsely low rCBV. Meningioma lacks the blood-brain barrier allowing immediate leakage of the contrast without any substantial recovery of T2* signal loss back to the baseline.

MR perfusion may help differentiate tumor from tumor mimicking lesions like infection, infarction and tumefactive demyelinating lesion (TDL). Histologically TDL consists of perivascular inflammatory infiltration and demyelination. TDL can be difficult to differentiate from tumors not only radiologically but also histologically. Hypervascularity is rare in this lesion with absence of frank neoangiogenesis. Hence MR perfusion will not show elevated rCBV in TDL.



Figs 16.3A to D: High grade versus low grade glioma. (A) Post-contrast T1-w axial image of the brain shows a nonenhancing tumor (arrows) in the right cerebral hemisphere. (B) CCBV map in the same patient shows the tumor to be hypervascular (red) suggestive of a high grade tumor. (C) Postcontrast T1-w axial image of the brain in another patient shows cystic solid lesion in the pons with some enhancement (arrows). (D) On the perfusion CCBV map, the lesion is hypovascular suggestive of a low grade tumor (arrows)



Figs 16.4A to D: Tumor recurrence versus necrosis. (A) Ill-defined tumor in the left temporal lobe after radiation therapy (arrows). (B) The tumor in (A) is hypervascular (red) on the CCBV map suggesting recurrent/residual tumor. (C) A resected and irradiated tumor in the left frontal lobe in another patient (arrows). (D) The tumor in (C) is hypovascular (arrows) suggestive of radiation necrosis

Other Clinical Uses

MR perfusion is also used to assess ischemic or under perfused areas in conditions like moyamoya disease (Fig. 16.5) and CNS vasculitis.

Arterial Spin Labeling (ASL)

ASL is a noninvasive method to assess tissue perfusion without exogenous contrast injection or radiation.

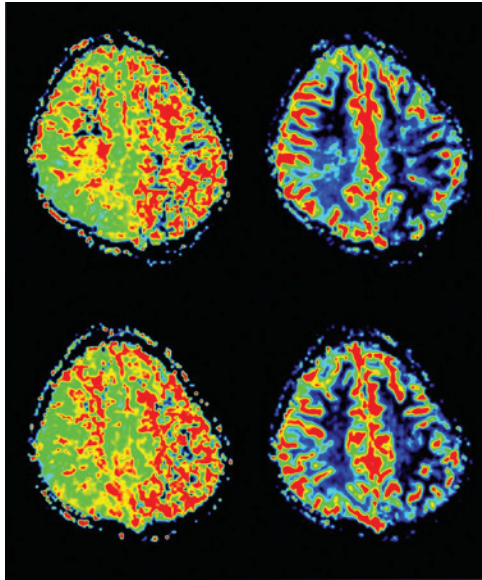


Fig. 16.5: Moyamoya disease. MTT maps (left side images) show increased MTT in the left cerebral hemisphere. CBV map (right side images) show reduced CBV in the left cerebral hemisphere. This is suggestive of perfusion compromise (reduction) in the left cerebral hemisphere.

ASL is done as follows (Fig. 16.6)—

Arterial blood flowing towards the region of interest is tagged by magnetic inversion pulses. The phase of the protons is changed.

After a delay to allow the tagged blood to enter in the slice of interest, images are acquired. This image is called 'tag image'.

Second image of the same slice of interest is again acquired without in-flowing tagged blood. This image is called 'control image'.

The tag image is subtracted from the control image.

This results into a perfusion image representing 'tagged blood' that flowed into the image slice.

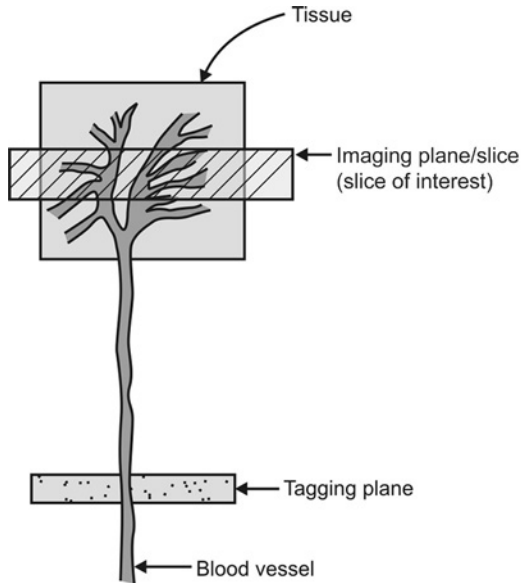


Fig. 16.6: ASL diagram

ASL involves T1-weighted imaging. It has poor signal-to-noise ratio, however, ASL has better spatial and temporal resolution than PET. Poor SNR and sensitivity to abnormally long transit delay of tagged protons have limited its application in clinical practice.

Magnetic Resonance Spectroscopy

CHAPTER 17

Magnetic resonance spectroscopy (MRS) is an exciting application of magnetic resonance to noninvasively assess various metabolites or biochemicals from the body tissues. This metabolite information is then used to diagnose diseases, monitoring diseases and assessing response to the treatment. Even though theoretically MRS can be performed with spins or nuclei of ^1H , ^{13}C , ^{19}F , ^{23}Na and ^{31}P , MRS in present clinical use are mainly ^1H (Hydrogen) and ^{31}P (Phosphorus) spectroscopy. Discussion in this chapter mainly relates to ^1H or proton spectroscopy because of its widespread use.

Basic Principles

The basic principles of MRS are same as magnetic resonance imaging (discussed in chapter 1). However, a few differences exist.

1. Usual MRI images are reconstructed from the signal from all protons in the tissue that is dominated by water and fat protons. The protons from other metabolites do not contribute to imaging because of their negligible concentration.

Contrary to routine MRI, the aim in MRS itself is to detect these small metabolites. Most metabolites of clinical interest have their signal resonate between resonant frequencies of water and fat. These small metabolites are detected only when the large signal from the water protons is suppressed.

2. *How are small metabolites from the tissue detected?*

Chemical shift forms the basis of MRS. The precessional frequency of protons is determined by the chemical environment or electron

cloud surrounding it. A proton in the water will precess at a different frequency than the proton in fat and the same proton in another metabolite (for example NAA) will precess at a different frequency than in water and fat. This change in the precessional frequency of protons in different chemical environment is *chemical shift*. So, by determining the frequency of protons we can detect their chemical environment, i.e. metabolites in which they are precessing.

In a homogeneous field,

Frequency of protons in a given metabolites = chemical shift = position of metabolite peak.

Since the precessional frequency of any proton is directly proportional to the external magnetic field strength (Larmor frequency), chemical shift in Hz will be different at different magnetic field strength. To avoid this confusion, chemical shift is expressed in parts per million (ppm), which will be same for a particular metabolite at all the field strengths.

Since chemical shift is proportional to the external magnetic field, smaller chemical shift will not be detected at low field strength. Even though MRS can be performed on 0.5 Tesla or above, field strength of 1.5 T or above is required for improved spectral separation and increased SNR.

3. Magnetic field homogeneity

Magnetic field should be homogeneous, i.e. of same strength through out its entire extent for all MR applications. MRS requires much more homogeneous field than MRI because the smaller concentration of metabolites with smaller chemical shift needs to be detected. Since the chemical shift is proportional to the external magnetic field, smaller chemical shift will be misinterpreted and incorrect concentration will be recorded in an inhomogeneous field. The homogeneity required for MRI is about 0.5 ppm whereas for MRS it is about 0.1 ppm. The process of making the magnetic field homogeneous is called as *shimming*.

4. No frequency encoding gradient in MRS

Similar to MRI, localization in MRS is done by slice selection and phase encoding gradients. However, the frequency encoding gradient is not used in MRS to preserve optimal homogeneity and chemical shift information.

One more phenomenon needs to be discussed in MRS, the *spin-spin* or *J-coupling*. Spins (protons) with a small difference of precessional frequency, for example spins within a molecule, interact with each other. This is facilitated by electrons around the nuclei. This spin-spin interaction modifies the resonant frequency of the spins involved in it. J-coupling causes fusion of peaks on spectral map, e.g. doublet of lactate at 1.3 ppm.

Localization Techniques in MRS

In initial days, localization of the volume of interest was done by the surface coil. The area (volume) covered by the coil was the volume of interest from which metabolite information is obtained. In present clinical practice, four methods are commonly used for the localization of volume of interest. They are STEAM, PRESS, ISIS and CSI (MRSI). STEAM, PRESS and ISIS are used for single voxel spectroscopy (SVS). CSI is a multivoxel (MVS) technique.

STEAM: Stimulated Echo Acquisition Method

The volume of interest is excited by three 90 degree pulses in three orthogonal planes. Since the echo is stimulated signal is weak. STEAM is used for short TE (20–30 ms) spectroscopy.

PRESS: Point Resolved Spectroscopy

In PRESS, one 90 degree and two 180 degree pulses are applied along three orthogonal planes. The signal is strong with better SNR hence PRESS is used for longer TE (135, 270 ms) spectroscopy. PRESS can not be used for shorter TEs.

ISIS: Image Selected In vivo Spectroscopy

Three frequency selective inversion pulses are applied in presence of the orthogonal gradients. Fourth non-selective pulse is used for the observation of signal. ISIS is used in the 31P spectroscopy.

CSI: Chemical Shift Imaging

CSI is used for the multivoxel spectroscopy, where a large area is covered and divided into multiple voxels. CSI is also called as Magnetic Resonance Spectroscopic Imaging (**MRSI**) as it combines features of both imaging and spectroscopy (Fig. 17.1). Spatial localization is done by phase encoding in one, two or three directions to get one, two or three

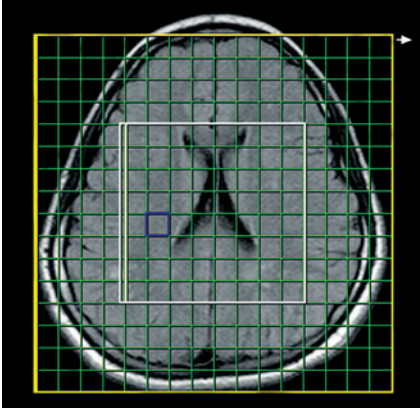


Fig. 17.1: Volume of interest (VOI) with Grid for multivoxel spectroscopy. Blue square = voxel, White square = volume of interest from which data is acquired and yellow square with green line = grid to prevent lipid contamination from the scalp interfering with signals

dimensional spectroscopy respectively. Metabolite maps or metabolic ratio maps can be seen overlaid over the images.

Steps in MRS Acquisition

Having seen the basics behind MRS, let's now go through the steps to obtain MRS.

1. Patient positioning
2. Global shimming
Optimization of the magnetic field homogeneity is done over the entire volume detected by the receiver coil. Global shimming provides starting value for local shimming.
3. Acquisition of MR images for localization
Images are obtained in all three planes (coronal, axial and sagittal) for placement of a voxel. In routine practice, MR images already obtained during routine imaging are used for the localization purpose if patient is not moved (Fig. 17.2).
4. Selection of MRS measurement and parameters
TR and TE are important parameters. Improved SNR is obtained at a longer TR.
Commonly used TEs are 20–30 ms, 135–145 ms and 270 ms (Fig. 17.3). At TEs longer than 135 ms, only peaks of major brain metabolites like choline, creatine, NAA and lactate are visible. The

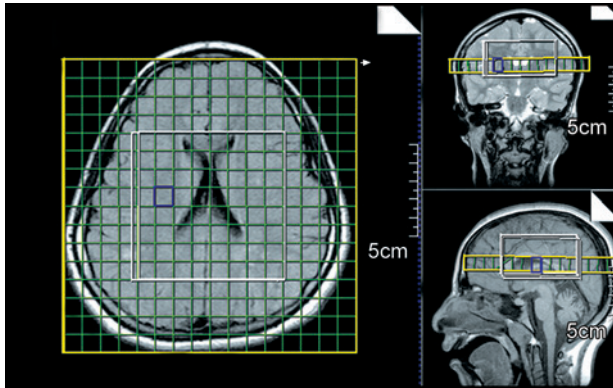


Fig. 17.2: Three plane localization of the voxel and VOI. Note position of the blue voxel in all three planes

lipid, glutamate, glutamine, GABA and inositol peaks are suppressed at higher TEs because of their short T2. Shorter TEs are used for detection of these metabolites. There is less noise at higher TEs.

5. Selection of VOI (volume of interest)

SVS can be used for local or diffuse diseases. CSI is used in irregularly shaped large lesion and where comparison on both sides is required (Fig. 17.4).

6. Local shimming

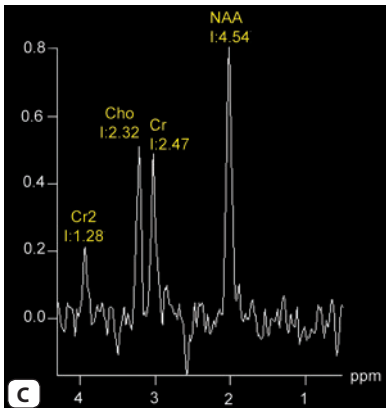
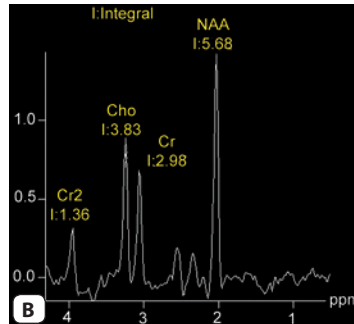
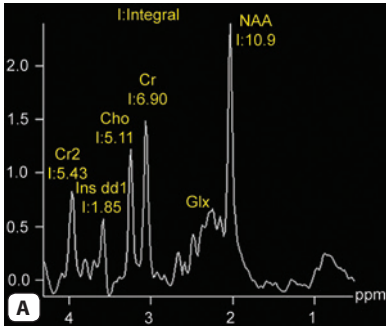
This is optimization of homogeneity over the selected volume of interest. Good local shim results into narrower metabolite peaks, better spectral resolution and good SNR. Full width at half height of the water peak is used as an indicator of shim. A local shim of 4-10 Hz is desirable.

7. Water suppression

The water peak is suppressed so that smaller metabolite peaks are visible. Water peak suppression is done by CHESS (Chemical shift selective spectroscopy) technique.

8. MRS data collection

On modern machines in use, SVS usually takes 3–6 minutes and CSI usually takes up to 12 minutes for data acquisition.



Figs 17.3A to C: Normal spectra at TE of 30 ms (A), 135 ms (B) and 270 ms (C). Smaller metabolite peaks like ml (Ins) and Glx can only be seen on low TE spectra

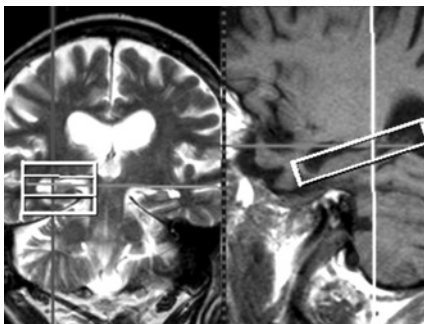


Fig. 17.4: Placement of VOI. In Alzheimer's disease hippocampus is the VOI (white box)

9. Data processing and display
Acquired data is processed to get spectrum and spectral maps. Zero point of spectrum is set in the software itself by frequency of a particular compound called Tetramethylsilane (TMS).
10. Interpretation
The area under the peak of any metabolite is directly proportional to the number of spins contributing to the peak. Absolute values for each metabolite may vary with age and population. Interpretation should always be based on ratios of metabolites and comparison with normal side.

Metabolites of 1H MRS

1. **NAA:** N- Acetylaspartate
Peak position: 2.02 ppm.
There is some contribution from NAAG and glutamate to the NAA peak.
It is a neuronal marker and any insult to the brain causing neuronal loss or degeneration causes reduction in NAA. It is absent in tissues/lesions with no neurons e.g. metastasis and meningioma.
NAA is reduced in: hypoxia, infarction, Alzheimer's, herpes encephalitis, hydrocephalus, Alexander's disease, epilepsy, some neoplasms, stroke, NPH, closed head trauma (diffuse axonal injury).
NAA is increased in: Canavan's disease (Fig. 17.5).

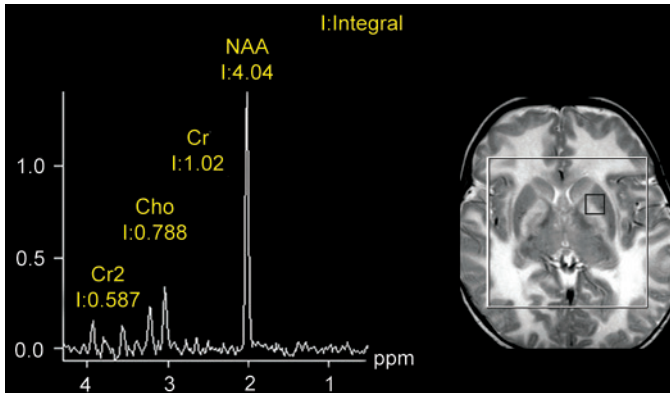


Fig. 17.5: Canavan's disease. Note markedly elevated NAA peak. T2-w axial image shows diffuse hyperintensity of the white matter

Table 17.1: Major Metabolites

Metabolites	Peak position in ppm	Approx concentration in mmol/kg in the white matter
NAA	2.02	10–15
Creatine	3.0	8
Choline	3.2	1.5
Myo-Inositol	3.56	5

2. **Cr:** Creatine

Peak position: 3.0 ppm. Second peak at 3.94 ppm

The Cr peak contains contribution from creatine, CrPO₄, GABA, Lysine and glutathione.

Cr serves as high energy phosphate and as a buffer in ATP/ADP reservoir. It increases in amount with age.

Cr is increased in: hypometabolic states and in trauma.

Cr is reduced in: hypermetabolic states, hypoxia, stroke and some tumor.

Cr remains stable in many diseases hence serves as reference or control peak for the comparison.

3. **Cho:** Choline

Peak position: 3.22 ppm.

Choline is a constituent of phospholipids of the cell membrane. It is a precursor of acetyl choline and phosphatidylcholine. Choline is indicator of cell membrane integrity. Cho increases with increased cell membrane synthesis and increased cell turnover.

Cho is increased in: Chronic hypoxia, epilepsy, Alzheimer's, gliomas and some other tumors, trauma, infarction, hyperosmolar states, diabetes mellitus.

Cho is reduced in: hepatic encephalopathy and stroke.

4. **ml:** Myo-Inositol

Peak position: 3.56 ppm. Second peak at 4.1 ppm.

MI acts as an osmolyte and is a marker of gliosis. It is involved in hormone sensitive neuroreception and is precursor of glucuronic acid. It is the dominant peak in newborn babies and decreases with age.

MI is increased in: Alzheimer's, frontal lobe dementias, diabetes and hyperosmolar states.

MI is decreased in: hepatic and hypoxic encephalopathy, stroke, tumor, osmotic pontine myelinolysis and hyponatremia.

5. **Lac:** Lactate

Peak position: 1.3 ppm.

It is a doublet. It is inverted at TE of 135 ms with PRESS, upright at other TEs on PRESS and at all the TEs with STEAM sequences. It is not seen in the normal brain spectrum.

It can be elevated in hypoxia, tumor, mitochondrial encephalopathy, intracranial hemorrhage, stroke, hypoventilation, Canavan's disease, Alexander's disease and hydrocephalus.

6. **Glx:** Glutamate (Glu) and Glutamine (Gln)

Peak position: 2–2.45 ppm for beta and gamma Glx. Second peak of alpha Glx at 3.6–3.8 ppm.

Glu is excitatory neurotransmitter and GABA is product of Glu. Gln has role in detoxification and regulation of neurotransmitter activities.

Glx peak is elevated in head injury, hepatic encephalopathy and hypoxia.

7. Lipids

Peak position: 0.9, 1.3, 1.5 ppm.

Not seen in the normal brain spectrum

Seen in acute destruction of myelin.

Increased in high grade tumors (reflects necrosis), stroke and multiple sclerosis lesions.

8. Aminoacids

Alanine (at 1.3-14 ppm), **Valine** (at 0.9 ppm), **leucine** (at 3.6 ppm) are usually multiplets visualized at short TE. They invert at TE of 135 ms.

Alanine is seen in the meningioma whereas valine and leucine are markers of an abscess.

9. Glucose

When present, it is seen next to Cho peak on its left side. It may increase in diabetes, parenteral feeding and hepatic encephalopathy.

10. GABA

Peak position: 1.9 and 2.3 ppm

Used for monitoring vigabatrin therapy given in children with myoclonic jerks.

Clinical Uses of MRS

¹H (Proton) MRS has its role in almost every neurological condition. Role of MRS in a few common conditions is discussed below.

1. Brain Tumors:

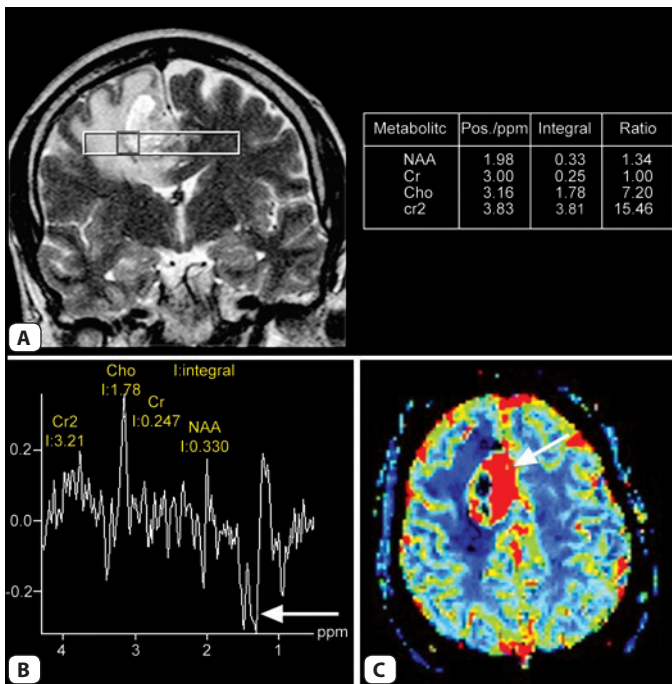
There is increase in Cho, lactate and lipid in tumors. There is reduction in NAA and Cr in tumors.

a. MRS in tumor evaluation—

MRS can differentiate neoplasm from nonneoplastic lesions. MRS also helps to grade gliomas based on metabolite ratios (Fig. 17.6).

b. In treatment planning

MRS guides the biopsy. Biopsy of higher choline area has been shown to have higher success and increased diagnostic confidence (Fig. 17.7). Inclusion of the peritumoral area with increased cho in the radiation field improves survival.



Figs 17.6A to C: High grade glioma. Coronal T2-w image (A) shows a heterogeneous tumor in the right fronto-parietal region. There is elevated choline/creatine ratio of 7.2 (the table in a) and elevated choline peak in the spectrum (B). A bifid inverted lactate peak (arrow) is also seen in the spectrum. The tumor is hypervascular (arrow) on the perfusion image CCBV map (C). All these findings are suggestive of a high grade tumor

c. In treatment monitoring

MRS helps to differentiate radiation necrosis and gliosis from the residual or recurrent neoplasm. Patient with radiation necrosis will have reduced peaks of all metabolites whereas recurrent/residual tumor will have characteristic spectrum of tumor with elevated choline (Fig. 17.8).

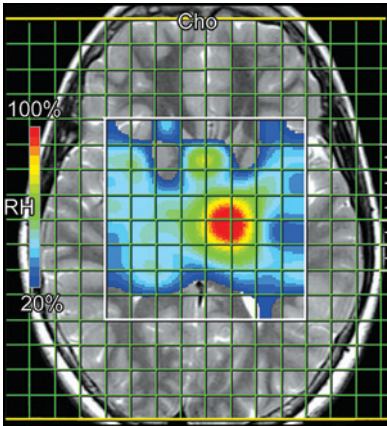
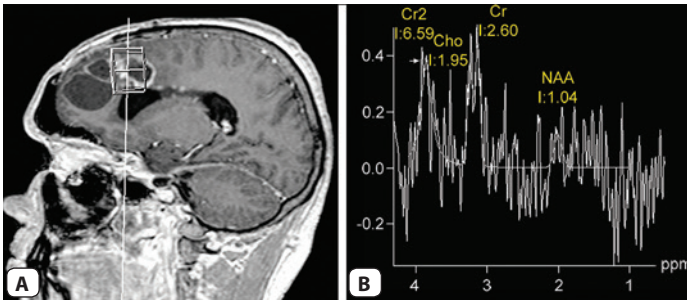


Fig. 17.7: Choline map for the biopsy guidance. MRSI choline map shows a red area in the tumor with very high choline concentration. Biopsy from such high choline area yields high diagnostic results



Figs 17.8A and B: Radiation necrosis. Sagittal post-contrast T1-w image (A) shows an irradiated tumor in the left frontal lobe (same patient as shown in Fig.16.4C and D). The spectrum (B) shows lots of noise and no dominant peak

2. Neonatal hypoxia

There may be decrease in NAA, Cr and MI, and increase in Cho and lactate/lipid peaks in the neonatal hypoxia. MRS can predict outcome of neonatal hypoxia. Progressive decrease in NAA, Cr and MI can be used to monitor the condition. In neonatal hemorrhage MRS can be used to determine hypoxia, which is one of the causes of neonatal hemorrhage.

3. Metabolic disorders and white matter diseases
 Elevation of lactate doublet is seen in mitochondrial disorders like MELAS (Mitochondrial Encephalopathy Lactic Acidosis and Stroke) and Leighs disease (Fig. 17.9).
 Canavan's disease can be differentiated easily from Alexander disease by MRS. It shows elevation of NAA peak.
4. Stroke
 NAA and Cr are reduced whereas Cho and lactate are elevated.
5. Closed head trauma
 In diffuse axonal injury, there is decrease in NAA/Cr ratio and absolute concentration of NAA.
6. Epilepsy
 NAA/Cr is reduced in the affected lobe. MRS may localize intractable epilepsy.
7. Multiple sclerosis
 In MS plaques, there is decrease in NAA/Cr and increased Cho/Cr and MI/Cr. Active plaque shows elevated lipid, lactate, Cho/Cr ratio and MI. Progression can be monitored by NAA/Cr ratio.
8. Alzheimer's dementia
 All dementias and aging brain show reduction in NAA/Cr, NAA and elevation of Cho/Cr ratio. However, Alzheimer's shows increased MI/Cr and absolute MI concentration. Similar findings are seen in the dementia associated with Down syndrome.

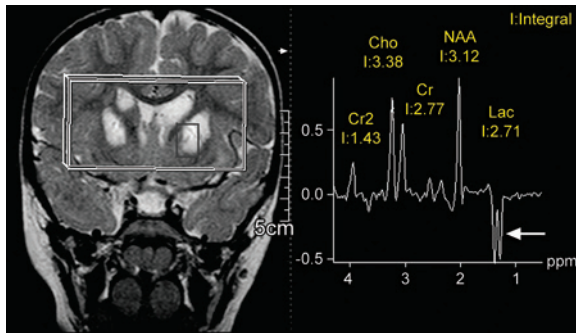


Fig. 17.9: Lactate peak in metabolic disorder. Bilateral basal ganglion hyperintensity is seen in this patient with Leigh's disease. Note a bifid inverted lactate peak at 1.3 ppm (arrow) in this spectrum at a TE of 135 ms

9. Hepatic encephalopathy (HE)
MI and Cho are reduced and Glx peak is elevated in hepatic encephalopathy. MRS may detect subclinical HE.
10. HIV and AIDS
There is steady decline in NAA/Cr in HIV patients. MRS may help to differentiate lymphoma, toxoplasma and progressive multifocal leukoencephalopathy (PML).
Lymphoma: shows elevation in lactate, lipids and choline; and reduction in NAA, Cr and MI.
Toxoplasma: shows elevation in lipids and lactate; and reduction in all other metabolites.
PML: shows elevation of Cho and slight elevation of lactate, lipid and MI; and reduction in NAA and Cr.
11. Abscess
Abscess can be difficult to differentiate from neoplasm. The changes in MR spectra in abscess include visualization of amino acid peaks at 0.9 ppm. These amino acids include valine, leucine and isoleucine. The abscess may show peaks representing acetate, pyruvate, lactate and succinate, which are end products arising from some microorganisms.

Cardiac Magnetic Resonance Imaging

CHAPTER 18

Cardiac magnetic resonance imaging (CMRI) opens a new era into cardiac imaging with the potential to provide virtually all of the information needed to assess the heart diseases. It provides anatomic and functional information in acquired and congenital heart diseases. It has already become the modality of choice in conditions like ARVD, differentiation of constrictive pericarditis from restrictive cardiomyopathy and aortic dissection. It gives precise quantification of ventricular dimensions and function. Most exciting application of CMRI is assessment of myocardial viability and perfusion. The technique, imaging planes and role of CMRI in various cardiac conditions are discussed in this chapter.

ECG Gating

Electrocardiographic (ECG/EKG) gating is essential for 'motion-free' images of the heart. Images are acquired in a particular phase of cardiac cycle in every cardiac cycle to avoid image blur and cardiac motion artifacts. The phase of the cardiac cycle during which images are acquired is decided by the ECG gating. Usually R-wave is used to trigger the acquisition after some trigger delay such that data is acquired in the diastolic phase (Fig. 18.1). Peripheral pulse also can be used for gating but it is less effective than ECG gating.

Imaging Sequences

Pulse sequences used for CMRI can be broadly divided into dark-blood and bright-blood techniques.

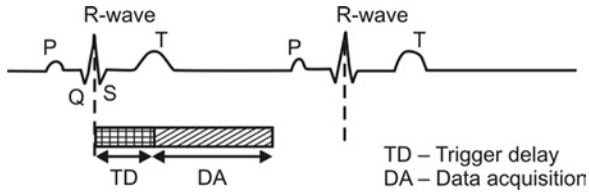


Fig. 18.1: Diagram of ECG gating

Dark-blood Technique

These are spin-echo sequences that show the flowing blood as flow void. These sequences include breath-hold turbo or fast spin-echo (TSE, FSE), single-shot FSE and double inversion recovery FSE (Double-IR-FSE) sequences.

Bright-blood Technique

These are gradient-echo (GRE) sequences that show the blood bright. GRE sequences used for CMRI include spoiled GRE (like turboFLASH/SPGR/T1-FFE) and balanced SSFP (TrueFISP/FIESTA/balanced TFE) sequences. Balanced SSFP sequences are the mainstay sequences for CMRI and are used in every aspect of cardiac imaging. A motion picture loop through out the various phases of a cardiac cycle can be produced with GRE sequences like balanced SSFP to *get rapid cine imaging*. Cine imaging is useful for functional assessment of ventricles with calculation of ejection fraction and stroke volume as well as for valvular and cardiac wall motion evaluation.

Phase contrast cine sequences are used for the measurement of velocity and assessment of flow direction in the vessels and across the cardiac valves.

As a general rule, imaging may begin with dark-blood sequences like single-shot FSE to obtain anatomic information and proceed with bright-blood techniques to assess functional abnormalities.

Imaging Planes

Orthogonal planes (axial, sagittal and coronal) used for general chest imaging are not suitable for cardiac imaging because cardiac axes are not parallel to body axes.

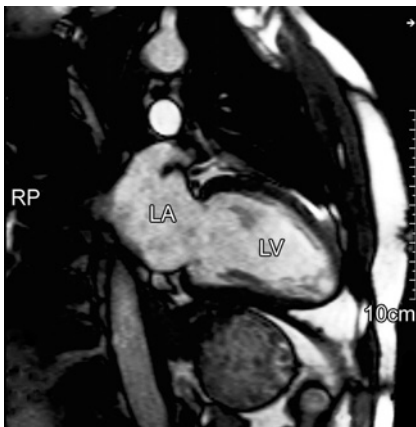


Fig. 18.2: Two Chamber view. LA = left atrium and LV = left ventricle

Imaging starts with routine axial, sagittal and coronal sections as localizers/scout images. Further imaging in the planes suitable for cardiac study is planned on these images as follows—

1. Vertical long-axis plane (two-chamber view) (Fig. 18.2)
This is prescribed from an axial image that shows the largest oblique diameter of the left ventricle (LV). The two chambers seen on this view are left atrium (LA) and LV. It is useful in assessing left heart structures and the mitral valve.
2. Horizontal long-axis (four-chamber view) (Fig. 18.3)
This is planned on the two-chamber view by drawing a line passing through LA, mitral valve and LV. All four chambers, mitral and tricuspid valves can be assessed together on this view.
Cine GRE images can be obtained in this plane to assess mitral, tricuspid and aortic valve function, and RV and LV wall motion.
3. Short-axis plane
Multiple cross sections are obtained perpendicular to LV long axis as seen on a two-chamber view (Fig. 18.4). These sections are taken from the base to apex of the heart.
Cine GRE images allow visualization and quantification of systolic myocardial wall thickening. Images in this plane are used to for calculating ventricular volume, mass and ejection fraction by post-processing.

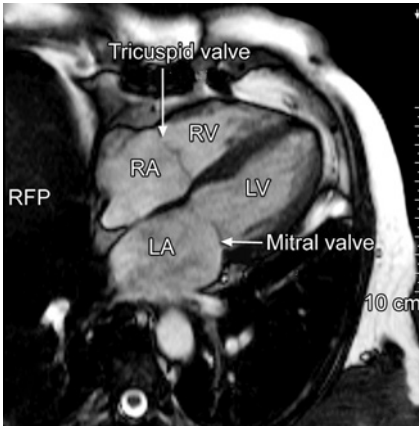


Fig. 18.3: Four Chamber view. LA = left atrium, LV = left ventricle, RA = right atrium and RV = right ventricle

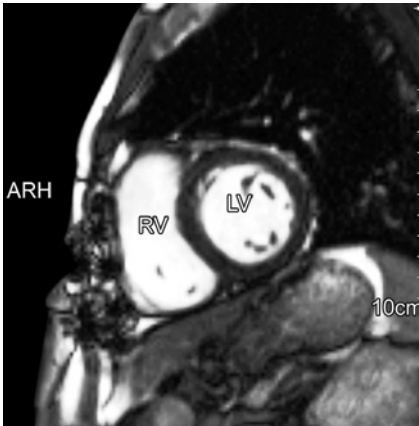


Fig. 18.4: Short axis view. RV = right ventricle and LV = left ventricle

4. Five-chamber view
This view is obtained parallel to the line passing through the LV apex and aortic outflow tract on the coronal images. Apart from all four chambers, this view also shows aortic root, the fifth chamber. This plane demonstrates both mitral and aortic valves.
5. RVOT
Plane passing through the RV outflow tract.

Clinical Applications of CMRI

1. *Congenital heart disease (CHD)*

CMRI is useful in understanding complex anatomy in CHD and gives the information not obtained by echocardiography. CMRI not only detects ASD, VSD with high sensitivity and specificity but also calculates shunt size with phase-velocity mapping. Using imaging planes aligned with cardiac chambers anatomic details of conditions like transposition of great arteries (TGA), truncus arteriosus, double outlet left ventricle and other complex cardiac diseases can be obtained. CMRI is also useful for the diagnosis of anomalies of systemic venous and arterial systems (Fig. 18.5). Survival has improved with availability of various treatment options for congenital heart diseases. CMRI plays important role in evaluating complex surgical shunts and baffles with their size as well as function. The need for sedation/anesthesia in most children is a major limitation of CMRI.



Fig. 18.5: Congenital heart disease, tetralogy of fallot. Coronal TrueFISP image shows right ventricular (RV) hypertrophy, a jet in the right ventricular outflow tract (arrow) indicating pulmonary regurgitation and right pulmonary artery stenosis (arrowhead). AO = arch of aorta

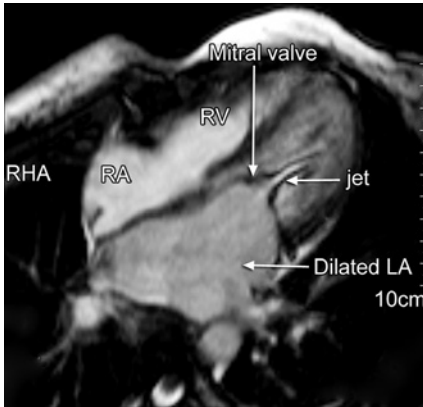


Fig. 18.6: Mitral stenosis. Four-chamber view shows stenosis of the mitral valve with a jet in the left ventricle and a dilated left atrium. The mitral valve stenosis was caused by rheumatic fever

2. **Valvular heart disease**

CMRI can demonstrate the presence and quantify the severity of valvular heart disease. Valvular stenosis or regurgitation results into a dark jet within the bright blood containing chambers (Fig. 18.6). The duration or extent of the signal void (jet) on MR images correlate with the severity of the aortic stenosis and total area of signal loss correlates with the severity of mitral regurgitation. Direct measurement of the jet velocity can be done using phase contrast technique for assessment of severity and quantification. Cine GRE sequence is useful for the assessment of the valve leaflets.

3. **Cardiomyopathies**

ARVD—Arrhythmogenic right ventricular dysplasia (ARVD) is characterized by fatty or fibrous infiltration (Fig. 18.7) with thinning or thickening of the RV free wall associated with wall motion abnormality. These changes are responsible for ventricular arrhythmias and are one of the causes of sudden cardiac death in young patients. MRI with its ability to give excellent soft tissue contrast is the modality of choice for the diagnosis of ARVD. Fat in the RV free wall is identified on T1-weighted images. Other findings include thinning of wall, enlargement and dilatation of RV, areas of dyskinesia, focal bulging of free wall during systole, decreased ejection fraction and impaired ventricular filling during the diastole.

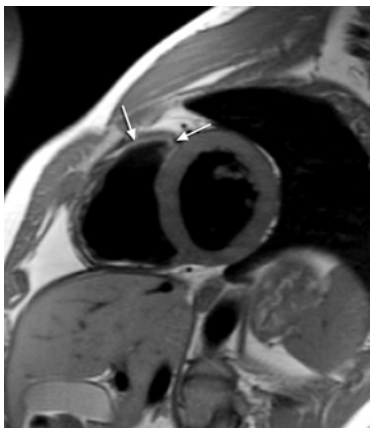
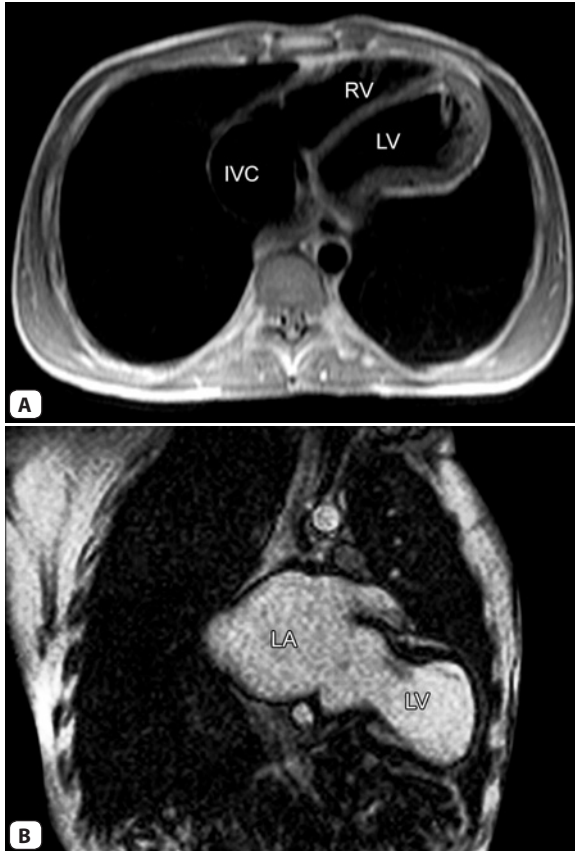


Fig. 18.7: Arrhythmogenic right ventricular dysplasia (ARVD). Short axis view T1-w image shows a linear high intensity fat in the right ventricular wall (arrows)

Hypertrophic cardiomyopathy—The diagnosis is usually made by echocardiography. CMRI is useful in the diagnosis of variant confined to the apex and assessment of RV involvement. Cine GRE sequences demonstrate the degree and extent of LV hypertrophy. The degree of associated LV outflow tract obstruction and mitral regurgitation can also be assessed by CMRI.

Restrictive cardiomyopathy versus constrictive pericarditis—This is a clinical dilemma as both conditions have the same clinical presentation. Differentiation is important because constrictive pericarditis can be treated surgically by stripping the pericardium. CMRI reliably differentiates constrictive pericarditis (Fig. 18.8) from restrictive cardiomyopathy by the presence of pericardial thickness more than 4 mm. Dark signal void can also be seen suggestive of calcifications in the pericardium. Restrictive cardiomyopathy will have normal pericardium with thickened ventricular walls. CMRI also shows associated complications like mitral regurgitation. Other associated findings seen in both conditions include dilated IVC/SVC, hepatic veins and RA. Causes of the restrictive cardiomyopathy include sarcoidosis, amyloidosis, hemochromatosis, scleroderma, storage disorder and idiopathic. Causes of the constrictive pericarditis include infective, connective tissue disorders, neoplasm, renal failure, postcardiac surgery and radiotherapy.



Figs 18.8A and B: Constrictive pericarditis. HASTE axial image (A) and T1-w GRE two chamber view (B) show small ventricular cavities (LV and RV), dilated inferior vena cava (IVC) and the left atrium (LA). The pericardium was thickened (not appreciated on these images)

Hemochromatosis—Myocardial iron deposition in transfusion dependant conditions like thalassemia major can be quantified by T2*-weighted sequence. CMRI is used to monitor these patients and to assess response to the chelating agents.

4. ***Ventricular function***

CMRI is reported to be more accurate than 2D echocardiography in the functional assessment of the heart. CMRI can accurately measure ventricular ejection fraction, end-diastolic and end-systolic volumes. Usually these measurements are done on short axis images using software. The sequence used is balanced SSFP that has good contrast between the blood pool and the myocardium.

5. ***Coronary artery assessment***

CMRI is still not good enough for the visualization of distal coronary arteries and its branches. The present role of MRI in coronary imaging include assessment of anomalous coronary arteries, aneurysm and bypass graft patency. Sequences used are standard GRE sequences like balanced SSFP with or without contrast injection.

6. ***Myocardial perfusion and viability***

Myocardial perfusion study—Gadolinium is injected intravenously as a tight bolus during pharmacologic stress. The pharmacologic stress for the myocardium is achieved by slow IV injection of adenosine 140 microgram per kg body weight. The sequence used is T1-weighted GRE sequence like turboFLASH with high temporal resolution. Low signal areas of underperfusion on these images correspond with regions of ischemia or infarct.

Myocardial viability—The imaging sequence for assessment of viability is run 10–15 minutes after gadolinium injection. The sequences used are either inversion recovery T1-w GRE or inversion recovery balanced SSFP sequence. Inversion pulse is used to suppress the myocardium so that any enhancement within it will be appreciated against the background of the black myocardium. Selection of proper inversion time (TI) is important to suppress signals from the normal myocardium. An infarcted area on viability imaging shows enhancement or bright signal. 'Bright is dead' on the viability imaging (Fig. 18.9).

MR viability answers a very important question, whether the patient will benefit from revascularization procedure like angioplasty and bypass or not. It shows the extent and severity of the non-viable myocardium. Recent studies have shown that myocardial viability determined by CMRI is superior to that determined by the PET.

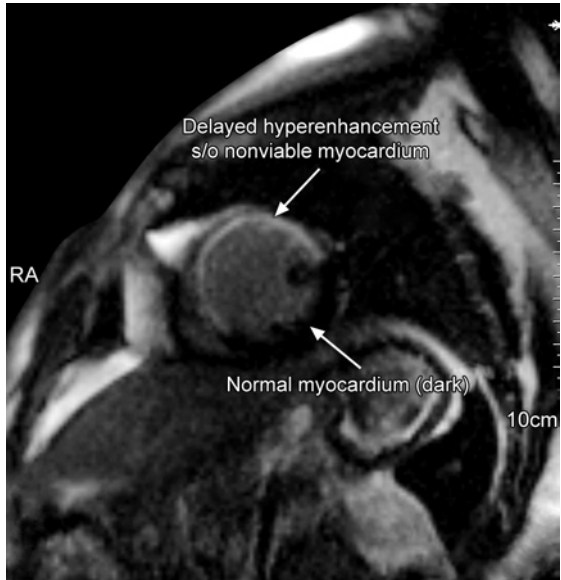
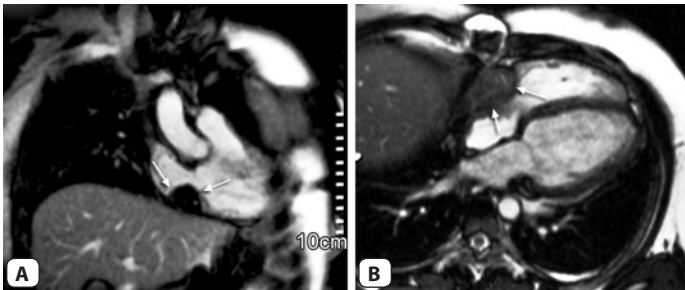


Fig. 18.9: Myocardial viability. Short axis view obtained after 15 minutes of contrast injection shows dark normal myocardium (suppressed by inversion recovery pulse) and enhancing non-viable myocardium



Figs 18.10A and B: Cardiac mass. Coronal (A) and four chamber view (B) images show a hypointense mass (arrows) in the right atrium likely representing a myxoma (pathology unavailable)

7. ***Cardiac and pericardial masses***

CMRI is an accurate method to evaluate cardiac and pericardial masses (Fig. 18.10). A thrombus is the most common filling defect in a cardiac chamber. Gadolinium enhancement differentiates the thrombus from a mass. Most of the cardiac neoplasms are secondary or metastatic. Primary cardiac tumors are rare and 80% are benign.

8. ***Pericardial disease***

Pericardium can be visualized with spin echo or GRE images. Normal pericardium is seen on the spin echo images as a line of low signal intensity located between the high signals of pericardial and epicardial fat. Normal thickness is 1–2 mm; more than 4 mm is considered thickening.

Magnetic Resonance Cholangiopancreatography

CHAPTER 19

Magnetic Resonance Cholangiopancreatography (MRCP) has got a widespread clinical acceptance and has almost completely replaced diagnostic ERCP. MRCP visualizes biliary and pancreatic tree non-invasively without use of any contrast injection or radiation. Principles, sequences, technique and clinical applications of MRCP are discussed.

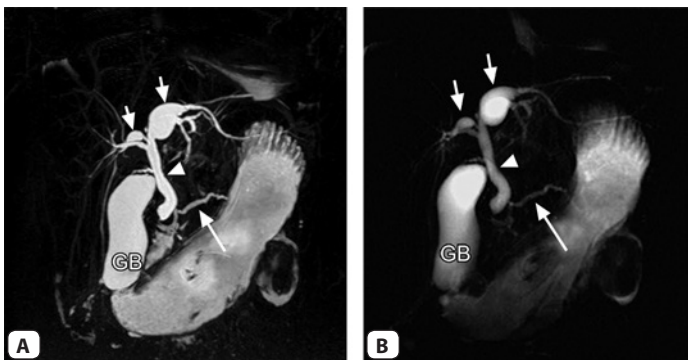
Principles

Heavily T2-w images are used to visualize static fluid or bile in the pancreatobiliary tree. The images are made heavily T2-w by using longer echo times (TE) in the range of 600–1200 ms. At this long TE, only fluid or tissues with high T2 relaxation time will retain signal. Background tissues with shorter T2 do not retain sufficient signal at longer TEs and are suppressed.

Sequences used in MRCP

Two main sequences used for MRCP are 3D FSE and single-shot FSE sequences. Other sequences that can be used include balanced SSFP and contrast-enhanced T1-w GRE sequences.

3D FSE sequence: This sequence (discussed in chapter 5) with high TE is acquired with respiratory triggering either by tying a bellows over the abdomen or by navigator technique. The 3D data is reformatted using MIP to get cholangiographic images (Fig. 19.1A). It takes long time, typically 4–5 minutes. It may not work if breathing is not regular.



Figs 19.1A and B: 3D MRCP versus single-shot radial slab MRCP. Coronal MIP image from 3D FSE sequence (A) and single-shot radial slab (B) show dilatation of extrahepatic (arrowhead) as well as intrahepatic (short arrows) bile ducts in this patient with choledochal cyst. Long arrow = pancreatic duct and GB = gallbladder

Single-shot FSE (SSFSE/HASTE): This sequence is acquired as slabs of 2–5 cm thickness. Most commonly it is acquired as radial coronal slabs. These slabs can be acquired with breath-hold or with respiratory triggering. There is no need to MIP these images as the slabs show ducts only with suppressed background tissues (Fig. 19.1B).

Balanced SSFP (TrueFISP/FIESTA/bTFE) sequence: It can be acquired with breath-hold or with respiratory triggering. It is a motion insensitive sequence and good quality images can be acquired in most of the patients. It can serve a problem solving complementary sequence as it can show ducts without motion artifacts.

Contrast-enhanced T1-w GRE sequences (THRIVE/VIBE/LAVA): These sequences can be acquired after injection of hepatobiliary specific contrast agents like gadobenate (Multihance), gadoxetate (Eovist/primovist) and mangafodifir trisodium (Mn-DPDP, Teslascan). These agents are excreted through bile opacifying the bile ducts on T1-w images. This type of *contrast-enhanced MR cholangiography* is useful for the detection of bile leak and for visualization of smaller ducts.

Secretin MR Cholangiopancreatography (S-MRCP): Secretin is a hormone secreted by duodenal mucosa in response to acid stimulation.

It increases secretion of water and bicarbonate by pancreas thereby distending pancreatic ducts. It is given intravenously (1 unit/Kg) and heavily T2-w images are acquired every 30 seconds for 10 minutes. It distends pancreatic duct up to 3 mm diameter. The peak response occurs at about 3–5 minutes after injection and the response completely vanes by 10 minutes. S-MRCP improves visualization of pancreatic side branches thereby increasing the sensitivity in diagnosing chronic pancreatitis. The main limitation of S-MRCP is the high cost of secretin.

MRCP Protocol and Technique

Patient preparation in the form of 8–12 hours of fasting to avoid any fluid in upper gastrointestinal tract especially in the stomach and duodenum is required in all patients. If fluid is still present in the stomach it can be suppressed by giving barium or blue-berry juice. Fasting also distends gallbladder and bile ducts.

The examination should start with a routine T2-w axial sequence for a gross look at upper abdominal organs and for planning MRCP sequences. Next, the 3D FSE sequence should be acquired. It takes 4–5 minutes and gives time to the technologist for planning other sequences. This is followed by single-shot radial slabs in the coronal plane. The axis of rotation of the radial slabs is kept at the porta on the axial images. Thin contiguous sections (3–4 mm) of the single-shot sequence in coronal and axial planes with intermediate TE of 200–300 ms should be acquired in all MRCP examinations. These images are very useful for small filling defects like calculi, and small ductal variations and anomalies that may not be picked up on other sequences. Axial or

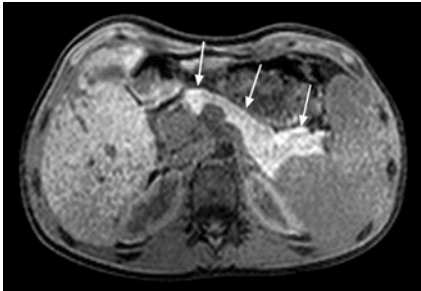


Fig. 19.2: T1-w GRE fat sat axial image (THRIVE) of the abdomen shows the pancreas as a bright homogeneous structure (arrows)

coronal balanced SSFP and axial T1-w fat sat sequence (for pancreas) (Fig. 19.2) complete the examination. Depending on the clinical question, additional sequences for the liver and contrast media injection can be performed.

Clinical Applications of MRCP

1. Cystic diseases of the bile duct.
MRCP is as effective as ERCP in evaluating choledochal cyst, choledochoceles and Caroli's disease (Fig. 19.3).
2. Congenital anomalies
MRCP is superior to ERCP in detecting pancreas divisum (Fig. 19.4). Congenital variations like low cystic duct insertion, medial cystic duct insertion, parallel course of the cystic and hepatic duct, and

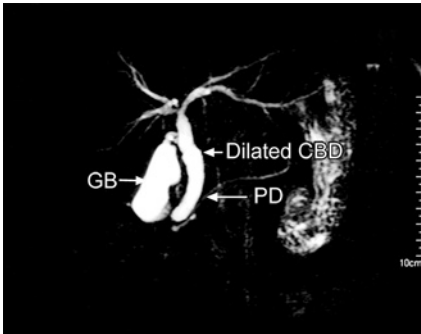


Fig. 19.3: Choledochal cyst. The CBD and common hepatic duct are dilated. The confluence and intrahepatic ducts are normal

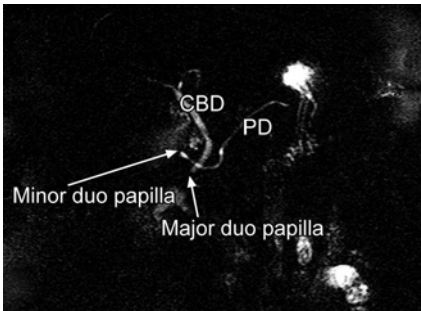


Fig. 19.4: Pancreas divisum. The main pancreatic duct (PD) drains into the minor papilla and crosses CBD instead of joining it at the major papilla. duo = duodenum

aberrant right hepatic duct are visualized on MRCP. Detection of these variations is important to avoid complications during the cholecystectomy especially the laproscopic.

3. Choledocholithiasis

Accurate diagnosis of stones in the CBD is important before cholecystectomy. MRCP is an excellent method to detect these stones, comparable to ERCP and superior to other modalities like USG and CT (Figs 19.5 and 19.6).

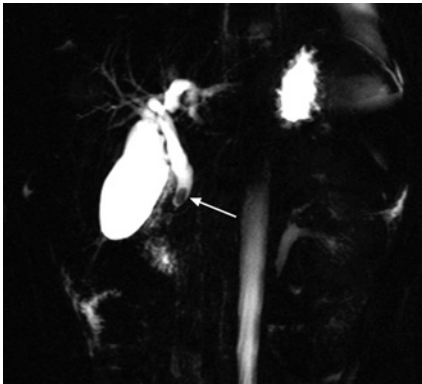


Fig. 19.5: Calculus in the CBD (arrow) with proximal dilatation of intra and extrahepatic biliary tree. The intrahepatic dilatation is asymmetric (left more than right) suggesting CBD stone to be a complication of congenital dilatation of ducts such as choledochal cyst rather than an obstructive calculus itself

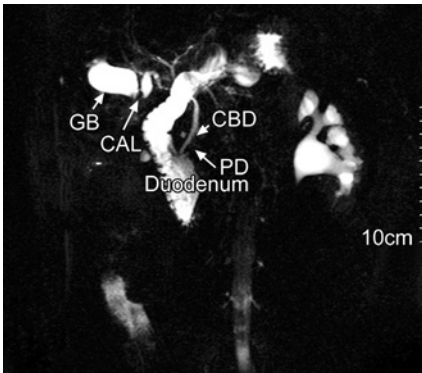


Fig. 19.6: Calculus in the gallbladder

4. Primary sclerosing cholangitis

It is characterized by multiple irregular strictures and saccular dilations of the intrahepatic and extrahepatic bile ducts producing beaded appearance (Fig. 19.7). MRCP is useful in the diagnosis and follow-up of primary sclerosing cholangitis. ERCP may result in progression of cholestasis and may not show ducts proximal to severe stenosis.

5. Postsurgical complications

Postsurgical complications like benign strictures, retained stones, biliary leak and biliary fistula can be effectively evaluated with MRCP. Patency of biliary-enteric anastomosis can be seen by MRCP (Fig. 19.8).

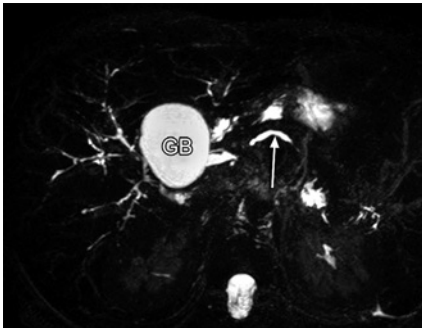


Fig. 19.7: Primary sclerosing cholangitis. Axial MIP image from 3D FSE MRCP shows diffuse irregularity of intrahepatic bile ducts with 'beading'. GB = gallbladder and arrow = pancreatic duct

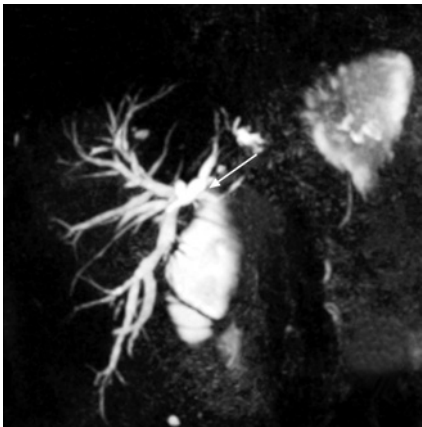


Fig. 19.8: Coronal MRCP image shows normal patent choledochο-jejunal anastomosis (arrow)

6. Chronic pancreatitis

Chronic pancreatitis is characterized by pancreatic duct dilatation, narrowing or stricture and irregularity. Alcoholic chronic pancreatitis is usually heterogeneous and characterized by side-branch dilatation and ductal calcifications. Whereas obstructive pancreatitis is more homogeneous, lacks calcification and is associated more often with main duct dilatation. MRCP is useful for detecting chronic pancreatitis and for the identification of a surgically or endoscopically correctable lesion.

7. Neoplastic lesions

MRCP can show duct proximal to the obstruction caused by neoplasms like cholangiocarcinoma and pancreatic head carcinoma. MRCP should be combined with fat saturated post-contrast T1-weighted images for the evaluation of extent and spread of the lesion.

Miscellaneous Neuroimaging MR Techniques

CHAPTER 20

In this chapter a few miscellaneous MRI techniques used in the neuroimaging are discussed. These techniques include functional MRI, susceptibility weighted imaging and CSF flow studies.

fMRI : Functional MRI

fMRI is a noninvasive MR technique to map or localize brain areas which are responsible for a particular task. Patient is asked to perform a particular activity, e.g. finger-thumb apposition and a T2*-weighted EPI sequence is run. The brain areas responsible for the activity (e.g. sensory or motor cortex) show increased signal.

Mechanism: fMRI is based on the concept of Blood Oxygen Level-Dependant (BOLD) imaging. Deoxyhemoglobin is paramagnetic while the oxyhemoglobin is diamagnetic relative to the surrounding tissues. Presence of deoxyhemoglobin causes microscopic field variation in and around the microvasculature resulting into signal drop on T2 or T2*-weighted images.

When any brain area is activated by the particular task blood flow to that area increases (Fig. 20.1). This increase in the blood flow is much more than the metabolic demand with resultant increased amount of oxyhemoglobin and relatively less deoxyhemoglobin in that area. This leads to increased signal in the area from less deoxyhemoglobin.

fMRI includes paradigm or tasks to stimulate brain areas. Active paradigms include motor, language and cognitive tasks and passive

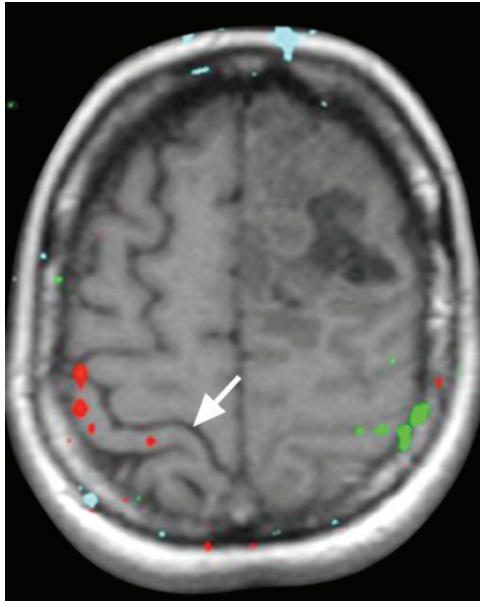


Fig. 20.1: Functional MRI. BOLD image shows activated red areas (on the right side) and green areas (on the left side) in the postcentral gyrus (motor cortex) from hand fingers movement. Arrow indicates right central sulcus. Patient has a tumor in the left frontal lobe

paradigms include tactile, auditory and visual stimuli. Usual areas mapped and tasks include—

1. Finger tapping /apposition of thumb with fingers for sensory motor cortex activation.
2. Light flashing for visual cortex.
3. Sound tones for auditory cortex.

Clinical Applications of fMRI

Apart from ongoing research in understanding brain functional areas and understanding psychiatric diseases, fMRI has clinical uses like—

1. Mapping of eloquent cortex in intracranial tumors, seizure foci and other lesions to determine the surgical risk and the optimal surgical approach.

2. Estimation of risk of postoperative deficit, e.g. if the particular functional area is more than 2 cm away from the tumor or lesion to be resected, then patient is less likely to develop postoperative deficit.
3. Determination of hemispheric dominance for the language.

Susceptibility Weighted Imaging

Susceptibility Weighted Imaging (SWI) is a new technique that uses susceptibility differences among tissues to differentiate them. It is a T2*-weighted imaging that uses both phase and magnitude information. Paramagnetic substances like deoxyhemoglobin, hemosiderin and ferritin cause positive phase shift relative to surrounding parenchyma while diamagnetic substances like calcium causes negative phase shift for a left handed system. Phase images are sensitive to this phase shift and can be used to differentiate these substances/tissues.

In SWI, a phase mask is created from the MR phase images and multiplied with the magnitude images. Automated postprocessing is performed at the end of the acquisition. Three sets of images available for viewing include phase images, magnitude images and minimum intensity projection images (Fig. 20.2).

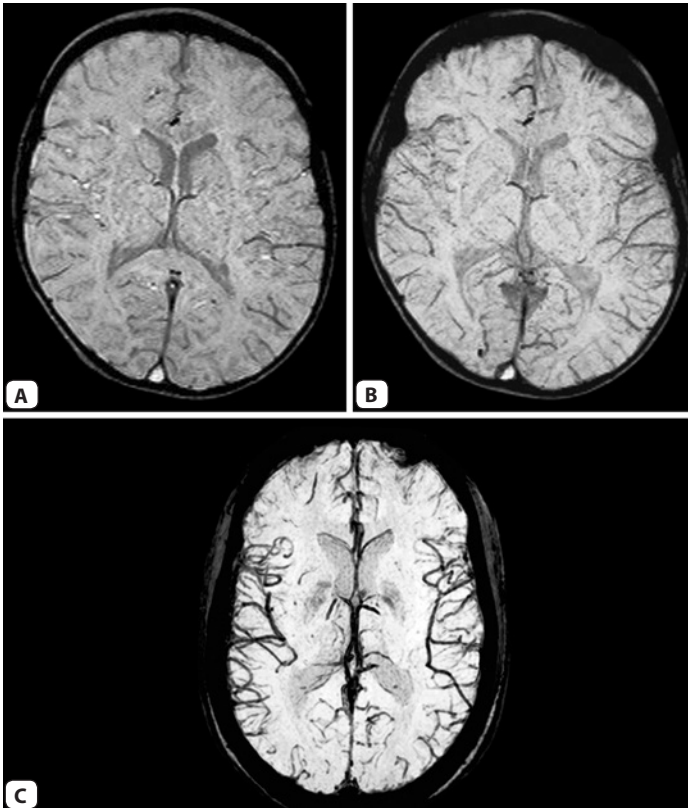
Susceptibility Weighted Imaging (SWI) has been increasingly used in various neuroimaging areas as well as in body imaging. It is more sensitive to conventional GRE sequences in detection of small hemorrhagic foci especially in conditions like diffuse axonal injury. Venous blood has lower T2* as compared to arterial blood. This difference is used to depict intracranial veins using long TE. SWI may differentiate calcification from hemorrhage on phase images.

Cerebrospinal Fluid Flow Study

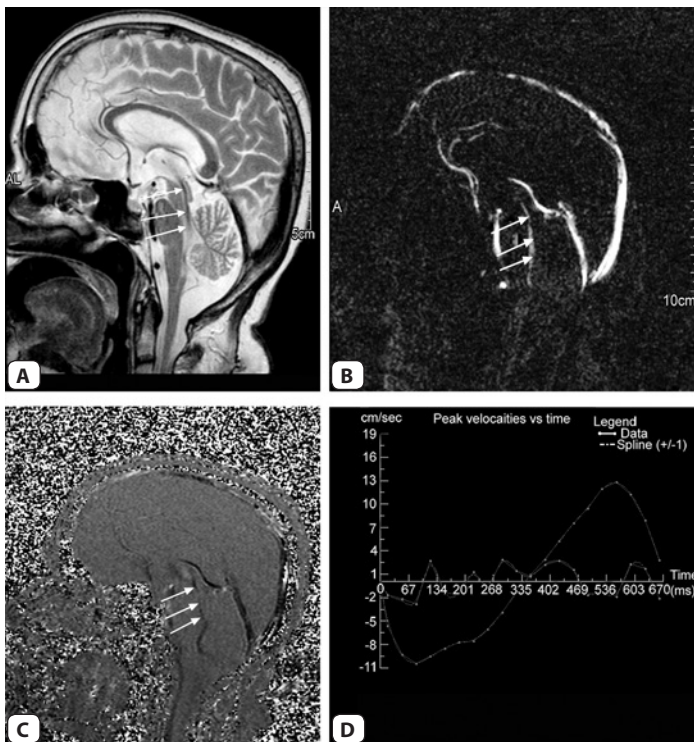
There is continuous to and fro movement of CSF during a cardiac cycle. During systole, because of expansion of cerebral hemispheres, there is craniocaudal movement of the CSF from lateral to third and third to fourth ventricles. CSF moves caudocranially during the diastole. These movements manifest as flow voids in the aqueduct of Sylvius on conventional MR imaging.

Cerebrospinal fluid (CSF) flow study is performed using phase contrast method, which is also used for MR angiography and venography. The study is performed with ECG gating that could be

prospective or retrospective. Most commonly, it is performed for assessment of flow in the aqueduct. The flow can be assessed in two ways: in-plane (along the aqueduct) and through-plane (perpendicular to the aqueduct). At the end of examination, magnitude images (showing anatomy) and phase or CSF flow images (giving information about CSF flow) are obtained (Fig. 20.3). The data is also used to calculate aqueductal stroke volume.



Figs 20.2A to C: Susceptibility weighted imaging. Magnitude (A) and minIP (B) SWI axial images of the brain are shown. SWI venography/ minIP image (C) in another patient shows dark vessels with increase visibility of small vessels



Figs 20.3A to D: CSF flow study in normal pressure hydrocephalus. T2-w sagittal image of the brain (A) shows hyperdynamic jet in the aqueduct (arrows). Magnitude image (B) and phase image (C) from an 'in-plane' CSF flow study show flow in the aqueduct (arrows). The graph of CSF flow plotted against cardiac cycle (D) shows flow below the baseline during systole and above the baseline during diastole

On CSF flow images, CSF in the aqueduct is bright during systole (craniocaudal flow) and dark during diastole (caudocranial flow). Normal aqueductal stroke volume is approximately 42 microliters. Stroke volume more than 42 microliters is suggestive of hyperdynamic flow. Clinical applications of CSF flow studies—

1. NPH -Normal Pressure Hydrocephalus

NPH is a condition in elderly patients with clinical triad of dementia, gait disturbances and incontinence of urine. Conventional MR images show ventricular dilatation out of proportion to the sulcal widening. In NPH, mean intraventricular pressure is normal (compensated hydrocephalus) but the pulse pressure is increased several times. This pulse pressure pounds against paracentral fibers like corona radiata ('waterhammer pulse') and also causes compression of the cerebral cortex. There is also hyperdynamic flow (increased to and fro motion) in NPH that manifests as increased flow void in the aqueduct on routine MR images. If this flow void is extensive then there is good response to the ventricular shunting, which is a treatment for NPH.

Aqueductal stroke volume more than 42 microliters on a CSF flow study usually indicates a good response to the ventricular shunting. NPH patient with stroke volume less than 42 microliters is less likely to benefit from the shunting. Thus CSF flow study has diagnostic as well as prognostic value in the NPH.

2. Shunt evaluation

Ventricular shunts have stop valve that allows unidirectional flow. On the flow images, the patent shunt signal during systole-diastole will be bright-gray-bright-gray respectively. If the shunt is blocked signal in the tube will be gray in both systole and diastole.

The flow through the aqueduct is reversed (caudocranial during the systole) after shunting because of low pressure pathways through the shunt for CSF. The CSF is pushed upwards by the cerebellum and choroid plexus in the fourth ventricle. So if the flow in the aqueduct is normal (i.e. craniocaudal during systole), it may represent a shunt block.

3. Cerebrospinal fluid (CSF) flow studies may be useful in differentiation of an arachnoid cyst from the mega cisterna magna. Arachnoid cyst will not show CSF movement during systole and diastole and will show different flow than the surrounding CSF.

Miscellaneous Body Imaging MR Techniques

CHAPTER 21

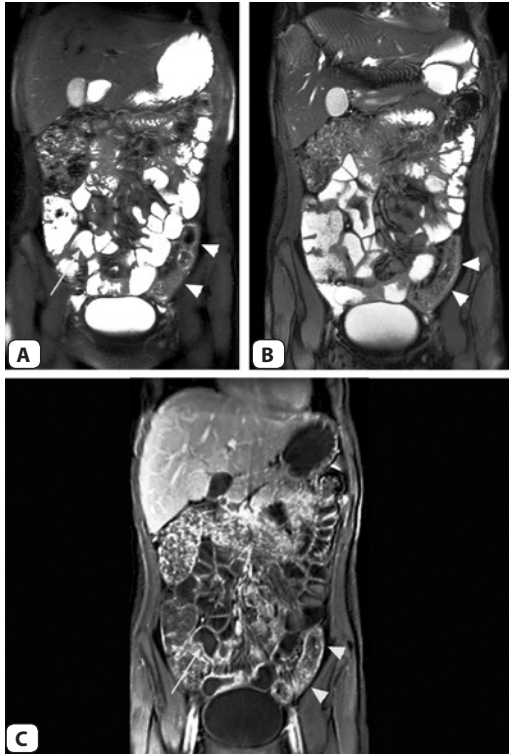
Some of the new, emerging and promising MR techniques in the body imaging are outlined in this chapter. These techniques include MR enterography, MR urography, Iron overload imaging, MR elastography and MR arthrography.

Magnetic Resonance Enterography

Magnetic resonance enterography (MRE) is a new technique for evaluation of the bowel. It is rapidly replacing barium studies.

Principles: MR evaluation of bowel was difficult until recently because of movement artifact from peristalsis and susceptibility artifact from gas in the bowel preventing bowel wall visualization. Faster sequences like single-shot FSE and balanced SSFP, and antiperistaltic agent are used to counteract motion and improve the visibility of thin bowel wall. Distension of the bowel loops by oral contrast helps to remove intraluminal gas and helps to better visualize the bowel wall.

Technique: The patient drinks 20 ml/kg of oral contrast about 45–60 minutes before the scan. The solutions that can be used as an oral contrast include Volumen (contains sorbitol, natural gum, simethicone and barium sulfate), polyethylene glycol and simple 3% sorbitol solution with some flavoring agents. Antiperistaltic agent is given intravenously in the beginning and at the time of contrast injection. These agents include hyoscine butylbromide (Buscopan) 0.3 mg/kg or glucagon 0.25–0.5 mg.



Figs 21.1A to C: MR Enterography in Crohn's disease. Coronal single-shot (A), balanced TFE (B) and postgadolinium T1-w 3D GRE THRIVE (C) images show thickened bowel loops. Arrow = terminal ileum and arrowheads = inflamed descending colon

Single-shot FSE and balanced SSFP sequences are acquired in axial and coronal planes before contrast injection. After gadolinium injection, T1-w 3D GRE images (VIBE/THRIVE/LAVA) in axial and coronal planes are acquired. Diffusion weighted imaging can be used to look at bowel wall inflammation, lymph nodes and abscesses.

Clinical applications: MRE can be used to evaluate any bowel pathology. It is mainly used in inflammatory bowel disease (IBD) to evaluate small bowel involvement (Fig. 21.1). It shows many extraintestinal findings in the IBD that are not seen on barium studies.

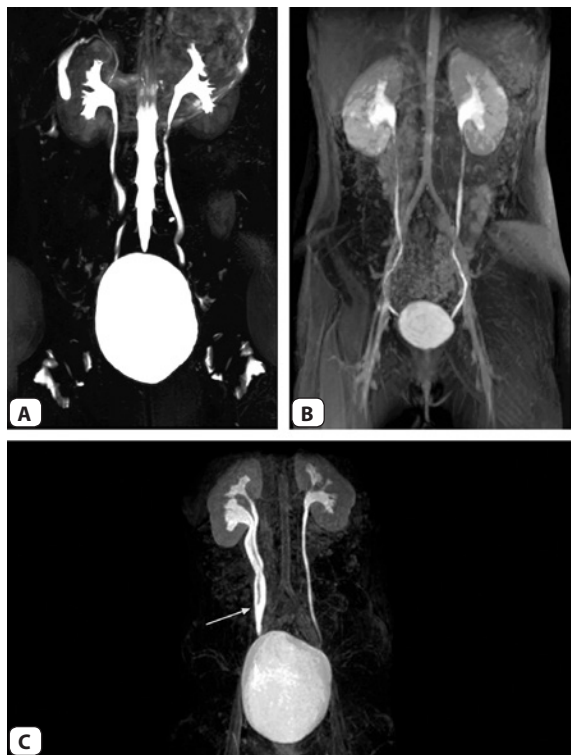
MR Urography

Principles: Urinary tract can be evaluated in two ways: by T2-w images with high TE and by T1-w images with excreted contrast in the collecting system. T2-w imaging is useful in visualization of a dilated system though visualization of a normal collecting system can be improved by intravenous hydration and diuretic injection. For nondilated collecting system, excreted IV contrast is useful but requires functioning renal parenchyma. A complete MRU is usually combination of both T1- and T2-w imaging and functional evaluation on dynamic post-contrast images.

Technique: Patient is started on intravenous ringer lactate (10 ml/kg) 30 minutes before the scan. Intravenous furosemide (1 mg/Kg) is injected approximately 15 minutes before the gadolinium injection. During these 15 minutes routine anatomical T1- and T2-w images of the kidneys and bladder are acquired followed by 3D MRU (a heavily T2-w 3D FSE same as 3D MRCP) covering kidneys, ureters and the bladder. Next, multiple runs of coronal oblique (along long axis of kidneys and ureters) T1-w 3D GRE (VIBE/THRIVE/LAVA) are acquired during dynamic intravenous injection of routine dose of gadolinium-based contrast media. The dynamic runs are continued till complete opacification of distal ureters and the bladder.

Postprocessing: The 3D MRU and post-contrast T1-w images can be reformatted in various planes using methods like MIP, MPR and VRT. The post-contrast images can be processed using various functional assessment software that are available free of cost on the internet. The functional information obtained includes differential renal function, renal transit time, time to excrete and symmetry between two kidneys.

Clinical applications: A complete MRU can serve as a one stop shop for evaluation of all urinary tract abnormalities including congenital (Fig. 21.2), obstructive and neoplastic.



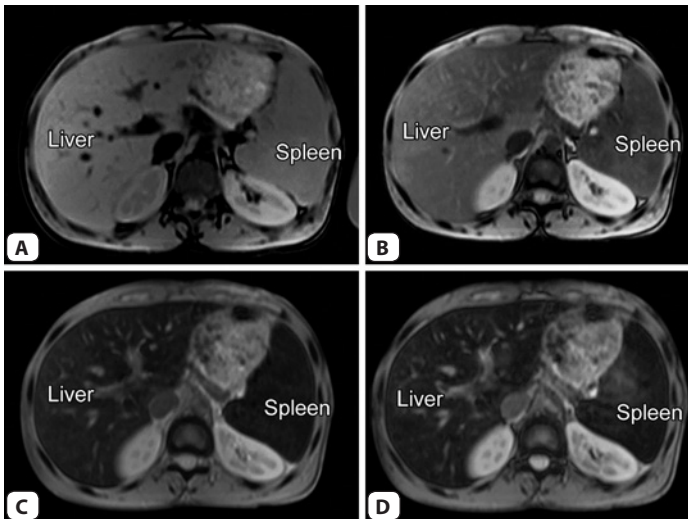
Figs 21.2A to C: MR Urography: Coronal MIP images of 3D MRU (T2-w FSE) (A) and postgadolinium dynamic MRU (B) show normal collecting system. MIP image of postcontrast T1-w MRU in another patient (C) shows right bifid collecting system with two ureters joining in their distal segments (arrow)

Iron Overload Imaging

Principles: Presence of ferritin and hemosiderin in the tissue causes faster decay of transverse magnetization and signal loss in that tissue. The signal loss in the tissue is proportional to the iron concentration and increases with the TE.

Technique: As the TE increases the darkening of the tissue containing iron increases. This can be quantified in two ways: comparing the signal intensity of the target organ with unaffected tissue such as muscle (signal intensity ratio) or determining decay pattern of T2 or T2* relaxation rates (relaxometry). Both these methods can be applied to spin-echo or gradient-echo images acquired with increasing TE. Gradient-echo images are faster and more sensitive to low iron content but have more susceptibility artifacts.

Clinical applications: Iron overload can be caused by long-term transfusion therapy, disorders of iron absorption such as hereditary hemochromatosis and defects in heme metabolism. Iron is toxic to the tissues and can cause dysfunction of the organs like liver, heart and endocrine organs. MR imaging can be used to detect and quantify iron deposition in various organs for initiating and monitoring treatment and determining the response to iron chelation therapy (Fig. 21.3). MR



Figs 21.3A to D: Iron overload imaging. T2*-w images of the abdomen (A to D) show progressive darkening of liver and splenic parenchyma with increasing TE suggestive of iron overload from multiple transfusions in this patient with thalassemia

quantification of iron overload has completely replaced liver biopsy in recent years.

Magnetic Resonance Elastography

This is a new technique used to measure stiffness of organs, in particular the liver. Mechanical waves at a predetermined frequency are sent by a device placed over the liver. Propagation of these waves through the liver is imaged using a gradient-echo sequence. The velocity and wavelength of the mechanical waves increases with greater tissue stiffness. Color coded quantitative stiffness maps (elastograms) are obtained. Liver stiffness increases with liver fibrosis. MR elastography can be indirectly used to evaluate and stage liver fibrosis. This method is still in its infancy but initial results are encouraging.

Magnetic Resonance Arthrography

Principles: MR arthrogram involves passive distension of the joint space followed by MR imaging for the joint. Passive distension of joint space allows better visualization of the labrum, joint capsule and various ligaments.

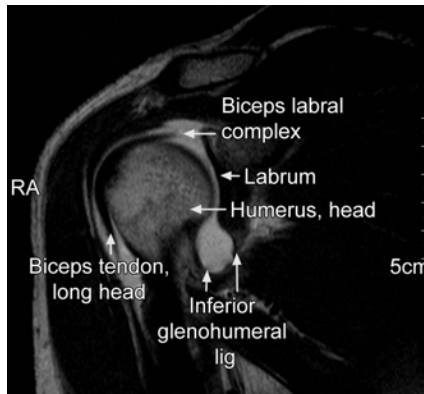


Fig. 21.4: MR Arthrogram of the shoulder.
Normal structures are shown

Technique: A solution is injected in the joint space under fluoroscopy guidance. The solution is usually made up of 0.1 cc of Gadolinium (for contrast in MR images), 2 cc of water soluble iodinated contrast media (for visualisation of joint space under fluoroscopy) and 20 cc of normal saline. MR imaging of the joint is performed within 45 minutes of the joint injection with routine sequences.

Indications:

1. Recurrent dislocation of the shoulder joint. MR shoulder arthrogram allows visualization of the glenoid labrum, glenohumeral ligaments and rotator cuff in exquisite detail (Fig. 21.4). MR arthrogram shows anteroinferior labral detachment (Bankart's lesion), APLSA (anterior labrum periosteal sleeve avulsion), GLOM (glenoid labrum ovoid mass) and SLAP (Superior labrum anterior-posterior) lesion in the recurrent dislocation.
2. Hip joint arthrogram for evaluation of the labrum. It is being performed less frequently because of good accuracy of routine hip imaging at 3Tesla MRI for the detection of labral abnormalities.

Index

Page numbers followed by *f* refer to figure and *t* refer to table

A

Abdominal imaging 122, 123*f*
Abscess 143, 171
Acoustic noise 86
Allergy 97
Alzheimer's
 dementia 170
 disease 164*f*
Aminoacids 167
Analog-to-digital converter 82
Aneurysm and hemostatic clips 88
Anterior labrum periosteal sleeve
 avulsion 202
Apparent diffusion coefficient 139
Arachnoid cyst 143
Array spatial sensitivity encoding
 technique 52
Arrhythmogenic right ventricular
 dysplasia 177, 178*f*
Arterial spin labeling 148, 155
Artificial sphincters 89
Ascending aorta 130*f*
ASL diagram 157*f*
Asthma 97
Atomic number 94

B

Bankart's lesion 202
Bilateral basal ganglion
 hyperintensity 170*f*
Bird cage coil 31*f*
Black blood imaging 129, 130*f*
Blood oxygen level-dependant 190

Body

 coil 30
 imaging 101
Bone growth stimulators 90
Brain tumor 99*f*
Bright blood
 imaging 130, 130*f*
 technique 173

C

Calculus in
 CBD 187*f*
 gallbladder 187*f*
Canavan's disease 165*f*, 170
Cardiac
 and pericardial masses 182
 magnetic resonance imaging 172
 mass 181*f*
Cardiomyopathies 177
Caroli's disease 186
Cartilage sensitive sequences 70
Cerebral
 blood
 flow 140, 149
 volume 149
 hemisphere 108*f*
Cerebrospinal fluid 192, 195
 flow study 192
Choledochal cyst 186*f*
Choline 166
Chronic
 infarct 143*f*
 pancreatitis 189

204 MRI Made Easy (For Beginners)

Circle of Willis arteries 129
CISS axial image of posterior cranial fossa 69*f*
Classification of MR contrast media 91
Closed head trauma 170
CNS
 infection 98
 neoplasm 98
Cochlear implants 90
Complication of congenital dilatation of ducts 187*f*
Congenital heart disease 176
Constrictive
 pericarditis 178, 179*f*
 interference at steady state 69
Contrast enhanced
 MRA 129, 136
 MRI 55
Coronary artery assessment 180
CP angle lesions 110
Crohn's disease 197*f*

D

Dark-blood technique 173
Demyelinating lesions 110
Dental devices and materials 88
Descending aorta 130*f*
DESS coronal image of knee 71*f*
Diagram of ECG gating 173*f*
Diffuse axonal injury 112*f*
Diffusion
 tensor imaging 146
 weighted imaging 137
Dipole-dipole interaction 92
Dixon method 51*f*
Double echo sequence 36*f*
Dual spin-echo sequence 35
DWI in
 abdomen 145*f*

 body imaging 146
 brain tumors 143
Dysprosium chelates 97

E

ECG gating 172
 for cardiac motion 74
Echo
 planar imaging 34, 44
 train length 36
Electromagnets 24
Endometrium 124
Epilepsy 108, 170
 protocol 109*f*
Extrahepatic biliary tree 187*f*

F

Faraday cage 29
Fast spin-echo sequence 37
Fat suppression techniques 50
Flair sequence 45*f*
Flip angle 19
Fluid-attenuated inversion recovery sequences 44
Fractional anisotropy 146
Functional MRI 190, 191*f*

G

Gadolinium 93, 94, 148
 chelates 94
Gibbs' artifact 78
Globus pallidus 56*f*
Glucose 167
Glutamate 166
Gradient
 echo sequence 34, 37, 39*f*, 46
 hemo axial image of brain 70*f*, 112*f*
 magnetic field 85
 moment nulling 74
 strength 29

H

- Heart valves 88
- Helium 26
- Hemochromatosis 179
- Hepatic encephalopathy 171
- High
 - grade
 - glioma 168*f*
 - versus low grade glioma 154*f*
 - signal intensity structure 121
- HIV and AIDS 171
- Hypoxic-ischemic injury 114
- Hypertrophic cardiomyopathy 178
- Hypertrophy of ligamentum flavum 116*f*
- Hypointense mass 181*f*

I

- Image quality determinants 20
- Implantable cardiac defibrillator 90
- Infection 108
- Inflamed descending colon 197*f*
- Integrated parallel acquisition technique 52
- Internal
 - auditory canal 110*f*
 - cardiac pacemaker 90
- Intracranial
 - arteries 132*f*
 - venous system 135*f*
- Intraocular foreign body 90
- Intravascular coils, filters and stents 89
- Inversion recovery sequence 34, 40, 41*f*
- Iron
 - overload imaging 199, 200*f*
 - oxide 97, 98
- Ischemic CNS diseases 98

J

- Joint imaging 121
- Junctional zone-inner myometrium 124

K

- Keyhole imaging 56, 57*f*
- K-space 17
 - and scanning parameters 17

L

- Lactate 166
 - peak in metabolic disorder 170*f*
- Lactation 97
- Left
 - cerebral hemisphere 156*f*
 - posterolateral herniation of disk 116*f*
- Leigh's disease 170*f*
- Lipids 167
- Liquid nitrogen 27
- Localization techniques in MRS 160
- Lymphoma 145*f*

M

- Magnetic field
 - homogeneity 28, 159
 - strength 23
- resonance
 - angiography 129
 - cholangiopancreatography 122, 183
 - contrast media 91
 - diffusion 137
 - elastography 201
 - enterography 196
 - imaging artifacts 73
 - instrumentation 22
 - perfusion 148
 - safety 85

- spectroscopy 158
- susceptibility artifact 78
- Magnetization transfer 55, 56f
 - diagram 55f
- Main pulmonary artery 130f
- Mangafodipir trisodium 97
- Manganese chloride 98
- Matrix 18
- Mean transit time 149
- Mechanism of MR contrast enhancement 92
- Medic axial image of cervical spine 72f
- Metabolic
 - diseases 114
 - disorders and white matter diseases 170
- Miscellaneous
 - body imaging MR techniques 196
 - neuroimaging MR techniques 190
- Mitral stenosis 177f
- Moyamoya disease 156f
- MR
 - abdominal imaging 122f
 - angiography 56, 129
 - arthrogram of shoulder 201f
 - perfusion in
 - brain tumors 153
 - stroke 150
 - urography 198
- MRI in pediatric brain 112
- Multi echo data image combination 71
- Multiple sclerosis 111f, 170
- Multivoxel technique 160
- Musculoskeletal neoplasms 120
- Myocardial
 - iron deposition 179
 - perfusion
 - and viability 180
 - study 180
 - viability 180, 181f

N

- Navigator technique 53
- Neonatal hypoxia 169
- Neoplastic lesions 189
- Nephrogenic systemic fibrosis 96, 129
- Neural foramina 116f
- Niobium-titanium 25
- Noncontrast MRA 129
 - techniques 131
- Non-titanium aneurysm clips 90
- Number of excitations number of signal averages 19

O

- Ocular implants 89
- Orthopedic implants 89
- Osteoarthritis 71f
- Otologic implants 89

P

- Pacemakers 89
- Pancreatic duct 186f, 188f
- Parallel imaging artifact 83f, 84
- Paramagnetic agent 92, 94
- Parameters of scanning 18
- Pelvic imaging 122
- Penile implants 89
- Penumbra of salvageable tissue 152f
- Perfusion imaging 152
- Pericardial disease 182
- Permanent magnet 24
- Phase encoding axis swap 73
- Point resolved spectroscopy 160
- Positron emission tomography 148
- Posterior circulation stroke 106f
- Post-excitation refocused steady-state sequences 40
- Postoperative spine 100f
- Pre-excitation refocused steady-state sequences 40

- Primary sclerosing cholangitis 188, 188*f*
- Principal Eigen value 146
- Principles of interpretation 102, 115
- Prostate imaging 123*f*
- Proton density image 16
- Pulmonary regurgitation and right pulmonary artery stenosis 176*f*

- R**
- Radial K-space filling 46
- Radiation necrosis 169*f*
- Radiofrequency coils 30
- Reformation of angiography 133
- Regional anisotropy 146
- Renal failure 96
- Respiratory compensation techniques 53, 54*f*
- Restrictive cardiomyopathy 178
- Rheumatic fever 177*f*
- Right ventricular hypertrophy 176*f*
- Ringing artifacts 78
- Role of contrast in MRI 98
- Routine contrast enhancement 152

- S**
- Sacroiliitis 118*f*
- Saddle coil 31*f*
- Safety issues 96, 126
- Saturation band 56, 74
- Selection of VOI 162
- Shading artifact 82*f*
- Short tau inversion recovery 49, 65
- Signal-to-noise ratio 20
- Simple cystic lesion 143
- Simultaneous acquisition of spatial harmonics 52
- Single-shot fast spin echo 62, 130*f* sequence 37, 38*f*
- Small petechial hemorrhages 112*f*
- Solenoid coil 31*f*
- Spatial resolution 21
- Spin
 - echo
 - pulse sequence 34
 - sequence 35*f*, 46
 - imaging 115
- Static magnetic field 85
- Steady state sequences 39
- Stenosis of mitral valve 177*f*
- Steps in diffusion weighting 138
- Stejskal-tanner' sequence 139*f*
- Stroke 140, 170
- Structure of superconducting magnet 26*f*
- Summary of sequences 46
- Superconducting magnets 24, 25
- wires 25
- Superior vena cava 130*f*
- Superparamagnetic iron oxides 92
- Surface coil 31
- Susceptibility artifact 79*f*

- T**
- T1 curves- pre and postcontrast 93*f*
- T1 weighted
 - image 13
 - sequences 58
- T2 weighted
 - image 14
 - sequences 61
- Tectal lipoma 76*f*
- Tetralogy of Fallot 176*f*
- Tetramethylsilane 164
- Time of flight MRA 131, 134
- Toxoplasma 171
- Transverse
 - magnetization 34
 - relaxation 9
- Tuberculomas 99*f*

208 MRI Made Easy (For Beginners)

Tumor 104
 recurrence versus necrosis
 155*f*
 vascularity 107*f*
Turbo spin echo sequence
 37*f*
Types of
 GRE sequences 38
 IR sequences 42
 MRA 129
Typical case of stroke 142*f*

U

Uterine imaging 124

V

Valvular heart disease 177
Vascular access ports 89
Venous infarct 105*f*
Vertical long-axis plane 174
Volume
 coil 30
 of interest 161*f*, 162

W

Water selective excitation 51

Z

Zipper artifact 80